16158-H019-R0-00

FINAL PROJECT REPORT

INVESTIGATION OF DATA COMPRESSION TECHNIQUES

NAS 9-10876

15 SEPTEMBER 1971

Prepared for
NATIONAL AERONAUTICS AND SPACE ADMINISTRATION
MANNED SPACECRAFT CENTER
HOUSTON, TEXAS

TRW
SYSTEMS GROUP

CR-115177

16158-H019-R0-00

FINAL PROJECT REPORT

INVESTIGATION OF DATA COMPRESSION TECHNIQUES

NAS 9-10876

15 SEPTEMBER 1971

Prepared for
NATIONAL AERONAUTICS AND SPACE ADMINISTRATION
MANNED SPACECRAFT CENTER
HOUSTON, TEXAS

M F Conover
Marshall F. Conover
Project Manager

Approved by: J W McCurry
J. W. McCurry, Manager
Systems Engineering Laboratory

TRW
SYSTEMS GROUP

Houston, Tex.

ACKNOWLEDGMENT

The Project Manager wishes to acknowledge the contributions of TRW programer/analysts W. Lee Hayden and William P. Bennett whose innovative support greatly enhanced this study.

ABSTRACT

This final project report is submitted to NASA/MSC by TRW Systems Group in accordance with Contract NAS 9-10876. The principal objective of this study was to apply actual electrocardiographic data to various data compression/reconstruction algorithms to determine how accurately these data could be reconstructed and with what data compression magnitudes. A candidate algorithm population was established and selection processes resulted in the application of electrocardiographic data from twenty individual subject/test conditions to the fast Fourier and fast Hadamard transforms; parallel adaptive composite; cycle-to-cycle with a filter; and a new fast Fourier cycle-to-cycle redundancy reduction algorithm. This study concluded that real electrocardiographic data can be compressed/reconstructed with statistical inaccuracies in the order of one-half to five percent. Further, the parallel adaptive composite algorithm was concluded to be the most desirable algorithm studied from the standpoints of accuracy, bandwidth compression ratio, software and computer requirements. Additional study is recommended in four areas: 1) investigate the effects of pre-compression filtering; 2) determine the values of data compression/reconstruction errors visually detectable by cardiologists; 3) study the effects of data compression techniques on vectorcardiographic parameters; and 4) examine principal and alternate means of implementing desirable algorithms in actual operational configurations.

CONTENTS

PRECEDING PAGE BLANK NOT FILMED

TABLES

ILLUSTRATIONS

PRECEDING PAGE BLANK NOT FILMED

NOMENCLATURE

algorithm - an ordered computational procedure for calculating a desired answer.

array - an ordered set of data stored in a computer memory.

bandwidth - the total frequency band about a carrier frequency that is required to communicate the needed information.

BCR - bandwidth compression ratio

binary word - a digital computer message composed of base-two symbols.

bit - a single element (1 or 0) of a binary word.

carrier - the basic frequency on which information is impressed to be transmitted.

channel capacity- the actual information rate capability of a communication channel.

control - a set-length period of baseline observation prior to a physiological test.

core - the central memory portion of a digital computer in which data and instructions are stored and executed.

CRT - cathode ray tube

C2C - cycle-to-cycle algorithm

DCR - data compression ratio

digitize - discrete sampling of analog signals with subsequent conversion to binary (digital) words.

distortion - the difference in fidelity between a reconstructed and an original waveform.

ECG - electrocardiogram, also EKG

ergometer - a device that can cause, measure and record work done by a subject under laboratory conditions.

FFC2C - fast Fourier cycle-to-cycle algorithm

FFT - fast Fourier transform algorithm

FHT - fast Hadamard transform algorithm

hertz - dimensional units for frequency

LBNP - lower body negative pressure (laboratory device)

information rate- the rate at which non-redundant data are transmitted.

Lissajous - an X-Y display (usually on a CRT) of two different signals that shows their time relationship (phase) to each other.

mm Hg - millimeters of mercury (pressure)

NOMEMCLATURE (Concluded)

ms	- millisecond
MSC	- Manned Spacecraft Center
mv	- millivolt
NASA	- National Aeronautics and Space Administration
PAC	- parallel adaptive composite algorithm
PCM	- pulse code modulation
p-p	- peak-to-peak
reconstruction	- building of a complete waveform using less than the original waveform as the foundation.
recovery	- a set-length period of observation after a physiological test.
rf	- radio frequency
rms	- root mean square
rss	- root sum square
sequency	- one-half the average number of zero level crossings per second.
software	- the stored programed instructions of a computer.
sps	- samples per second
transform	- changing the mathematical representation of a signal from one domain to another.
truncate	- cut off
VCG	- vectorcardiogram

1. INTRODUCTION

Today, as never before, data compression may supply the answer to a problem that faces manned space flight biomedical data gathering. This problem is manifested in biomedical data requirements which are expanding as the mission durations, crew sizes and sophistication increase. Additionally, biomedical data seem to demand an inordinate share of data processing capabilities--particularly electrocardiac signals--which tax the checkout activities, manned space flight networks and post flight data processing facilities. Data compression techniques may well be able to reduce the biomedical information bandwidth--a natural resource--requirements while simultaneously satisfying the demands of the medical community.

1.1 STUDY PURPOSE

The purpose of this study was to investigate data compression (and subsequent reconstruction) techniques of electrocardiogram (ECG) and vectorcardiogram (VCG) signals. A variety of data compression techniques was studied by evaluating their operations on real physiological (ECG/VCG) signals via error analyses.

1.2 DATA COMPRESSION DEFINITION

Data compression is an expression with broad meaning and can embody any or all of the following terms: *data compaction, bandwidth compression, redundancy removal, redundancy reduction, adaptive sampling* and *adaptive telemetry*. In 1965 Weber[1], recognizing the need for standardizing the terminology to reduce confusion and misunderstandings, produced an exemplary paper to this end.

A data compression/reconstruction technique--as it relates to this study--*identifies the minimum data elements of a biomedical measurement continuum that are required to reconstruct the original data continuum within established limits of error so that the biomedical information bandwidth can be reduced.* Accordingly, data compression techniques can allow transmission of the desired information utilizing less of the radio spectrum; i.e., less bandwidth. In this manner, the *data* will have seemed to be *compressed* into a smaller bandwidth--hence the term.

Bandwidth concepts are the key to understanding the need for data compression. It has been shown[2] that a frequency at least equal (depending on the transmission mode) to the highest information frequency content of any measurement being telemetered resides on both sides of the transmitted radio frequency (rf) carrier. This segment of the rf spectrum is called the *bandwidth*. Because many other disciplines are impacted by the width--or size--of the information bandwidth, a bandwidth reduction will yield beneficial effects of which the data requestor or analyst is not even aware.

Presented below are a few major relationships between bandwidth requirements and other disciplines.

a) transmitter size. As bandwidth decreases, less power is required to reach a given distance because of antenna and receiver design considerations.

b) receiver design. Because receiver-generated noise decreases with bandwidth, an increase in system range is realized with a decrease in bandwidth. In the converse, if receiving, transmitting and antenna systems are already maximized, the required spacecraft range will necessarily limit the bandwidth.

c) spacecraft power. A low power transmitter eases the total demands on the spacecraft prime energy source.

d) data handling and storage. A small bandwidth results in fewer data samples which results in less handling and storage requirements.

e) data processing. Fewer data samples may result in less ground computation time and costs.

f) wire ground-communication links. The number of wire circuits required to reach the control center is reduced directly with bandwidth.

2. INVESTIGATION OF DATA COMPRESSION TECHNIQUES

In summary, during the conduct of this study TRW surveyed the field of data compression. Thirty-five different data compression algorithms were found and are documented in Table 2-1. A synopsis of each algorithm is presented in Appendix A. The algorithm population was narrowed to seven candidates by the application of acquired qualitative guidelines and the quantitative guidelines contained in the contract statement of work. Five of the seven candidate algorithms were tested--in addition to a sixth TRW-developed algorithm--using real ECG and VCG data from nine different subjects. The ECG/VCG data--recorded by NASA/MSC during manned space flight and earth-based laboratory work--were subdivided into four activity groups containing twenty individual subject/test conditions. The ECG/VCG data were digitized at a 500 samples per second rate which preserves a practical frequency response of from 100 to 125 hertz in keeping with high-frequency ECG investigations done by Franke[3] and Langner[4].

2.1 ALGORITHM POPULATION DEVELOPMENT

2.1.1 Literature Survey

An extensive literature survey on data compression was conducted to establish a basis on the present state-of-the-art. Although the subject of data compression (in the late 1950's) addressed speech and television signals, papers and articles on aerospace telemeters were not found before 1961 when Ellersick[5] appears to have identified the need. The preponderance of aerospace data compression papers were published between 1964 and 1969.

The most recent algorithms (suitable for data compression) found were by Bergland[6] and Harmuth[7] who in 1969 published works on the fast Fourier and fast Hadamard transforms. These two computationally-fast transformation algorithms probably represent the most recent software-type algorithms that are applicable to data compression and reconstruction.

Table 2-1 presents the data compression algorithm population developed from the literature survey. Naturally, each algorithm found is not listed in Table 2-1 for some papers report on a slightly different modification or application of an established data compression concept. Table 2-1 further presents a generalized estimate regarding the complexity of the algorithm implementation; prior test results; and a rationale for the desirability of further study using actual ECG data. Appendix A contains a synopsis on each specific algorithm listed in Table 2-1.

2.1.2 Candidate Algorithm Selections

Three conditions provided the principal screening factors in the selection of candidate algorithms from Table 2-1. These conditions -- which are presented below -- were implicit in the statement of work.

a) An accurate reconstruction of the original ECG waveform must be possible from the compressed data.

b) The algorithm must be able to operate in real time; i.e., it must be able to operate as fast, or faster, as the data samples arrive.

c) There must be evidence that a reasonable bandwidth compression ratio (BCR) is achievable using real ECG/VCG data.

In evaluations of prior work done on the algorithm population and applying the above conditions, the following seven algorithms were selected as candidates for further study:

a) Fast Fourier Transform[6] (FFT)

b) Fast Hadamard Transform[7] (FHT)

c) Filtering[8,9]

d) Cyclic Pattern[10] (CP)

e) Cycle-to-Cycle[8] (C2C)

f) First-Order Interpolator-Fan[11] (FOI-Fan)

g) Parallel Adaptive Composite[11] (PAC)

Table 2-1. Data Compression Algorithm Population*

Algorithm Terminology		Estimated Complexity of Implementation			Literature Search Data		Desirable for Further Study	
Generic	Specific	Software	Core	Speed	DCR	Error	Yes/No	Rationale
Transformation	Fast Fourier Transform	Moderately Complex	Large	Moderately Fast	--	--	Yes	Transform domain promises high DCR
	Fast Hadamard Transform	Moderately Simple	Large	Moderately Fast	--	--	Yes	Similar and faster than fast Fourier
	Spectrum Analysis	Complex	Large	Moderately Slow	--	--	No	Output precludes ECG reconstruction
	Thresholding	Simple	Small	Fast	--	--	No	Output precludes ECG reconstruction
	Frequency Discrimination	Complex	Large	Moderately Slow	--	--	No	Output precludes ECG reconstruction
	Hotelling's Method	Very Complex	Large	Slow	--	--	No	Real time operation precluded by speed
	Filtering	Moderately Simple	Small	Slow-Fast	--	--	Yes	Will enhance other algorithm operations
Adaptive Sampling	Associative	Moderately Complex	Medium	Moderately Fast	--	--	No	Excluded by near-future NASA telemeters
	Command Adaptive	Moderately Complex	Medium	Moderately Fast	--	--	No	Excluded by near-future NASA telemeters
	Self-Adaptive	Moderately Complex	Medium	Moderately Fast	--	--	No	Excluded by near-future NASA telemeters
	Transient Event	Moderately Complex	Medium	Moderately Fast	--	--	No	Excluded by near-future NASA telemeters
Redundancy Reduction	Predictors							
	ZOP	Simple	Small	Very Fast	5.4	25.0%	No	Most suitable for discrete data
	ZOP-FA	Simple	Small	Very Fast	5.5	7.7%	No	Most suitable for discrete data
	ZOP-O	Simple	Small	Very Fast	5.5	9.0%	No	Most suitable for discrete data
	Exponential	Moderately Simple	Small	Fast	--	--	No	ECG signal is not exponential in nature
	Cyclic Pattern	Complex	Large	Moderately Slow	--	--	Yes	ECG signals are cyclic in nature
	Cycle-to-Cycle	Moderately Complex	Large	Moderately Slow	1800	1.4%	Yes	Has achieved good DCR with clean signals
	Interpolators							
	ZOI	Simple	Small	Very Fast	--	--	No	Most suitable for discrete data
	FOI-2DF	Simple	Small	Very Fast	4.4	7.1%	No	Rejected in favor of FOI-Fan
	FOI-Fan	Simple	Small	Very Fast	5.6	1.0%	Yes	Best of FOI group-- accepts analog data
	FOIM	Simple	Small	Very Fast	4.5	7.0%	No	Rejected in favor of FOI-Fan
	FOI-3DF/-4DF	Moderately Complex	Medium	Moderately Fast	5.5/ 10.0	7.5%/ 8.0%	No	Gains over 2DF do not justify costs
	Sync Function	Moderately Complex	Large	Moderately Fast	8.0	18.0%	No	Rejected for complexity and error
	Fourier	Very Complex	Large	Moderately Slow	10.0	35.0%	No	Speed precludes real time operation
	Least Squares	Very Complex	Large	Very Slow	--	--	No	Speed precludes real time operation
	Lagrange	Very Complex	Large	Slow	--	--	No	Speed precludes real time operation
	Difference Method	Very Complex	Large	Slow	--	--	No	Speed precludes real time operation
	Fourier Coefficients	Very Complex	Large	Slow	--	--	No	Speed precludes real time operation
	Composite							
	Parallel Adaptive	Moderately Simple	Small	Very Fast	6.3	7.6%	Yes	Combines good elements of ZOP-FA&FOI-Fan
Encoding	Non-Adaptive							
	Delta Modulation	Moderately Complex	Medium	Moderately Fast	--	--	No	Anticipated DCR very small
	Difference Modulation	Moderately Simple	Medium	Moderately Fast	--	--	No	Requires slowly changing signals
	Probabilistic	Very Complex	Large	Very Slow	--	--	No	Real time operation precluded by speed
	Adaptive							
	Bit Plane	Very Complex	Large	Very Slow	--	--	No	Real time operation precluded by speed
	Probabilistic	Very Complex	Large	Very Slow	--	--	No	Real time operation precluded by speed

* Refer to Appendix A for a synopsis on each algorithm.

Detailed comparison between the CP and C2C disqualified the CP from this study in that a substantial ECG library would be required to develop a catalog of ECG patterns--in addition to a moderately complex program. An inordinate amount of resources would have therefore been required to study the CP technique thereby restricting the number of candidate algorithms.

Another candidate algorithm--the FOI-Fan--was discounted from individual study because the algorithm is utilized in the PAC and will be studied along with the Zero-Order Predictor-Floating Aperture (ZOP-FA) algorithm.

The remaining five algorithms emerged as the study candidates to be tested.

2.2 QUALITATIVE ECG CRITERIA

A survey of two NASA/MSC flight surgeons and an independent consultant was conducted to accumulate qualitative ECG guidelines to be considered along with the quantitative ECG guidelines from the contract statement of work (the principal quantitative guideline required that the reconstructed ECG/VCG waveform be as close as possible to one per cent error).

To provide a standard basis for discussion among the consultants, a sample vectorcardiogram (VCG), shown in Figure 2-1, was used. A Frank[12] lead system and standard recorder sensitivities were used to obtain the VCG from a subject at rest. In order to better identify cardiac waveform complexities and subtleties as they might apply to qualitative factors, the Figure 2-1 VCG waveforms were magnified by 225 percent.

Presented below are the consultants' principal opinions regarding factors important to their purview of compression and reconstruction of ECG/VCG data. These factors were weighed with the quantitative criteria during the study.

a) Consultant No. 1 — Doctor of Medicine, MSC Flight Surgeon

1. Continuous, full-time cardiac data are required.
2. The most important cardiac components in manned space flight are;

   Primary : QRS Complex
   Secondary: T Wave
   Tertiary : P Wave

3. An amplitude error of up to five per cent (between the reconstructed and original waveform) on a standard ECG record probably cannot be readily discerned nor will affect the cardiologist's reading of the record.

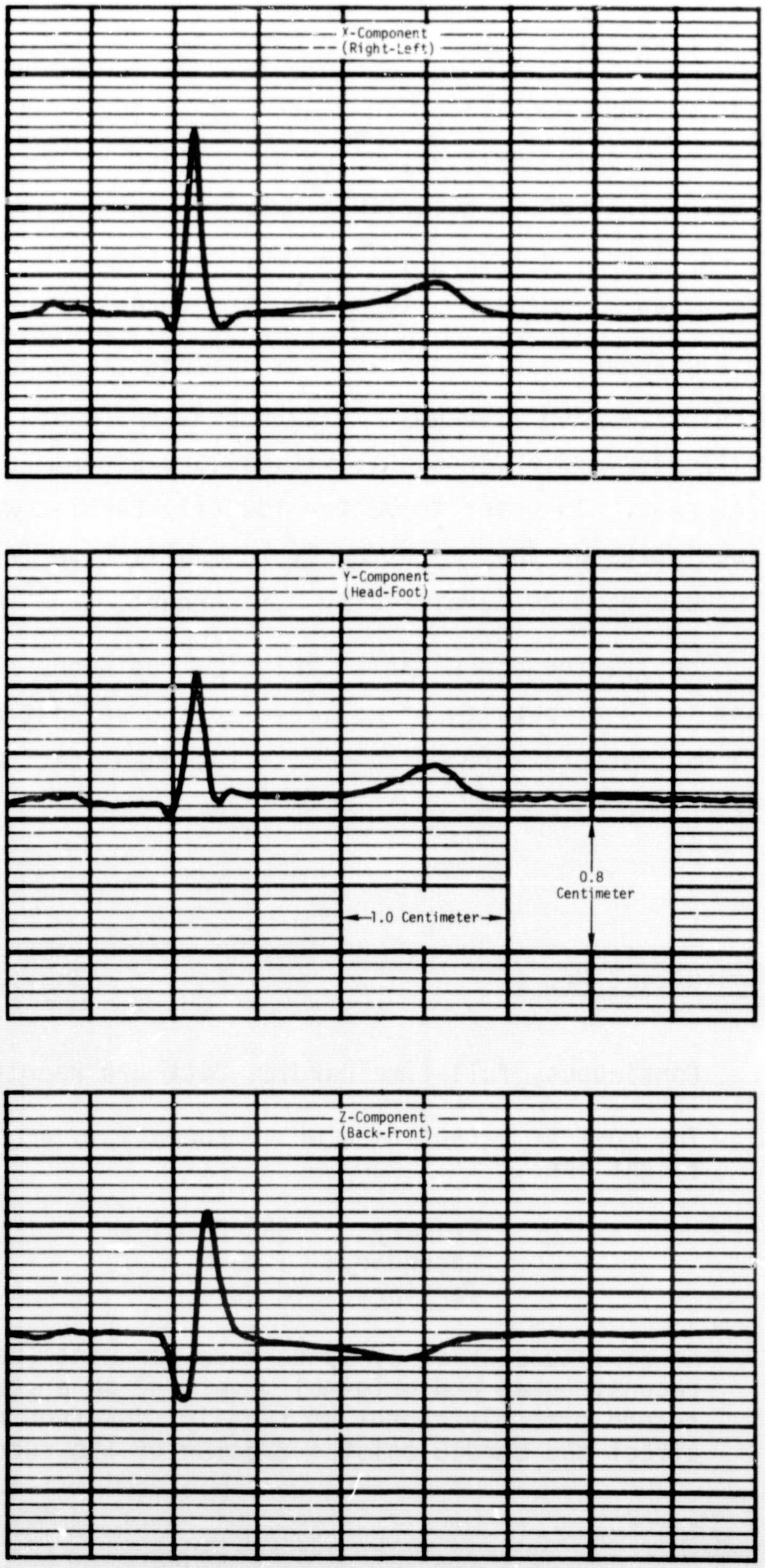

Figure 2-1. VCG Waveforms for Qualitative Criteria Discussions

b) Consultant No. 2 — Doctor of Medicine, MSC Flight Surgeon

1. Cardiac waves/segments/complexes durations and amplitudes are not routinely measured relative to exercise monitoring.

2. Astronaut cardiac rates and rhythm are very important during exercise periods.

3. The ST segment is closely monitored for depressions as small as one millimeter during exercise. The depression existence may indicate ischemia.

c) Consultant No. 3 — Doctor of Medicine, Independent Cardiologist

1. Wave "rise times," per se, are of small concern in ECG analyses.

2. The most important cardiac components in clinical cardiology are:

Primary :	QRS Complex
Secondary :	ST Segment
Tertiary :	T Wave
Quaternary:	P Wave

3. Junctional (J) depression has no meaning without ST segment depression during exercise.

4. Reconstruction of the compressed ECG by connecting all wave peaks and valleys by straight lines would not seriously hamper the clinical ECG analyses.

   However, the ST segment slope is important and a non-straight line reconstruction would better show a "drooping" ST segment which can be produced by Digitalis.

2.3 TEST GROUP DESCRIPTION

Magnetic tape recordings were obtained from NASA/MSC which contained ECG signals from three subjects in earth orbit and VCG signals from six subjects undergoing various physiological tests in the MSC cardiovascular laboratories. The signals were transferred to stripcharts (oscillograms) and reviewed for selection of appropriate areas to be used as standard input data for algorithm testing. Four types of physiological test conditions were performed by the group of nine subjects mentioned above.

Condition	Duration (minutes)	Physiological Tests Types			
		A	B	C	D
Earth Orbit	---	X			
Control	5		X	X	X
LBNP @ -20 mmHg	5		X		
LBNP @ -30 mmHg	5		X		
LBNP @ -40 mmHg	5		X		
LBNP @ -40 mmHg	15			X	
Ergometer Testing	2				X
Recovery	5		X	X	
Recovery	10				X

Twenty sections of different, individual subject/test conditions were selected and are shown in Figures 2-2 through 2-5. The test sections were divided into groups of similar, or identical, physiological activities. A total of four different groups was devised. Table 2-2 summarizes the activity groups and subject identifications which are used throughout this report. Members of each group were selected by considering such parameters as: the number of available samples; a satisfactory range of heart rates; unique cardiac complexes; and the presence of certain artifacts such as isoelectric variances or muscle noise.

Thus, a population of twenty different test cases of actual ECG/VCG data were considered to represent a satisfactory cross-section for testing of data compression and reconstruction techniques.

FOLDOUT FRAME 1

* * * * * * * * * * *
* A T T E N T I O N *
* * * * * * * * * * *

Stripchart speed for Figures 2-2 through 2-5 is 25 mm/second. However, Y-axis sensitivities are unknown but are known not to be the usual 1.0 mv/cm. These ECG/VCG mountings are presented for general comparisons only.

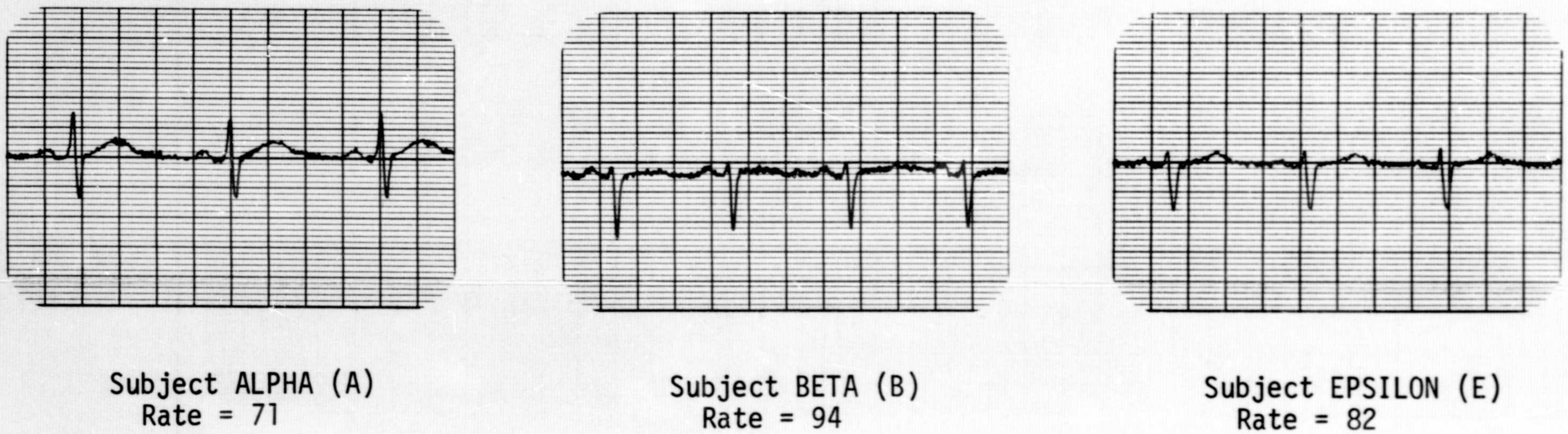

Figure 2-2. Activity Group I - Earth Orbit Station Keeping (ECG)

FOLDOUT FRAME 1

Subject	X-Component	Y-Component	Z-Component
ZETA (Z) LBNP Recovery R = 58	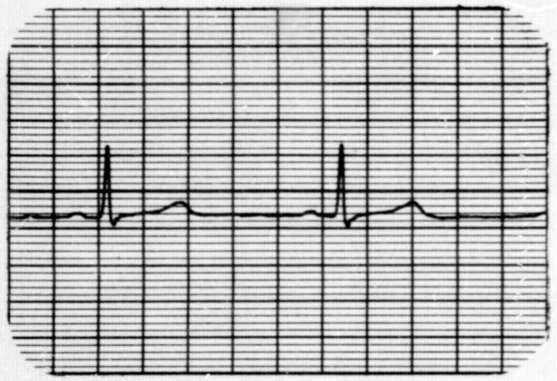	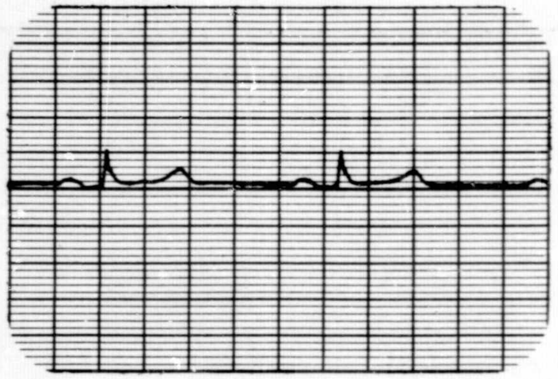	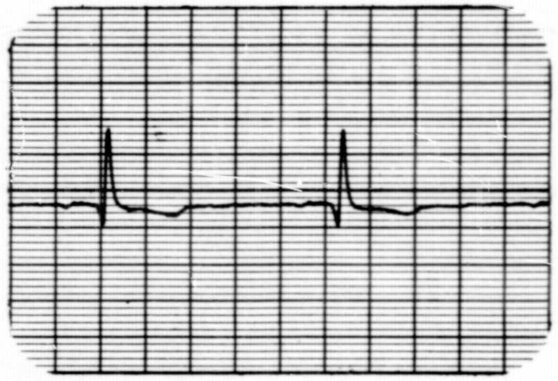
ETA (H) LBNP Control R = 52	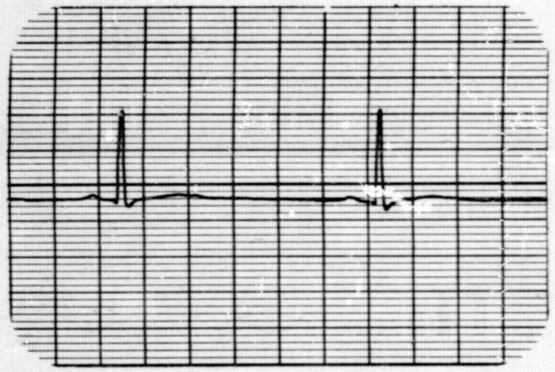	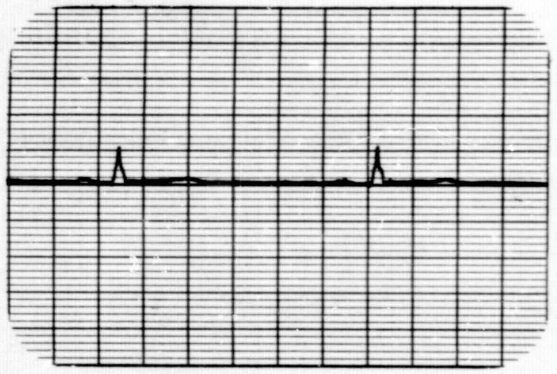	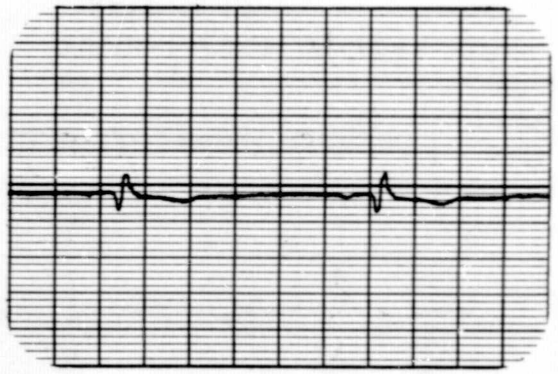
IOTA (I) LBNP Control R = 52	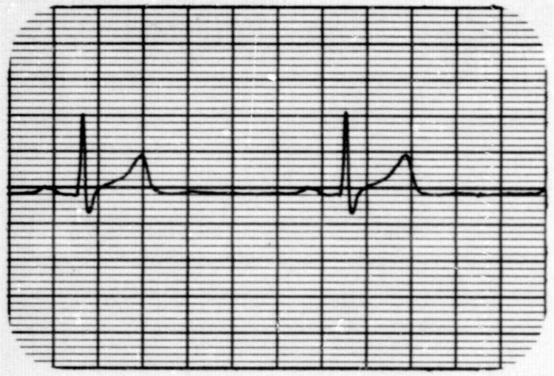	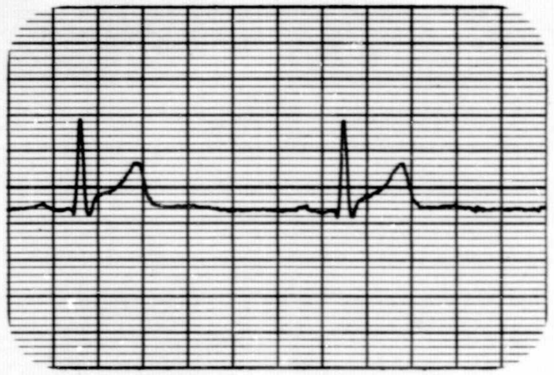	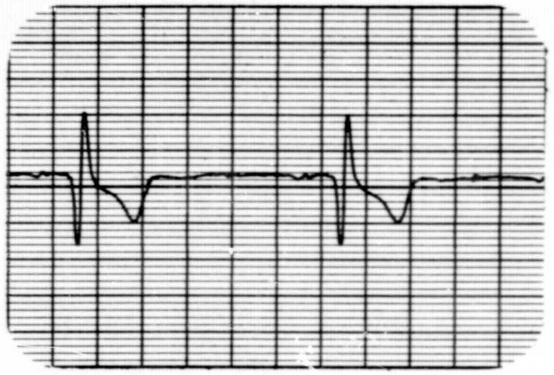
IOTA (I) Ergometer Recovery R = 84	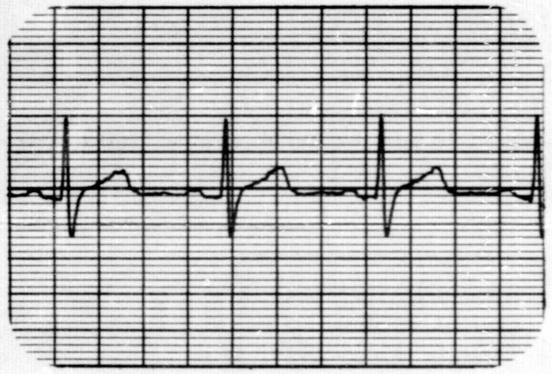		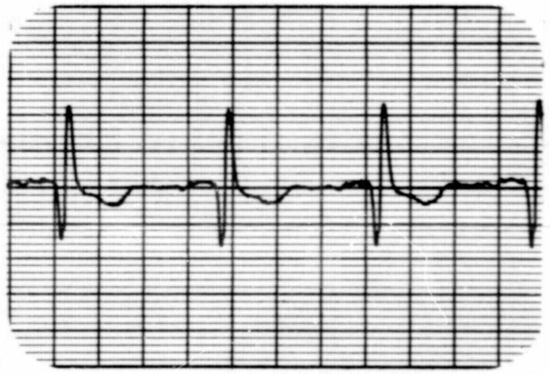

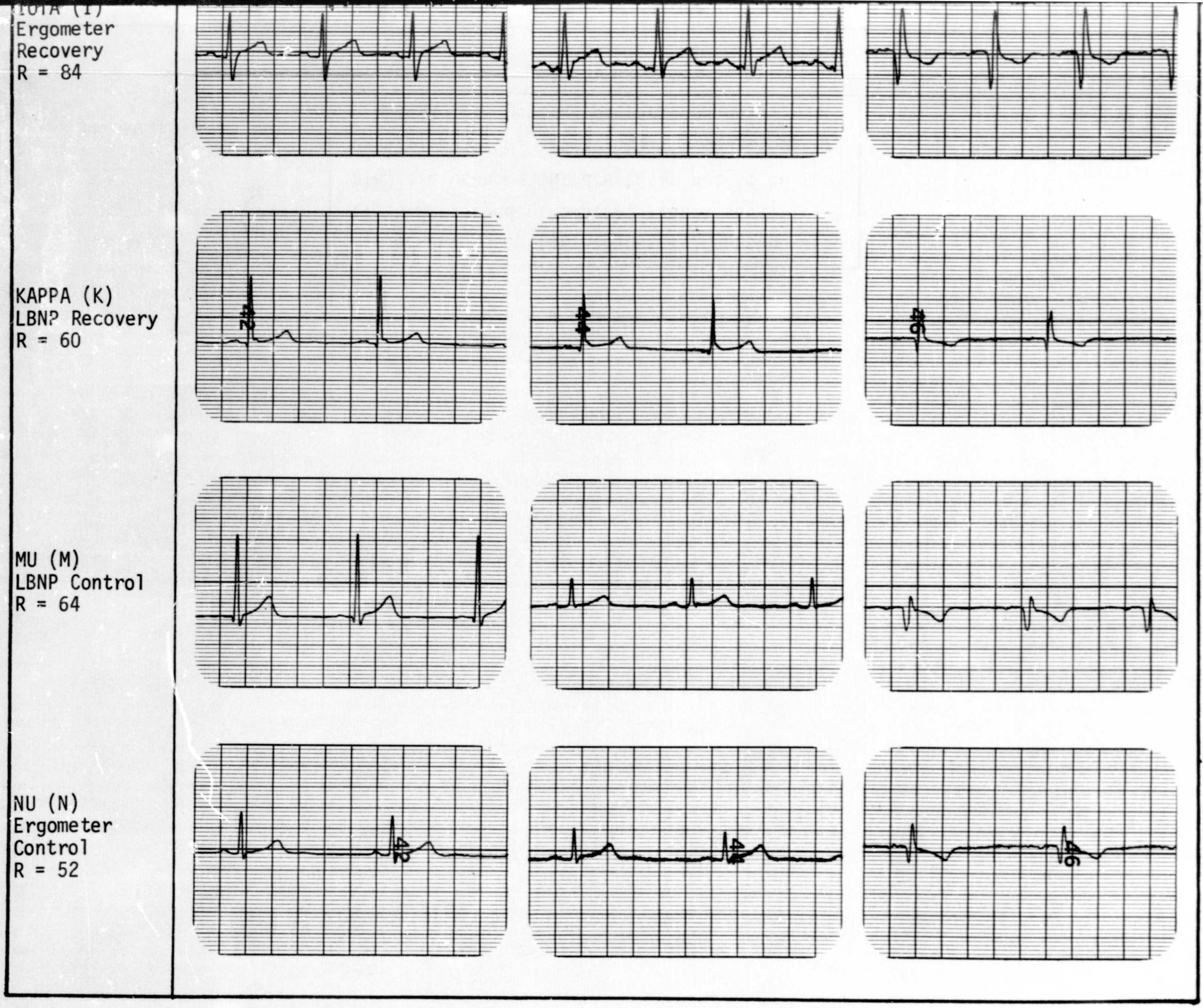

Figure 2-3. Activity Group II - Controls and Recoveries (VCG)

16158-H019-R0-00

FOLDOUT FRAME 1

Subject	X-Component	Y-Component	Z-Component
ZETA (Z) R = 55	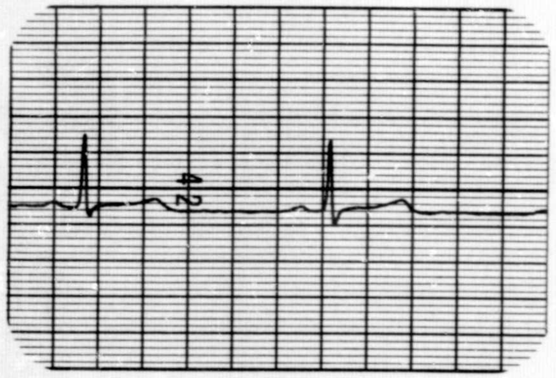	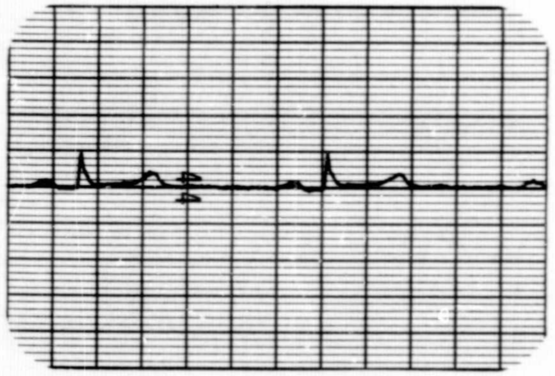	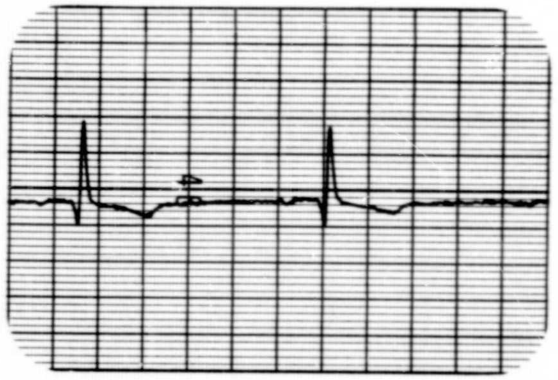
ETA (H) R = 68	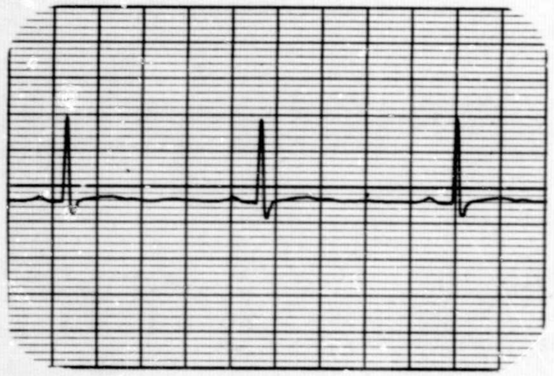	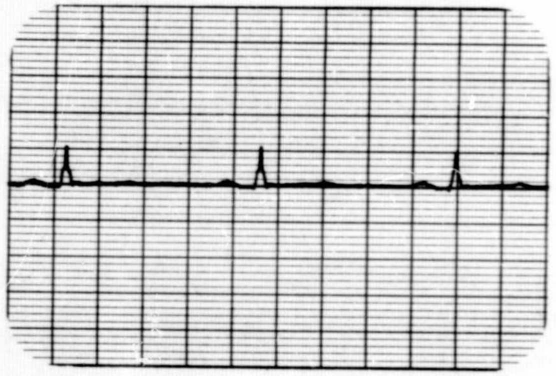	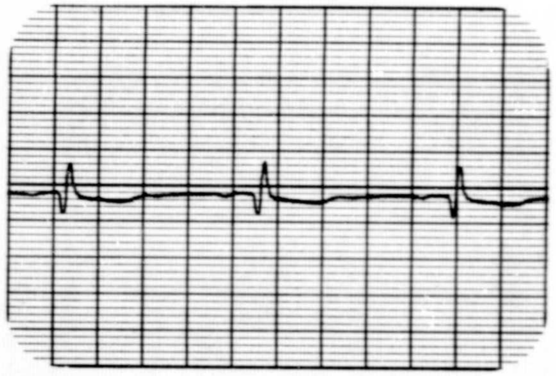
IOTA (I) R = 64	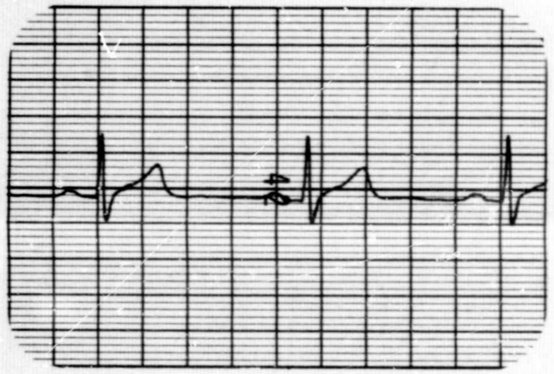	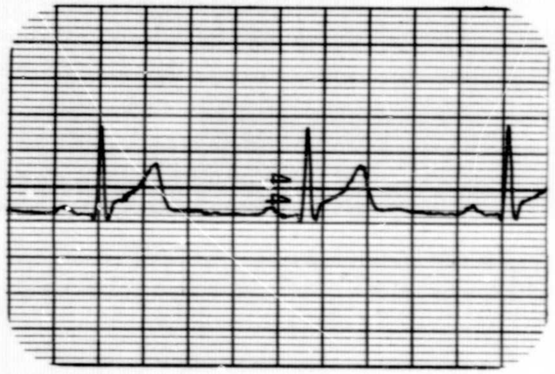	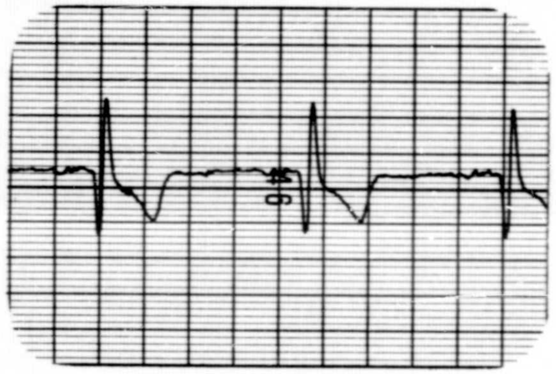
KAPPA (K) R = 86	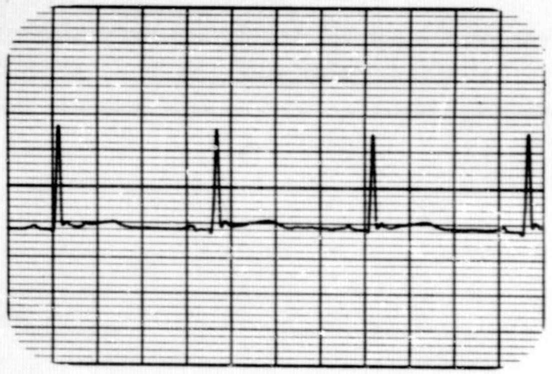	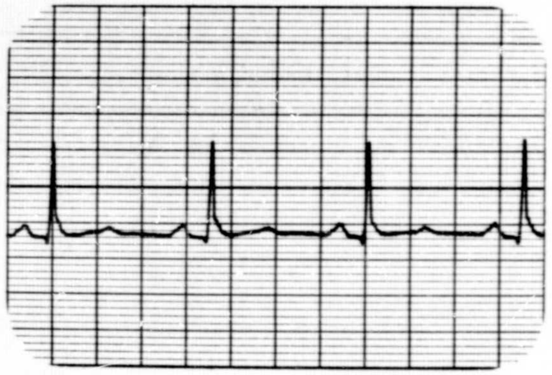	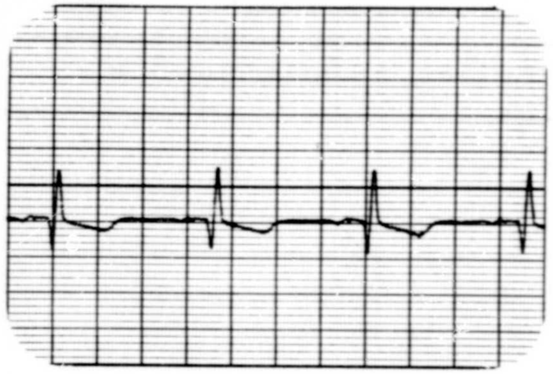

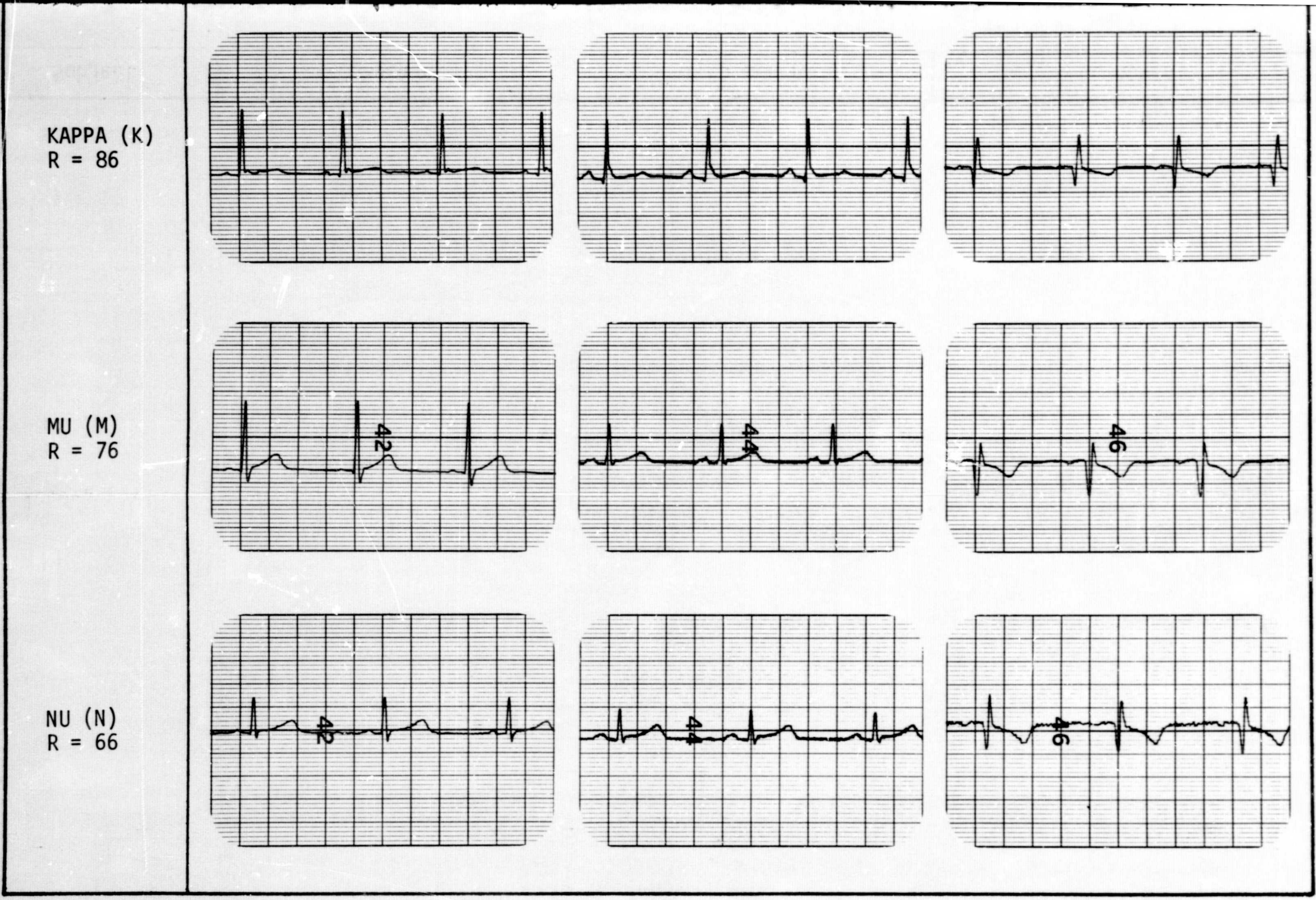

Figure 2-4. Activity Group III - Lower Body Negative Pressure at -40 mmHg (VCG)

16158-H019-R0-00

FOLDOUT FRAME 1

Subject	X-Component	Y-Component	Z-Component
IOTA (I) Erect R = 150	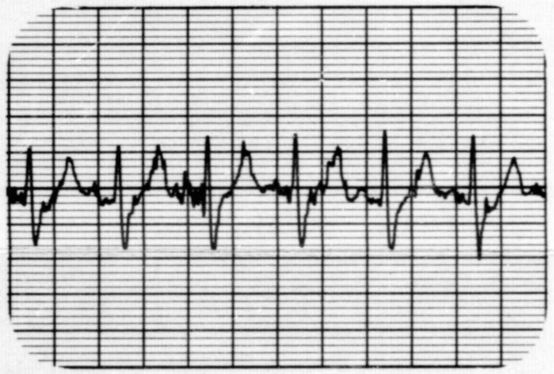	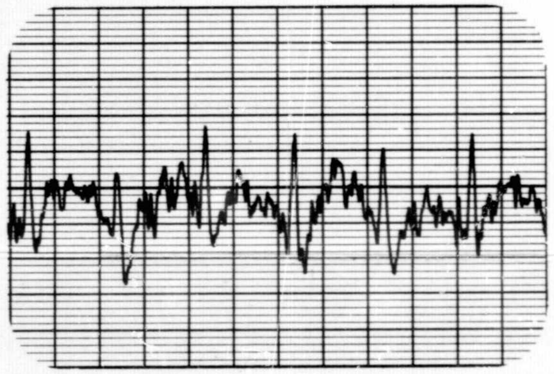	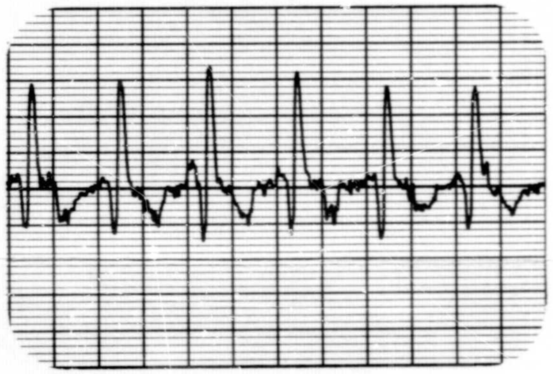
IOTA (I) Supine R = 135	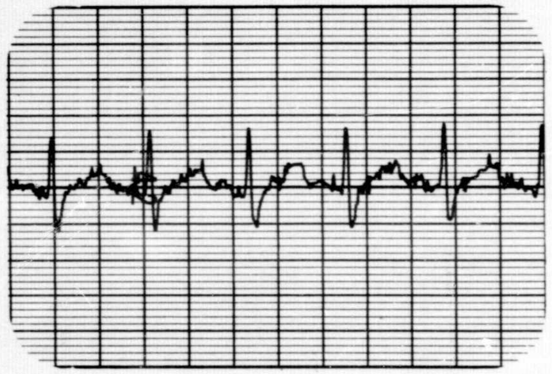	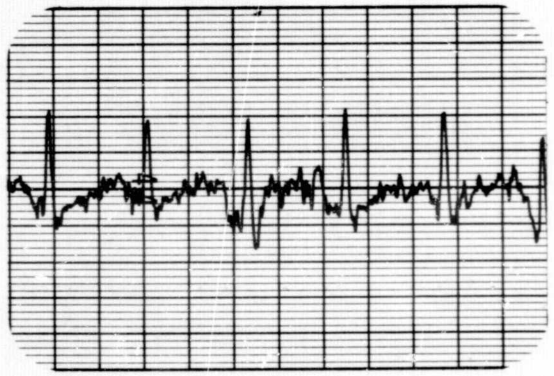	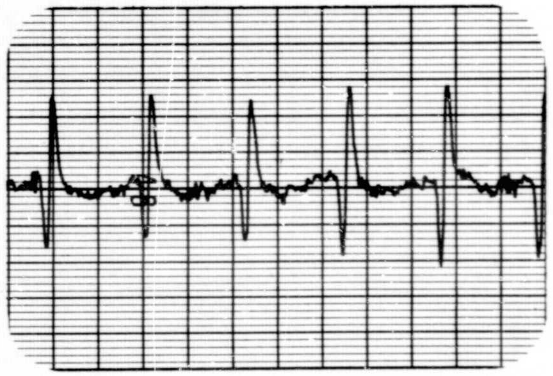

16158-H019-R0-00

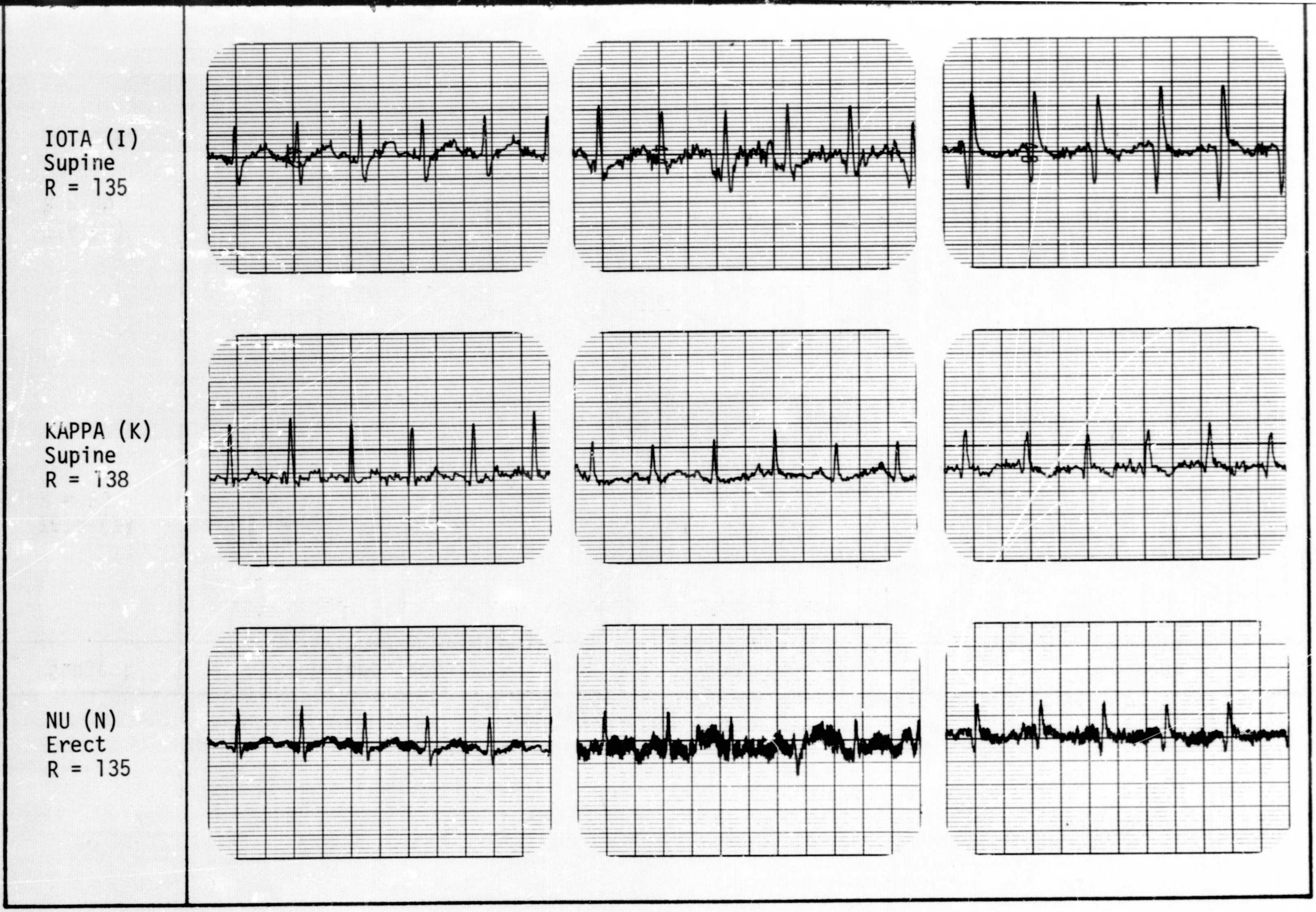

Figure 2-5. Activity Group IV - Erect and Supine Ergometer Tests (VCG)

Table 2-2. Definition of ECG/VCG Activity Groups

Activity Group	Subject	Test Condition	Signal Type	Heart Rate
I	Alpha (A)	Earth Orbit	ECG	71
	Beta (B)	Earth Orbit	ECG	94
	Epsilon (E)	Earth Orbit	ECG	82
II	Zeta (Z)	Recovery, LBNP	VCG	58
	Eta (H)	Control, LBNP	VCG	52
	Iota (I)	Control, LBNP	VCG	52
	Iota (I)	Recovery, Ergometer	VCG	84
	Kappa (K)	Recovery, LBNP	VCG	60
	Mu (M)	Control, LBNP	VCG	64
	Nu (N)	Control, Ergometer	VCG	52
III	Zeta (Z)	LBNP @ -40 mmHg	VCG	55
	Eta (H)	LBNP @ -40 mmHg	VCG	68
	Iota (I)	LBNP @ -40 mmHg	VCG	64
	Kappa (K)	LBNP @ -40 mmHg	VCG	86
	Mu (M)	LBNP @ -40 mmHg	VCG	76
	Nu (N)	LBNP @ -40 mmHg	VCG	66
IV	Iota (I)	Ergometer, Erect	VCG	150
	Iota (I)	Ergometer, Supine	VCG	135
	Kappa (K)	Ergometer, Supine	VCG	138
	Nu (N)	Ergometer, Erect	VCG	135

2.3.1 Test Group ECG/VCG Digitizing Philosophy

The analog ECG/VCG signals were converted to digital form for compatibility with digital computer input requirements. This preparation process is done by periodically sampling the analog ECG signal and converting the voltage levels into a binary word representation which is recorded on a computer compatible magnetic tape. The rate of data sampling is of primary importance. From a data systems point of view, the sampling rate must be four to five times the highest frequency content in the signal.

A digitizing rate of 500 samples per second (sps) was selected after considering many affirming factors.

a) Modern electrocardiographic equipments have frequency response capabilities in excess of 100 hertz. A 500 sps rate would allow a 100-125 hertz data response.

b) All the VCG data were acquired via modern VCG equipment. (The ECG acquired during manned space flight was limited to about 50 hertz.)

c) Many other works[8] have used 500 sps and therefore the study results would be comparable on that basis.

d) A growing community of researchers--in particularly Franke[3] and Langner[4]--feel that high frequency ECG components of clinical importance may exist in certain cases.

e) While automated ECG diagnostic capabilities are being developed by the use of digital computer programs, this study does not address that subject, per se. Although one-half of the 1000 sps rate recommended by the American Heart Association[13] and Pipberger[14] for ECG digital computer analysis, the 500 sps rate will yield an rss uncertainty of 2.83 ms in cardiac wave/complex determinations. Thus the 500 sps digitizing rate will provide a compromise and allow for possible future use of these tapes with digital, diagnostic computer programs.

2.4 TESTING AND ANALYSES

2.4.1 Test Bed Program (TBED)

A computer program for testing and analysis of the candidate algorithms was developed and designated TBED. The TBED program was written for the UNIVAC 1108 systems at the MSC computation and analysis center and is shown--in block diagram form--in Figure 2-6. Four subprograms were devised under the main driver program called TBED. Tantamount among TBED requirements was that the program must be able to receive data; compress data; transmit compressed data to the reconstructor; reconstruct the waveform; compare the reconstructed waveform to the original; generate and print out all the required statistical information; and finally, create a plot tape from which microfilm plots could be made.

The above program requirements were designed into TBED so that all functions could be executed in a single computer run which was of paramount importance in terms of the utilization efficiency of manpower and computer-time resources.

To present a general insight into TBED--particularly the statistics subprogram--a short explanation of each subprogram is included. Refer to Figure 2-6.

2.4.1.1 Data Compression Subprogram (COMP)

Two principal functions were accomplished by this first subprogram under the control of the TBED driver.

a) ECG/VCG input data were read from the input tapes, tagged for identification, and stored in an array.

b) The specific data compression algorithm under test resided in COMP and operated on all the ECG/VCG data from the input array transmitting the results on to the next subprogram.

2.4.1.2 Data Reconstruction Subprogram (RECON)

RECON also performed two principal functions under the control of the TBED driver.

a) RECON first acted as a data-with-tag receiver accepting the results from COMP.

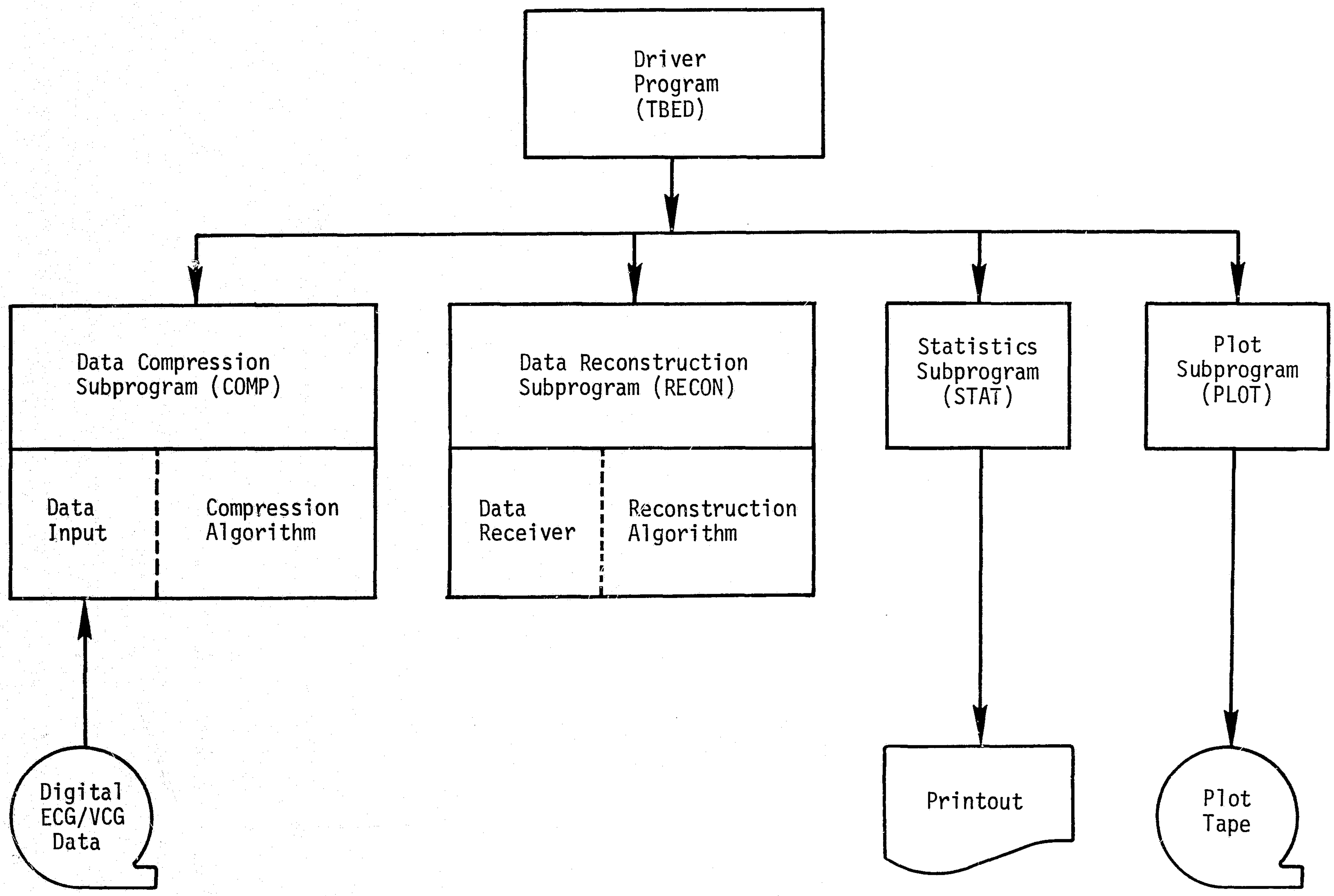

Figure 2-6. Test Bed Program Block Diagram

b) The data reconstruction algorithm under test resided in RECON and reconstructed the original ECG/VCG waveform using the COMP output as its basis. The reconstructed data points were also stored in an array similar to the original ECG/VCG data points. After reconstruction the statistics subprogram was ready to operate.

2.4.1.3 Statistics Subprogram (STAT)

Error analysis of the data compression/reconstruction testing activity was performed by STAT under control of the TBED driver. A total of 18 statistical parameters were computed by STAT of which less than one-half dealt directly with the data compression/reconstruction error analysis--hence STAT. Presented below is a synopsis of the STAT subprogram outputs.

a) Total Data Samples. This parameter identifies the total input ECG/VCG data samples that were processed by the data compression algorithm.

b) Total Compressed Samples. For later computations this total is acquired by noting the total data samples transmitted from the COMP algorithm to the RECON algorithm.

c) Data Compression Ratio (DCR). A measure of effectiveness of a compression algorithm is expressed by the following ratio:

$$DCR = \frac{\text{Total Data Samples}}{\text{Total Compressed Samples}}.$$

For example, if 2000 data samples (equal to four seconds of digital data) are compressed and 200 compressed samples are received by the RECON, then the DCR is:

$$DCR = \frac{2000}{200} = \frac{10}{1} = 10{:}1 = 10.$$

d) Data Word Length. The length of the information portion of the input ECG/VCG binary data word is used in (g) below.

e) Transmitted Word Length. Like (d) above this parameter is also used in (g) below.

f) Position Tag Word Length. If a compression algorithm removes redundant data samples, then the non-redundant transmitted data samples must be identified by an information tag to denote their time relationship to other non-redundant ECG/VCG data samples. This parameter is also used in (g) below.

g) Bandwidth Compression Ratio (BCR). The most comprehensive expression for the effectiveness of any data compression/reconstruction algorithm is a ratio stating how much bandwidth reduction has been accomplished. An examination of the total number of binary digits--or bits--will yield the desired results, for in PCM telemetry the bandwidth is a function of the bit rate rather than an analog frequency. Thus the BCR may be stated as:

$$BCR = \frac{N_o L_o}{N_c L_c + N_c L_t}$$

where N_o and N_c equal the number of original and compressed ECG/VCG data words; L_o and L_c are the length (number of bits) of each original and compressed data words; and L_t represents the number of bits that have to be added to identify the compressor output data samples.

Therefore the BCR equation yields a ratio of the number of original bits to the number of transmitted bits which is a ratio indicative of real applications and will always be $<$DCR.

h) Maximum Distortion. Distortion is defined in this study to be the difference--in millivolt (mv) amplitude--between a reconstructed data sample and its corresponding original data sample. Maximum distortion is the largest mv difference found in the entire set of data tested by a given algorithm.

i) Mean Distortion. The mean distortion is derived by the following:

$$M = \text{Mean distortion} = \frac{\sum_{1}^{N} d}{N}$$

N is the number of samples under test; and $d = (A_o - A_r)$, where A_o and A_r are the millivolt amplitudes of the original and reconstructed data samples.

j) rms Distortion. An rms distortion is computed by:

$$\text{rms distortion} = \sqrt{\frac{\sum_{1}^{N} d^2}{N}}$$

where d and N are defined above.

k) Standard Deviation (σ). An equation that shows the standard deviation of the reconstructed waveform from the original is given by:

$$\sigma = \sqrt{\frac{\sum_{1}^{N}(M-A_r)^2}{N}}$$

where A_r, M and N are defined above.

l) Minimum Amplitude. This parameter represents the most negative voltage magnitude of any data sample tested and was always within the QRS complex.

m) Mean Amplitude. Although not used in other computations this parameter states the mean of all data samples tested.

n) Maximum Amplitude. Also in the QRS complex, this value records the largest R-wave peak of any ECG/VCG waveform being tested.

o) rms Error. Error is defined in this study as the ratio of distortion to the QRS peak-to-peak (p-p) amplitude in percent, viz:

$$\text{rms error} = \frac{\text{rms distortion}}{\text{QRS p-p}} \times 100.$$

Peak-to-peak QRS amplitude is item (n)-(l) above and rms distortion is defined in (j).

p) Maximum Error. Like rms error, the maximum error states maximum distortion in terms of the percent of QRS p-p amplitude;

$$\text{maximum error} = \frac{\text{maximum distortion}}{\text{QRS p-p}} \times 100.$$

where maximum distortion is defined in (h) above.

q) Compression Time. An expression of the algorithm speed, this parameter recorded the total time for the compression algorithm to process the original data samples.

r) Reconstruction Time. In similar manner this parameter recorded the total time for the reconstruction algorithm to process the compressed data and result in the same number of data samples as the original waveform.

2.4.1.4 Plot Subprogram (PLOT)

Under TBED control an existing TRW plotting subprogram was utilized to write the necessary tape for the production of cathode ray tube (CRT) microfilm plots. These CRT plots are used later in this report to show the original and reconstructed ECG/VCG waveforms.

2.4.2 Fast Hadamard Transform (FHT) and Fast Fourier Transform (FFT) Algorithms Test Results

A mathematical description of each algorithm has been included in Appendix B.

2.4.2.1 Fast Hadamard Transform (FHT) Analysis

Because the FHT and FFT algorithm operations are similar in nature, their test results have been combined into a single presentation in Figure 2-7. Reconstruction rms errors versus subjects by activity groups are shown in Figure 2-7 for an FHT mean DCR/BCR = 4.0/2.3. All tests were conducted utilizing a four-second section of subject data.

Experimentation with the FHT revealed that when using the zonal filtering techniques--explained in Appendix B--to achieve a DCR of 8.0 and larger, a "stairstep" ECG/VCG waveform representation of the various cardiac complexes could be observed. Therefore, a smaller FHT DCR of 4.0 was chosen for these studies. Figure 2-7 shows the rms errors to consistently fall between two and three percent except for subject III Eta and subject IV Nu. These anomalies were created by two different factors. Subject Eta's original VCG analog tape signals were very small (approximately 0.1 to 0.3 mv p-p) compared to a more nominal value of about one millivolt. Therefore, since rms errors are expressed relative to the p-p QRS amplitude, the apparent rms error will seem to be 3 to 10 times others in the same group.

Subject IV Nu had a nominal QRS amplitude; however, this subject's signals possess considerable instrumentation noise (not to be confused with the normal muscle noise artifacts) as can readily be varified in Figure 2-5. Both subjects II and III Eta and IV Nu will be penalized in all study test results for these two systematic factors.

Listed below are the group rms errors for the FHT as computed from Figure 2-7. Because subject Eta will not produce meaningful results in subsequent algorithms, two sets of data are presented to allow better correlation of these results with other algorithm results.

Activity Group	Group Mean (%)	Group - Eta Mean (%)
I	2.3	- -
II	2.7	3.2
III	3.7	2.7
IV	4.0	- -

Two VCG plots for the FHT are presented on pages 25 and 26 along with complete substantiating statistical data.

2.4.2.2 Fast Fourier Transform (FFT) Analysis

Two sets of FFT results at a mean DCR = 8.0/4.5 and a mean DCR = 32.0/17.9 are presented in Figure 2-7. Tests of the FFT were also conducted utilizing a four-second section of subject data.

Similar experimentation with the FFT zonal filtering (see Appendix B) revealed an acceptable reconstructed waveform could be achieved up to a maximum DCR = 8.0. Increased zonal filtering to produce a large DCR = 32.0 revealed that the desirable effects of filtering--or smoothing--intrinsic in the FFT caused substantial QRS amplitude degradation and other distortions which are easily seen on pages 27 and 28. A worst case in the form of subject IV Nu is shown on page 29 for the FFT at DCR = 8.0 and the resulting reconstructed waveform appears to be admirably improved while still maintaining proper cardiac wave amplitudes and durations.

Listed below are the mean group rms errors for the two sets of FFT test results computed from Figure 2-7. Subject Eta has similarly been removed in one column.

Activity Group	FFT DCR	Group Mean (%)	Group - Eta Mean (%)
I	8.0	0.8	- -
	32.0	5.2	- -
II	8.0	1.7	2.0
	32.0	5.1	5.4
III	8.0	2.3	1.5
	32.0	6.2	6.0
IV	8.0	2.8	- -
	32.0	7.6	- -

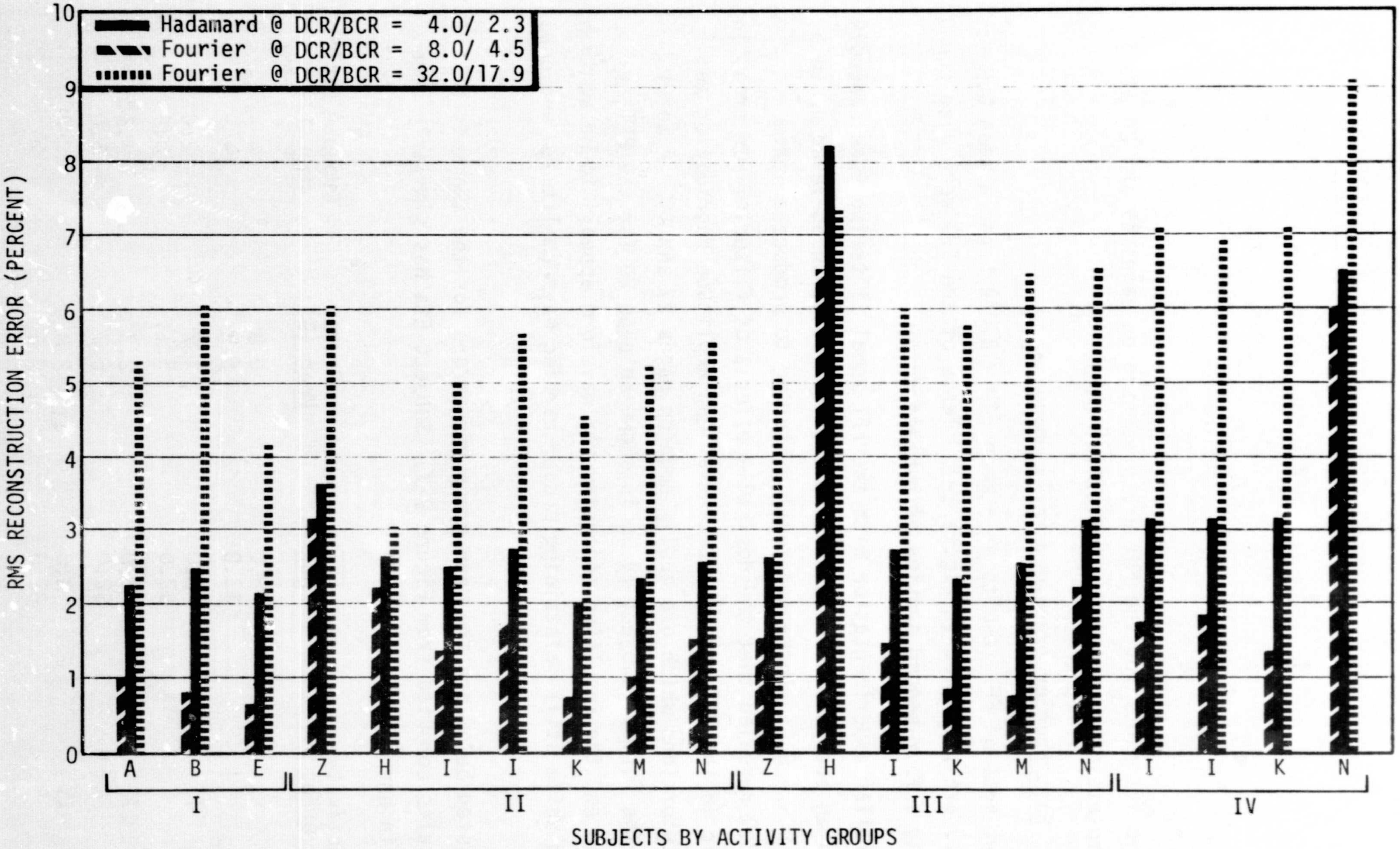

Figure 2-7. Test Results for the FHT and FFT Algorithms

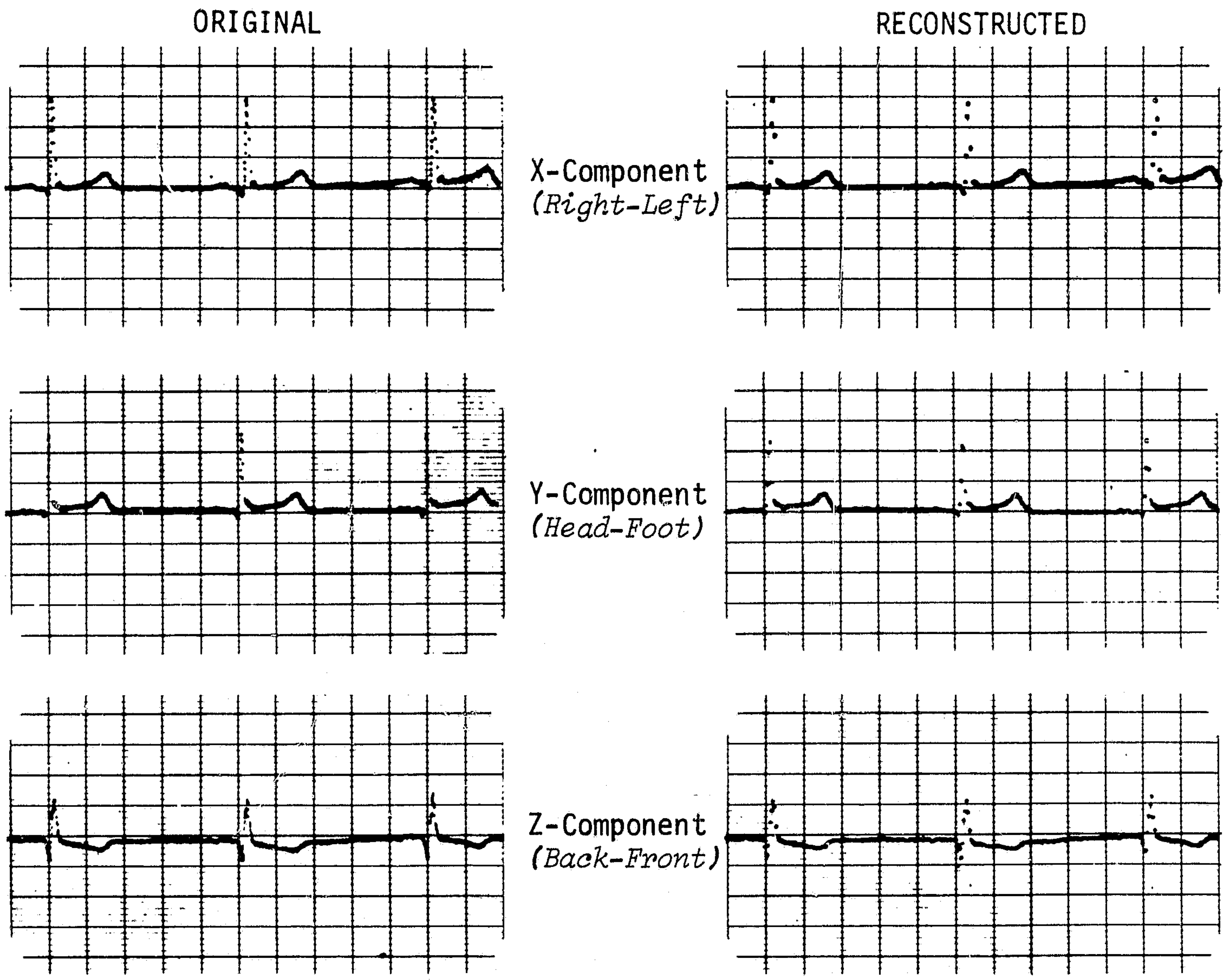

STUDY INPUT DATA DESCRIPTION

ACTIVITY GROUP:

I □ *II* ■ *III* □ *IV* □

SUBJECT IDENTIFICATION: Kappa

SUBJECT TEST CONDITION:

0-g □ *Orbit* □ *Control/Recovery* ■

1-g ■ *Ergometer* □ *LBNP @ -40 mmHg* □

CARDIOGRAM CHARACTERISTICS:

VCG ■ *ECG* □ *Heart Rate* 60

QRS Amplitude (mv p-p): *Upper* 1.46 *Middle* 1.22 *Lower* 0.89

DATA COMPRESSION/RECONSTRUCTION RESULTS
(VCG Component Mean)

ALGORITHM:

Fast-Fourier □ *Cycle-to-Cycle* □

Fast-Hadamard ■ *FFC2C* □

PAC □

COMPRESSION RATIOS:

Data (DCR) 4.0

Bandwidth (BCR) 2.1

DISTORTION (mv):

Maximum 0.0233 *Average* 0.0019 σ 0.0236

ERROR (%):

Maximum 19.3 *rms* 2.0

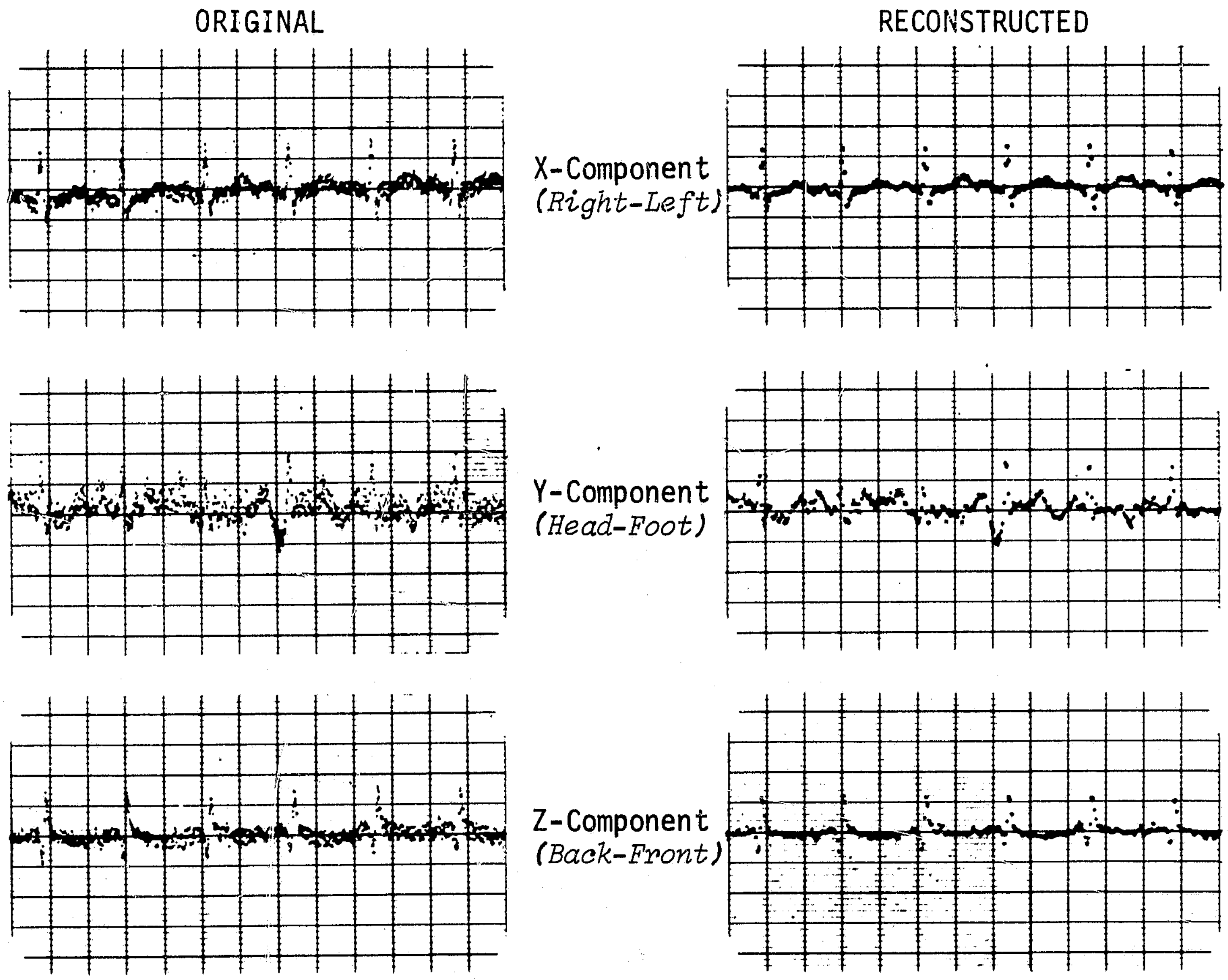

STUDY INPUT DATA DESCRIPTION

ACTIVITY GROUP:

I ☐ *II* ☐ *III* ☐ *IV* ■

SUBJECT IDENTIFICATION: Nu

SUBJECT TEST CONDITION:

0-g ☐ *Orbit* ☐ *Control/Recovery* ☐

1-g ■ *Ergometer* ■ *LBNP @ -40 mmHg* ☐

CARDIOGRAM CHARACTERISTICS:

VCG ■ *ECG* ☐ *Heart Rate* 136

QRS Amplitude (mv p-p): *Upper* 1.04 *Middle* 1.30 *Lower* 0.99

DATA COMPRESSION/RECONSTRUCTION RESULTS
(VCG Component Mean)

ALGORITHM:

Fast-Fourier ☐ *Cycle-to-Cycle* ☐

Fast-Hadamard ■ *FFC2C* ☐

PAC ☐

COMPRESSION RATIOS:

Data (DCR) 4.0

Bandwidth (BCR) 2.1

DISTORTION (mv):

Maximum 0.263 *Average* 0.0001 σ 0.073

ERROR (%):

Maximum 23.9 *rms* 6.5

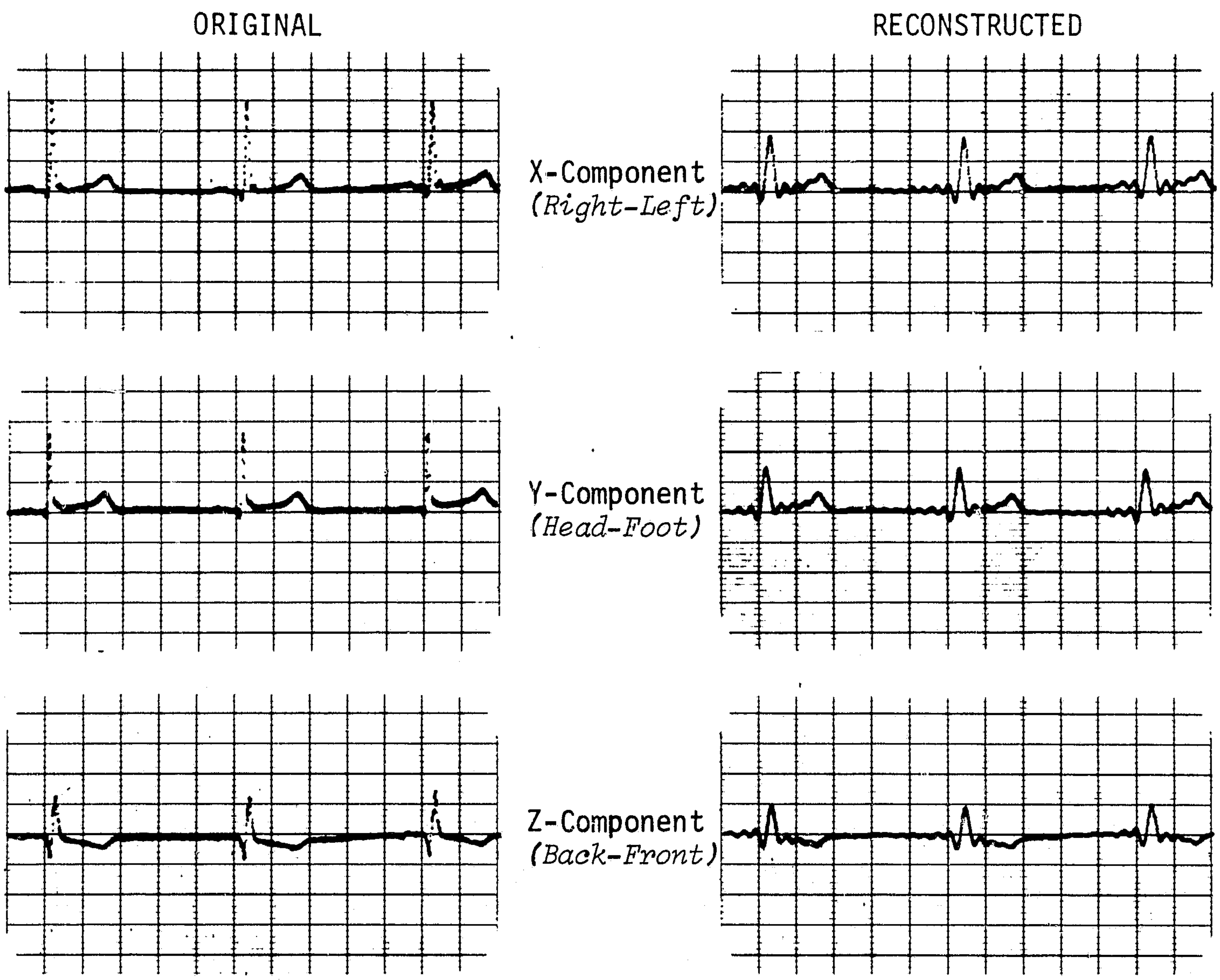

STUDY INPUT DATA DESCRIPTION

ACTIVITY GROUP:

I ☐ *II* ■ *III* ☐ *IV* ☐

SUBJECT IDENTIFICATION: Kappa

SUBJECT TEST CONDITION:

0-g ☐ *Orbit* ☐ *Control/Recovery* ■

1-g ■ *Ergometer* ☐ *LBNP @ -40 mmHg* ☐

CARDIOGRAM CHARACTERISTICS:

VCG ■ *ECG* ☐ *Heart Rate* 60

QRS Amplitude (mv p-p): *Upper* 1.46 *Middle* 1.22 *Lower* 0.89

DATA COMPRESSION/RECONSTRUCTION RESULTS
(VCG Component Mean)

ALGORITHM:

Fast-Fourier ■ *Cycle-to-Cycle* ☐

Fast-Hadamard ☐ *FFC2C* ☐

PAC ☐

COMPRESSION RATIOS:

Data (DCR) 32.0

Bandwidth (BCR) 10.7

DISTORTION (mv):

Maximum 0.0391 *Average* 0.0 σ 0.0556

ERROR (%):

Maximum 31.9 *rms* 4.59

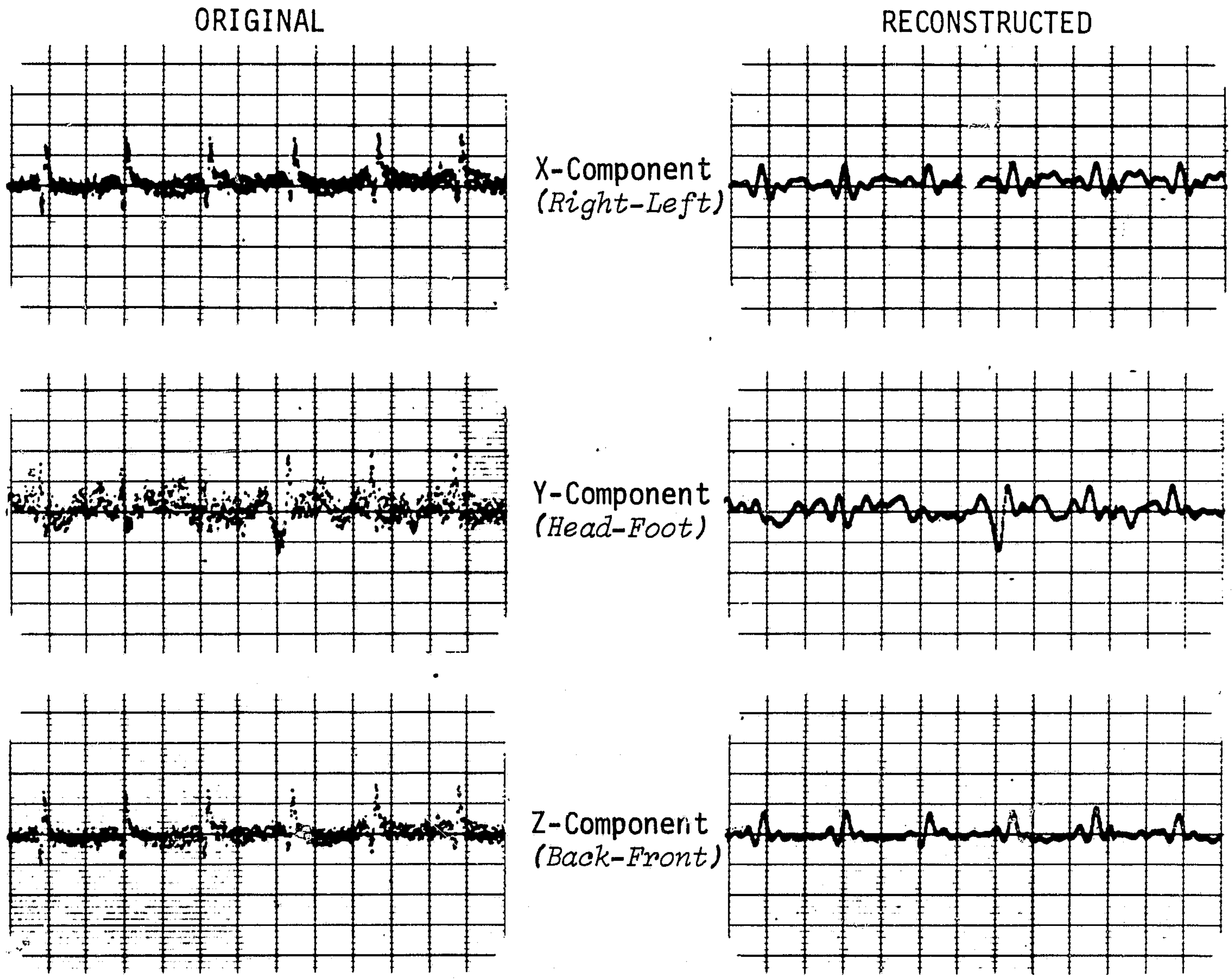

STUDY INPUT DATA DESCRIPTION

ACTIVITY GROUP:

I ☐ *II* ☐ *III* ☐ *IV* ■

SUBJECT IDENTIFICATION:	SUBJECT TEST CONDITION:		
Nu	*0-g* ☐	*Orbit* ☐	*Control/Recovery* ☐
	1-g ■	*Ergometer* ■	*LBNP @ -40 mmHg* ☐

CARDIOGRAM CHARACTERISTICS:

VCG ■ *ECG* ☐ *Heart Rate* 136 — *QRS Amplitude (mv p-p)*: *Upper* 1.04 *Middle* 1.30 *Lower* 0.99

DATA COMPRESSION/RECONSTRUCTION RESULTS
(VCG Component Mean)

ALGORITHM:		COMPRESSION RATIOS:	
Fast-Fourier ■	*Cycle-to-Cycle* ☐	*Data (DCR)*	32.0
Fast-Hadamard ☐	*FFC2C* ☐	*Bandwidth (BCR)*	19.7
PAC ☐			

DISTORTION (mv):			ERROR (%):	
Maximum 0.414	*Average* 0.0	σ 0.102	*Maximum* 37.5	*rms* 9.19

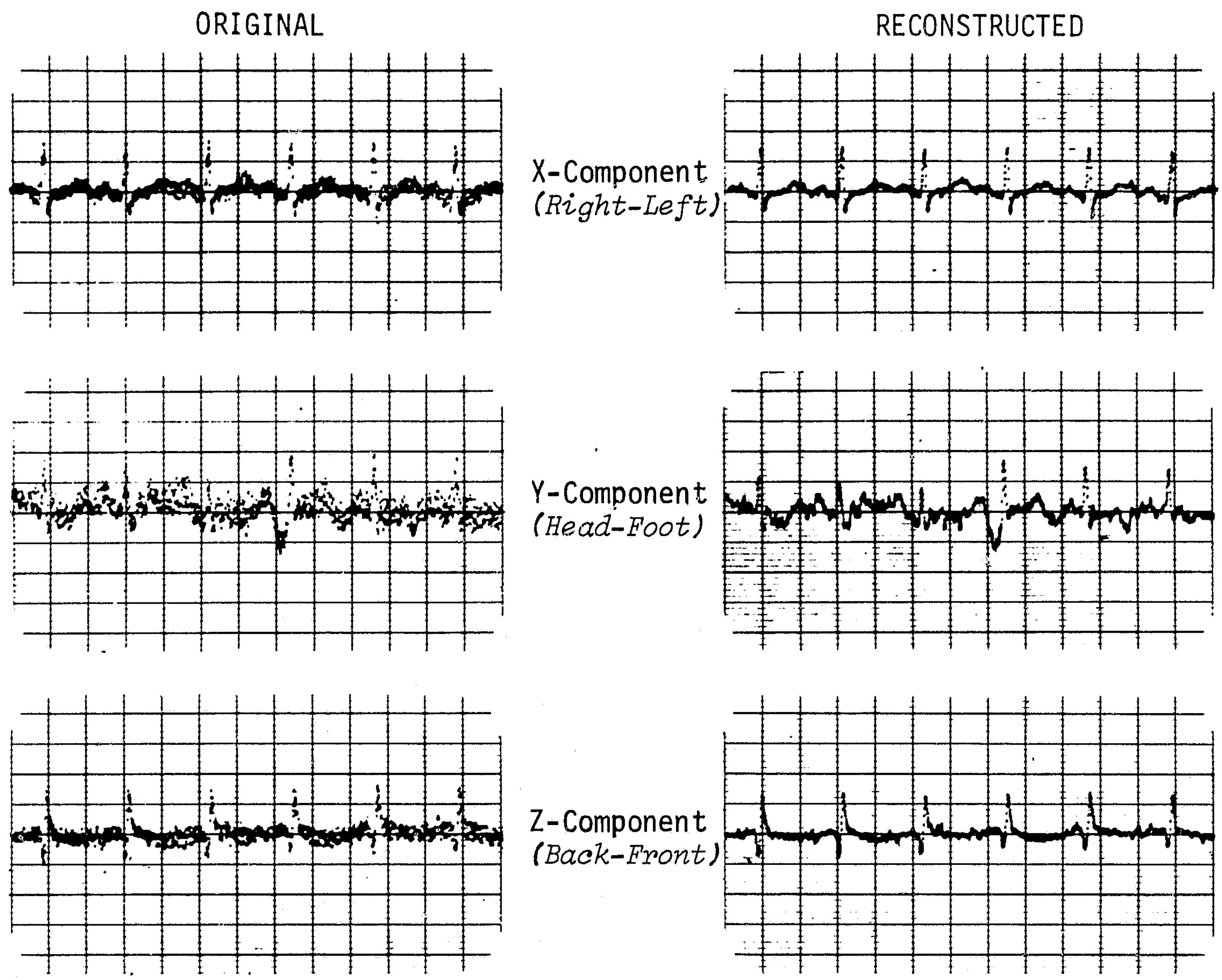

STUDY INPUT DATA DESCRIPTION

ACTIVITY GROUP:

I ☐ *II* ☐ *III* ☐ *IV* ■

SUBJECT IDENTIFICATION: Nu

SUBJECT TEST CONDITION:

0-g ☐ *Orbit* ☐ *Control/Recovery* ☐

1-g ■ *Ergometer* ■ *LBNP @ -40 mmHg* ☐

CARDIOGRAM CHARACTERISTICS:

VCG ■ *ECG* ☐ *Heart Rate* 136

QRS Amplitude (mv p-p): *Upper* 1.04 *Middle* 1.30 *Lower* 0.99

DATA COMPRESSION/RECONSTRUCTION RESULTS
(VCG Component Mean)

ALGORITHM:

Fast-Fourier ■ *Cycle-to-Cycle* ☐

Fast-Hadamard ☐ *FFC2C* ☐

PAC ☐

COMPRESSION RATIOS:

Data (DCR) 8.0

Bandwidth (BCR) 4.9

DISTORTION (mv):

Maximum 0.187 *Average* 0.00 σ 0.068

ERROR (%):

Maximum 16.8 *rms* 6.0

2.4.2.3 Algorithm Speed

Both the FHT and FFT algorithms are capable of operating in real time while receiving input ECG/VCG data at 500 sps. Listed below are the percents of time utilized by each algorithm to compress and reconstruct a four-second slice of real ECG/VCG data; i.e., if two seconds were required to compress four seconds (2000 samples) of data, the indication would be 50% which would show the algorithm is working only one-half of the time.

Algorithm	Percent of Real Time Required	
	Compression	Reconstruction
FHT	53	53
FFT	55	55

2.4.3 Parallel Adaptive Composite (PAC) Algorithm Test Results

A mathematical description of the PAC algorithm has been included in Appendix B.

2.4.3.1 Analysis

Table 2-3 lists the results of testing the PAC algorithm with all subjects using three different aperture (tolerance) combinations. As explained in Appendix B, each subalgorithm (ZOP-FA and FOI-Fan) has an aperture that decides if a data sample is redundant or non-redundant.

Analysis of the PAC operation--confirmed through testing of the PAC at various aperture combinations--substantiated that an excellent cross-section of the PAC capability would be displayed by the three aperture combinations shown in Table 2-3, viz: both subalgorithm (Z and F) apertures at one millivolt; both apertures at three millivolts; and the third combination where Z = 5 mv and F = 3 mv.

Reviewing the numerical results compiled in Table 2-3 shows an encouraging range of data compression/reconstruction effectiveness. For groups II, III and IV, only the mean result of all three VCG components is shown for each subject.

Subalgorithm Apertures	Test Result Ranges DCR	BCR	RMS Error (%)
Z1-F1	1.3- 5.6	0.5- 2.2	0.30-0.89
Z3-F3	1.7-19.1	0.7- 8.0	1.08-2.24
Z5-F3	1.9-26.6	0.8-11.3	1.60-3.38

Again, the effects of subject Eta have been removed because the PAC could not process such a small p-p QRS amplitude for two out of three aperture combinations. Subject IV Nu, because of its aforementioned noise, has put an unsatisfactory lower bound on the BCR as shown above. A BCR<1 naturally means more bits are generated by the PAC algorithm than are inputed--a most undesirable data compression demonstration. However, assuming that such a noise problem would not be acceptable for manned space flight, Table 2-3 shows that BCR>1 for all subjects of Z3-F3 and Z5-F3 apertures except subject IV Nu. A re-evaluation of the PAC algorithm software design has shown that a 25 percent increase in BCR can be easily achieved if a slightly different philosophy is applied to the outputted identification tag attached to each non-redundant data sample.

Although the Z1-F1 aperture produced very small rms errors, it unfortunately was too small an aperture for practical use causing BCR<1 for about one-third of the subjects.

A unique result of testing the PAC algorithm was the simultaneous determination of the relative data compressing effectiveness of both the ZOP-FA and FOI-Fan subalgorithms. Since by definition, the PAC utilizes both subalgorithms in parallel and outputs the results of the better compressing subalgorithm, one subalgorithm would have completely suppressed the other had it been the better. However, the test results indicated each subalgorithm performed where it was best suited. Therefore neither subalgorithm can be said to work well with all of a cardiac complex; but the two operating together produce a resulting DCR/BCR and waveform fidelity better than either could do separately.

Ten PAC plots from selected subjects at different algorithm apertures are included to allow visual correlation of the reconstructed waveforms with the data in Table 2-3. The included plots were selected to give a good overview of the demonstrated PAC algorithm statistics using real ECG/VCG data.

Table 2-3. PAC Algorithm Test Results for Three Different Apertures

Activity Group	Subject	Test Condition	Test Results by PAC Apertures Z1-F1/Z3-F3/Z5-F3 Millivolts					
			Compression Ratios		Distortion (mv)		Error (%)	
			Data	Bandwidth	RMS	Maximum	RMS	Maximum
I	ALPHA	Orbit	3.2/ 7.3/12.3	1.3/2.9/ 4.9	0.0059/0.0154/0.0241	0.01/0.03/0.05	0.50/1.31/2.04	0.85/2.54/4.24
(ECG)	BETA	Orbit	4.4/11.8/18.0	1.8/4.7/ 7.2	0.0062/0.0153/0.0230	0.01/0.03/0.05	0.65/1.62/2.47	1.06/3.19/5.32
	EPSILON	Orbit	5.6/15.2/26.6	2.2/6.1/10.6	0.0062/0.0157/0.0237	0.01/0.03/0.05	0.89/2.24/3.38	1.43/4.29/7.14
	Group I Means		4.4/11.4/19.0	1.8/4.6/ 7.6	0.0061/0.0155/0.0237	0.01/0.03/0.05	0.68/1.72/2.63	1.11/3.34/5.57
II	ZETA	Recovery (LBNP)	1.5/ 2.5/ 4.1	0.6/1.0/ 1.6	0.0044/0.0145/0.0232	0.01/0.03/0.05	0.38/1.29/2.08	0.89/2.69/4.49
(VCG)	ETA	Control	16.1/ * / *	6.4/ * / *	0.0068/ * / *	0.01/ * / *	2.37/ * / *	3.52/ * / *
	IOTA	Control	2.5/ 8.9/20.4	1.0/3.6/ 8.2	0.0058/0.0156/0.0220	0.01/0.03/0.05	0.78/2.08/2.91	1.33/3.98/6.63
	IOTA	Recovery (Ergometer)	2.5/ 8.1/15.9	1.0/3.2/ 6.4	0.0058/0.0153/0.0222	0.01/0.03/0.05	0.67/1.78/2.58	1.16/3.49/5.82
	KAPPA	Recovery (LBNP)	3.5/20.0/28.3	1.4/8.0/11.3	0.0064/0.0136/0.0218	0.01/0.03/0.05	0.55/1.21/1.93	0.87/2.63/4.38
	MU	Control	2.9/12.4/19.7	1.2/5.0/ 7.9	0.0061/0.0152/0.0229	0.01/0.03/0.05	0.54/1.37/2.05	0.90/2.68/4.47
	NU	Control	2.3/10.8/23.0	0.9/4.3/ 9.2	0.0057/0.0156/0.0227	0.01/0.03/0.05	0.69/1.88/2.14	1.20/3.60/6.00
	Group II Means		4.5/10.5/18.6	1.8/4.2/ 7.4	0.0059/0.0150/0.0225	0.01/0.03/0.05	0.85/1.60/2.28	1.41/3.18/5.30
III	ZETA	LBNP @-40 mmHg	1.9/ 4.7/11.3	0.8/1.9/ 4.5	0.0052/0.0156/0.0243	0.01/0.03/0.05	0.50/1.51/2.36	0.97/2.93/4.87
(VCG)	ETA	LBNP @-40 mmHg	13.7/ * / *	5.5/ * / *	0.0068/ * / *	0.01/ * / *	7.29/ * / *	10.87/ * / *
	IOTA	LBNP @-40 mmHg	2.5/ 9.0/20.1	1.0/3.6/ 8.0	0.0057/0.0156/0.0228	0.01/0.03/0.05	0.78/2.14/3.11	1.36/4.09/6.81
	KAPPA	LBNP @-40 mmHg	3.8/19.1/26.4	1.5/7.6/10.6	0.0063/0.0135/0.0218	0.01/0.03/0.05	0.60/1.29/2.08	0.95/2.86/4.76
	MU	LBNP @-40 mmHg	2.6/10.7/15.3	1.0/4.3/ 6.1	0.0060/0.0149/0.0219	0.01/0.03/0.05	0.44/1.09/1.60	0.73/2.19/3.66
	NU	LBNP @-40 mmHg	2.1/ 5.7/12.2	0.8/2.3/ 4.9	0.0054/0.0158/0.0238	0.01/0.03/0.05	0.64/1.88/2.84	1.19/3.56/5.93
	Group III Means		4.4/ 9.8/17.1	1.8/3.9/ 6.8	0.0059/0.0151/0.0229	0.01/0.03/0.05	1.71/1.58/2.40	2.68/3.13/5.21
IV	IOTA	Ergometer (Erect)	2.1/ 4.8/ 6.9	0.8/1.9/ 2.8	0.0054/0.0153/0.0228	0.01/0.03/0.05	0.53/1.48/2.21	0.96/2.89/4.83
(VCG)	IOTA	Ergometer (Supine)	2.2/ 4.8/ 7.4	0.9/1.9/ 3.0	0.0053/0.0153/0.0232	0.01/0.03/0.05	0.56/1.60/2.42	1.04/3.13/5.22
	KAPPA	Ergometer (Supine)	2.5/ 5.8/ 8.4	1.0/2.3/ 3.4	0.0057/0.0152/0.0225	0.01/0.03/0.05	0.58/1.54/2.29	1.01/3.04/5.06
	NU	Ergometer (Erect)	1.3/ 1.7/ 1.9	0.5/0.7/ 0.8	0.0032/0.0117/0.0186	0.01/0.03/0.05	0.30/1.08/1.71	0.91/2.74/4.57
	Group IV Means		2.0/ 4.3/ 6.2	0.8/1.7/ 2.5	0.0049/0.0144/0.0218	0.01/0.03/0.05	0.49/1.43/2.16	0.98/2.95/4.92

* Data are meaningless due to abnormally small signal amplitude versus aperture size.

ORIGINAL

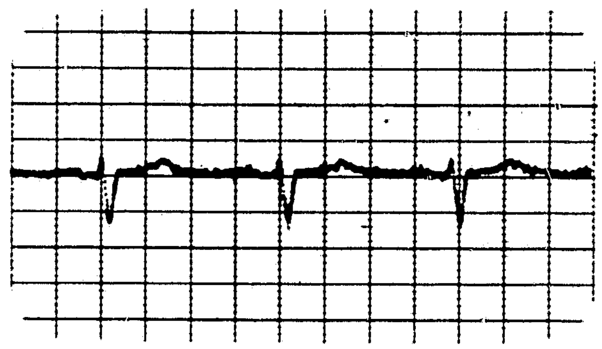

RECONSTRUCTED

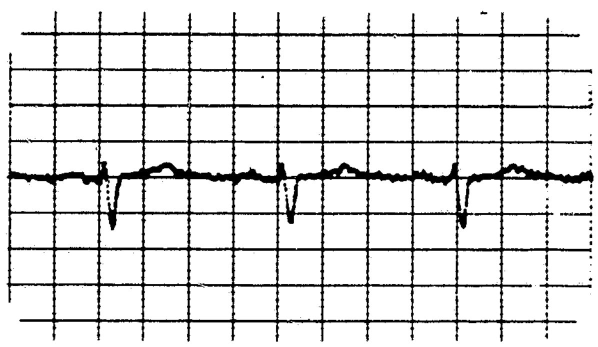

STUDY INPUT DATA DESCRIPTION

ACTIVITY GROUP:

I ■ *II* ☐ *III* ☐ *IV* ☐

SUBJECT IDENTIFICATION:	SUBJECT TEST CONDITION:		
Epsilon	*0-g* ■	*Orbit* ■	*Control/Recovery* ☐
	1-g ☐	*Ergometer* ☐	*LBNP @ -40 mmHg* ☐

CARDIOGRAM CHARACTERISTICS:

VCG ☐ *ECG* ■ *Heart Rate* 75 — *QRS Amplitude (mv p-p)*: *Upper* 0.70 *Middle* -- *Lower* 0.70

DATA COMPRESSION/RECONSTRUCTION RESULTS

ALGORITHM:		COMPRESSION RATIOS:	
Fast-Fourier ☐	*Cycle-to-Cycle* ☐	*Data (DCR)*	5.6
Fast-Hadamard ☐	*FFC2C* ☐	*Bandwidth (BCR)*	2.2
PAC Z1/F1 Apertures ■			

DISTORTION (mv):

Maximum 0.01 *Average* 0.0002 σ 0.0062

ERROR (%):

Maximum 1.43 *rms* 0.89

ORIGINAL

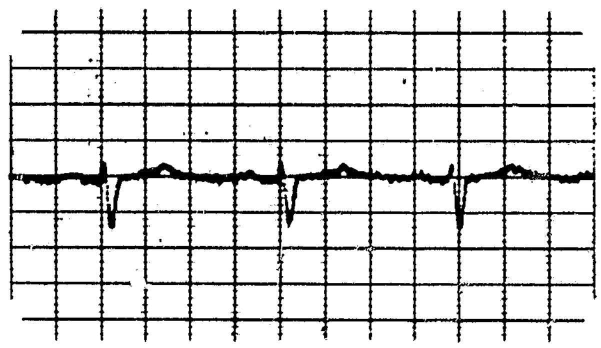

RECONSTRUCTED

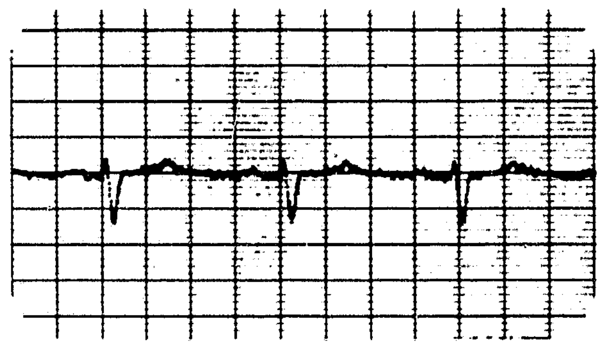

STUDY INPUT DATA DESCRIPTION

ACTIVITY GROUP:

I ■ *II* □ *III* □ *IV* □

SUBJECT IDENTIFICATION:	SUBJECT TEST CONDITION:					
Epsilon	*0-g*	■	*Orbit*	■	*Control/Recovery*	□
	1-g	□	*Ergometer*	□	*LBNP @ -40 mmHg*	□

CARDIOGRAM CHARACTERISTICS:

VCG □ *ECG* ■ *Heart Rate* 75

QRS Amplitude (mv p-p): *Upper* 0.70 *Middle* --- *Lower* 0.70

DATA COMPRESSION/RECONSTRUCTION RESULTS

ALGORITHM:				COMPRESSION RATIOS:	
Fast-Fourier	□	*Cycle-to-Cycle*	□	*Data (DCR)*	26.6
Fast-Hadamard	□	*FFC2C*	□	*Bandwidth (BCR)*	10.6
PAC Z5/F3 Apertures	■				

DISTORTION (mv):

Maximum 0.05 *Average* 0.0013 σ 0.0237

ERROR (%):

Maximum 7.14 *rms* 3.36

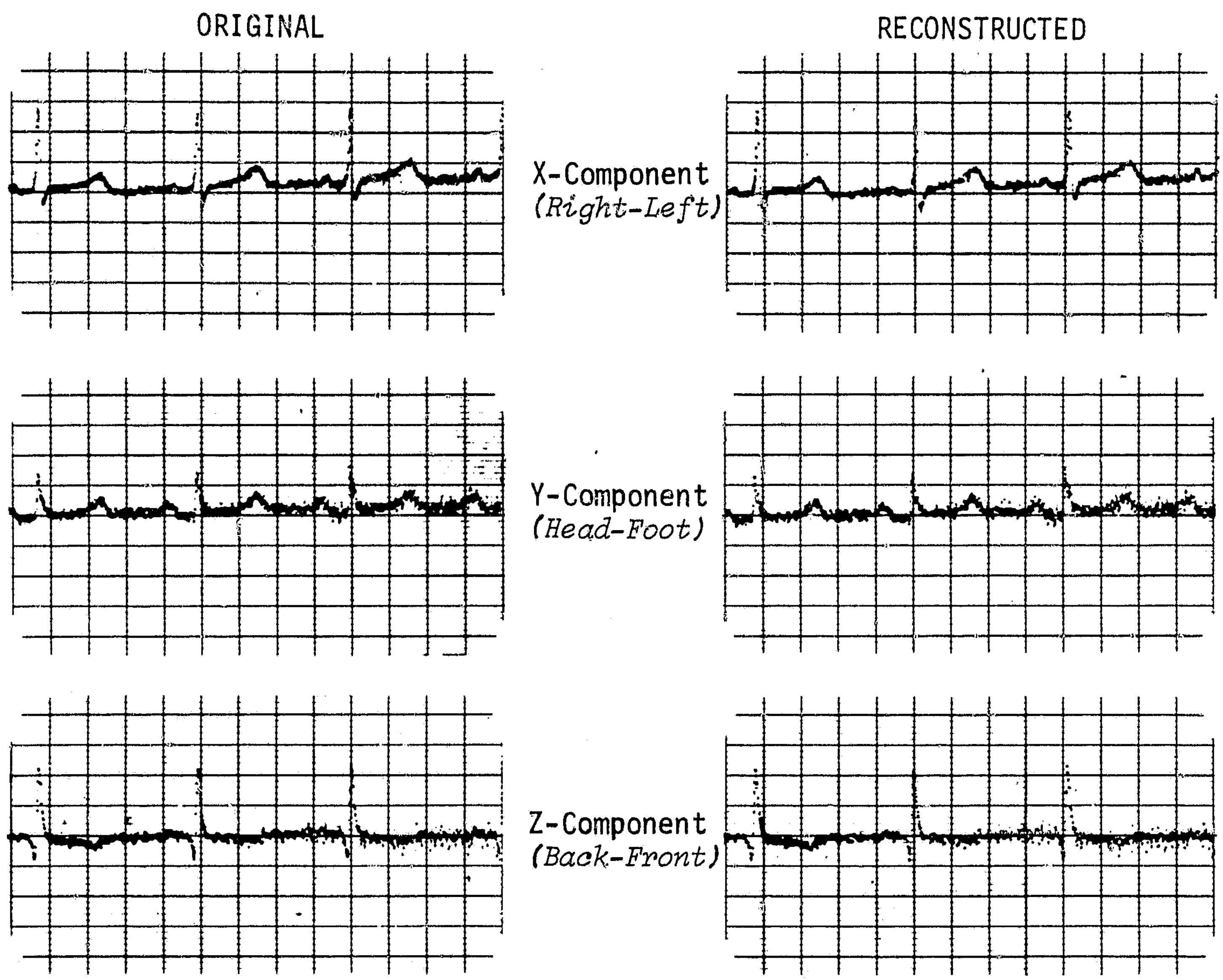

STUDY INPUT DATA DESCRIPTION

ACTIVITY GROUP:

I ☐ *II* ■ *III* ☐ *IV* ☐

SUBJECT IDENTIFICATION: Zeta

SUBJECT TEST CONDITION:

0-g ☐ *Orbit* ☐ *Control/Recovery* ■

1-g ■ *Ergometer* ☐ *LBNP @ -40 mmHg* ☐

CARDIOGRAM CHARACTERISTICS:

VCG ■ *ECG* ☐ *Heart Rate* 72

QRS Amplitude (mv p-p): *Upper* 1.41 *Middle* 0.78 *Lower* 1.43

DATA COMPRESSION/RECONSTRUCTION RESULTS
(VCG Component Mean)

ALGORITHM:

Fast-Fourier ☐ *Cycle-to-Cycle* ☐

Fast-Hadamard ☐ *FFC2C* ☐

PAC Z1/F1 Apertures ■

COMPRESSION RATIOS:

Data (DCR) 1.5

Bandwidth (BCR) 0.6

DISTORTION (mv):

Maximum 0.01 *Average* -0.0002 σ 0.0044

ERROR (%):

Maximum 0.89 *rms* 0.38

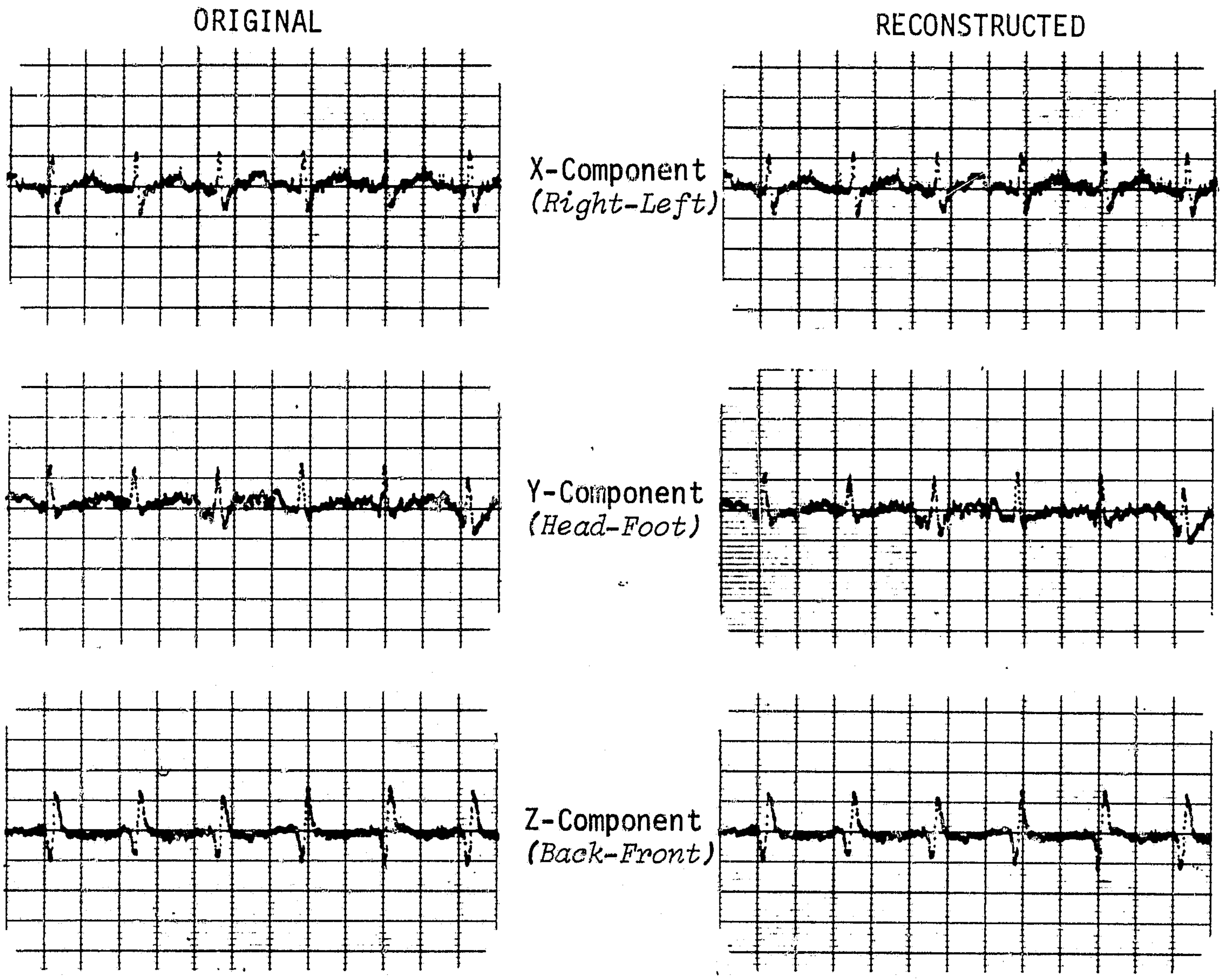

STUDY INPUT DATA DESCRIPTION

ACTIVITY GROUP:

I ☐ *II* ☐ *III* ☐ *IV* ■

SUBJECT IDENTIFICATION: Iota

SUBJECT TEST CONDITION:

0-g ☐ *Orbit* ☐ *Control/Recovery* ☐

1-g ■ *Ergometer* ■ *LBNP @ -40 mmHg* ☐

CARDIOGRAM CHARACTERISTICS:

VCG ■ *ECG* ☐ *Heart Rate* 135

QRS Amplitude (mv p-p): *Upper* 0.88 *Middle* 0.96 *Lower* 1.05

DATA COMPRESSION/RECONSTRUCTION RESULTS
(VCG Component Mean)

ALGORITHM:

Fast-Fourier ☐ *Cycle-to-Cycle* ☐

Fast-Hadamard ☐ *FFC2C* ☐

PAC Z3/F3 Apertures ■

COMPRESSION RATIOS:

Data (DCR) 4.8

Bandwidth (BCR) 1.9

DISTORTION (mv):

Maximum 0.03 *Average* -0.0004 σ 0.0153

ERROR (%):

Maximum 3.13 *rms* 1.60

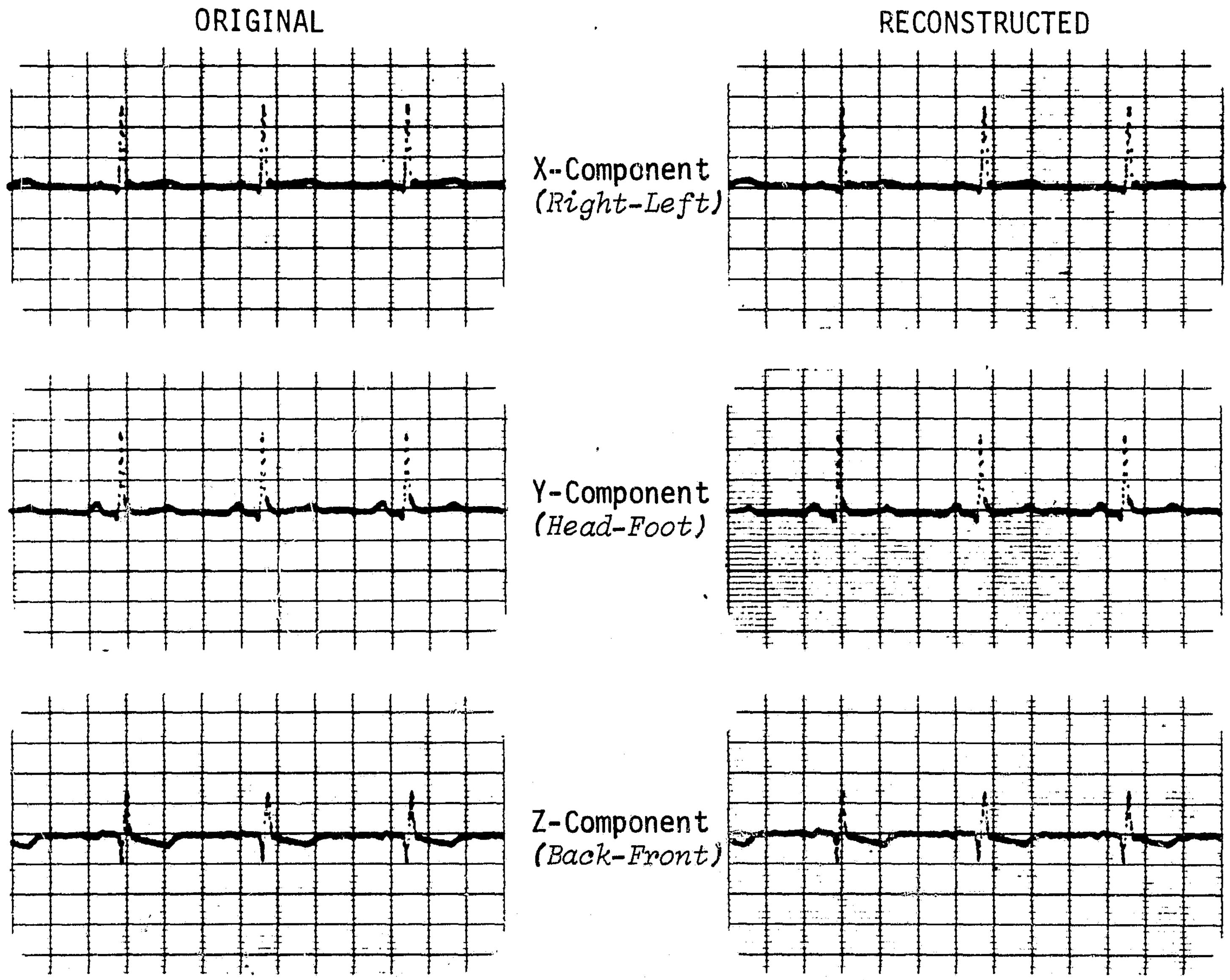

STUDY INPUT DATA DESCRIPTION

ACTIVITY GROUP:

I ☐ *II* ■ *III* ☐ *IV* ☐

SUBJECT IDENTIFICATION: Kappa

SUBJECT TEST CONDITION:

0-g ☐ *Orbit* ☐ *Control/Recovery* ■

1-g ■ *Ergometer* ☐ *LBNP @ -40 mmHg* ☐

CARDIOGRAM CHARACTERISTICS:

VCG ■ *ECG* ☐ *Heart Rate* 80

QRS Amplitude (mv p-p): *Upper* 1.11 *Middle* 1.42 *Lower* 0.92

DATA COMPRESSION/RECONSTRUCTION RESULTS
(VCG Component Mean)

ALGORITHM:

Fast-Fourier ☐ *Cycle-to-Cycle* ☐

Fast-Hadamard ☐ *FFC2C* ☐

PAC Z3/F3 Apertures ■

COMPRESSION RATIOS:

Data (DCR) 3.5

Bandwidth (BCR) 1.4

DISTORTION (mv):

Maximum 0.01 *Average* 0.0 σ 0.0063

ERROR (%):

Maximum 0.87 *rms* 0.55

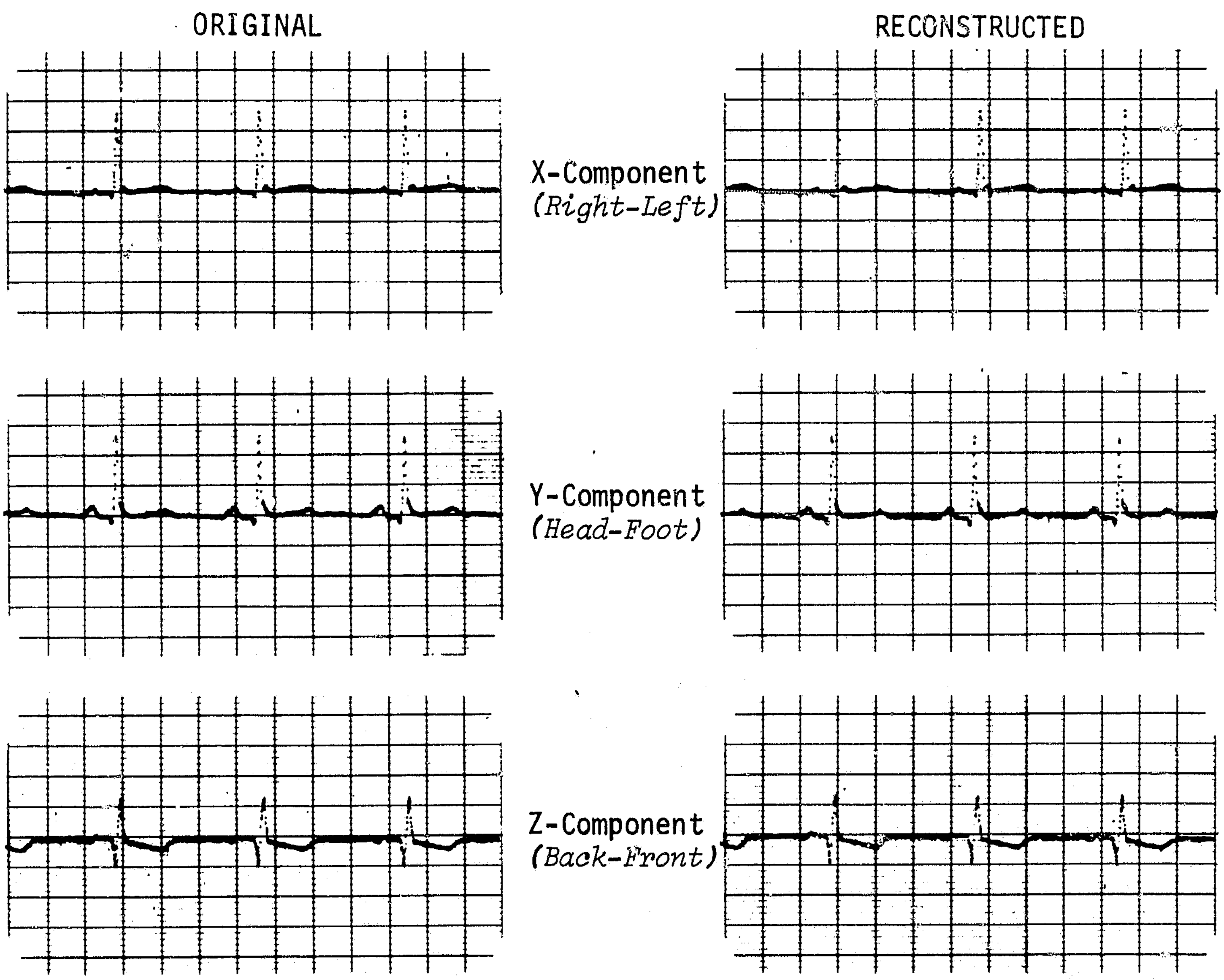

STUDY INPUT DATA DESCRIPTION

ACTIVITY GROUP:

I □ *II* ■ *III* □ *IV* □

SUBJECT IDENTIFICATION: Kappa

SUBJECT TEST CONDITION:

0-g □ *Orbit* □ *Control/Recovery* ■

1-g ■ *Ergometer* □ *LBNP @ -40 mmHg* □

CARDIOGRAM CHARACTERISTICS:

VCG ■ *ECG* □ *Heart Rate* 80

QRS Amplitude (mv p-p) — *Upper* 1.11 *Middle* 1.42 *Lower* 0.92

DATA COMPRESSION/RECONSTRUCTION RESULTS
(VCG Component Mean)

ALGORITHM:

Fast-Fourier □ *Cycle-to-Cycle* □

Fast-Hadamard □ *FFC2C* □

PAC Z5/F3 Apertures ■

COMPRESSION RATIOS:

Data (DCR) 28.3

Bandwidth (BCR) 11.3

DISTORTION (mv):

Maximum 0.05 *Average* -0.0027 σ 0.0217

ERROR (%):

Maximum 4.38 *rms* 1.93

ORIGINAL | RECONSTRUCTED

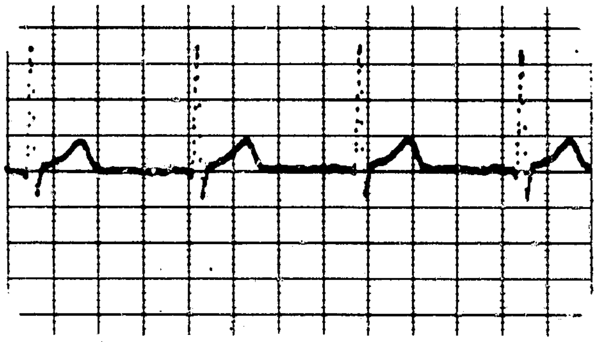

X-Component (*Right-Left*)

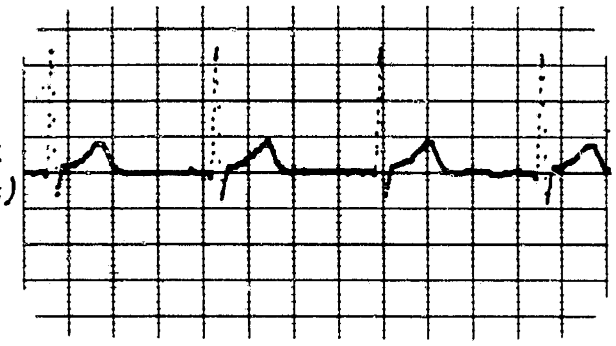

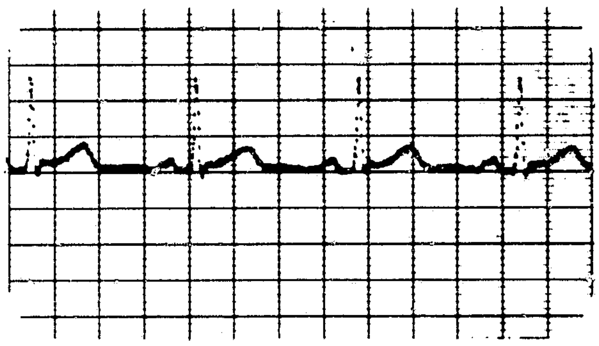

Y-Component (*Head-Foot*)

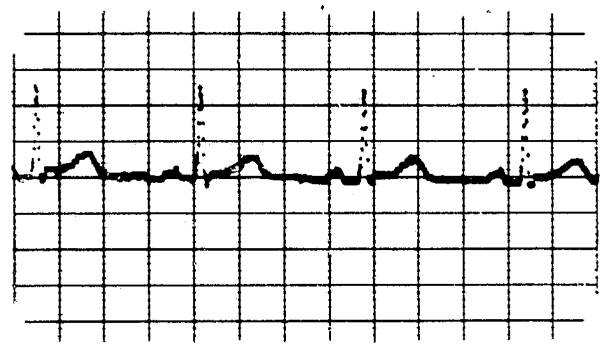

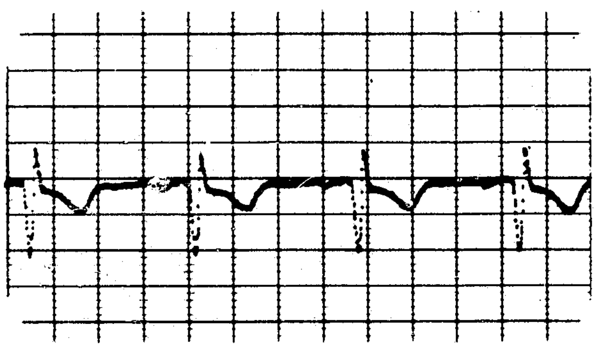

Z-Component (*Back-Front*)

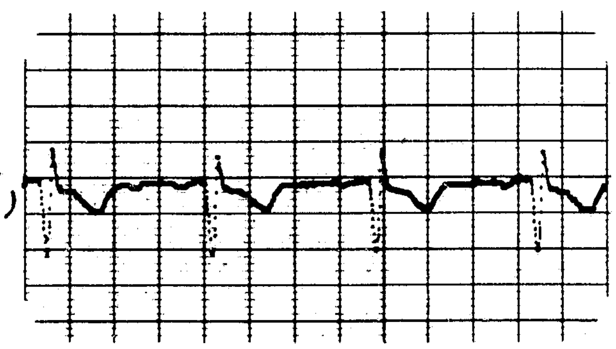

STUDY INPUT DATA DESCRIPTION

ACTIVITY GROUP:

I ☐ *II* ☐ *III* ■ *IV* ☐

SUBJECT IDENTIFICATION: Mu

SUBJECT TEST CONDITION:

0-g ☐ *Orbit* ☐ *Control/Recovery* ☐

1-g ■ *Ergometer* ☐ *LBNP @ -40 mmHg* ■

CARDIOGRAM CHARACTERISTICS:

VCG ■ *ECG* ☐ *Heart Rate* 83

QRS Amplitude (mv p-p): *Upper* 1.76 *Middle* 1.19 *Lower* 1.27

DATA COMPRESSION/RECONSTRUCTION RESULTS
(VCG Component Mean)

ALGORITHM:

Fast-Fourier ☐ *Cycle-to-Cycle* ☐

Fast-Hadamard ☐ *FFC2C* ☐

PAC Z5/F3 Apertures ■

COMPRESSION RATIOS:

Data (DCR) 15.3

Bandwidth (BCR) 6.1

DISTORTION (mv):

Maximum 0.05 *Average* 0.0013 σ 0.0217

ERROR (%):

Maximum 3.66 *rms* 1.60

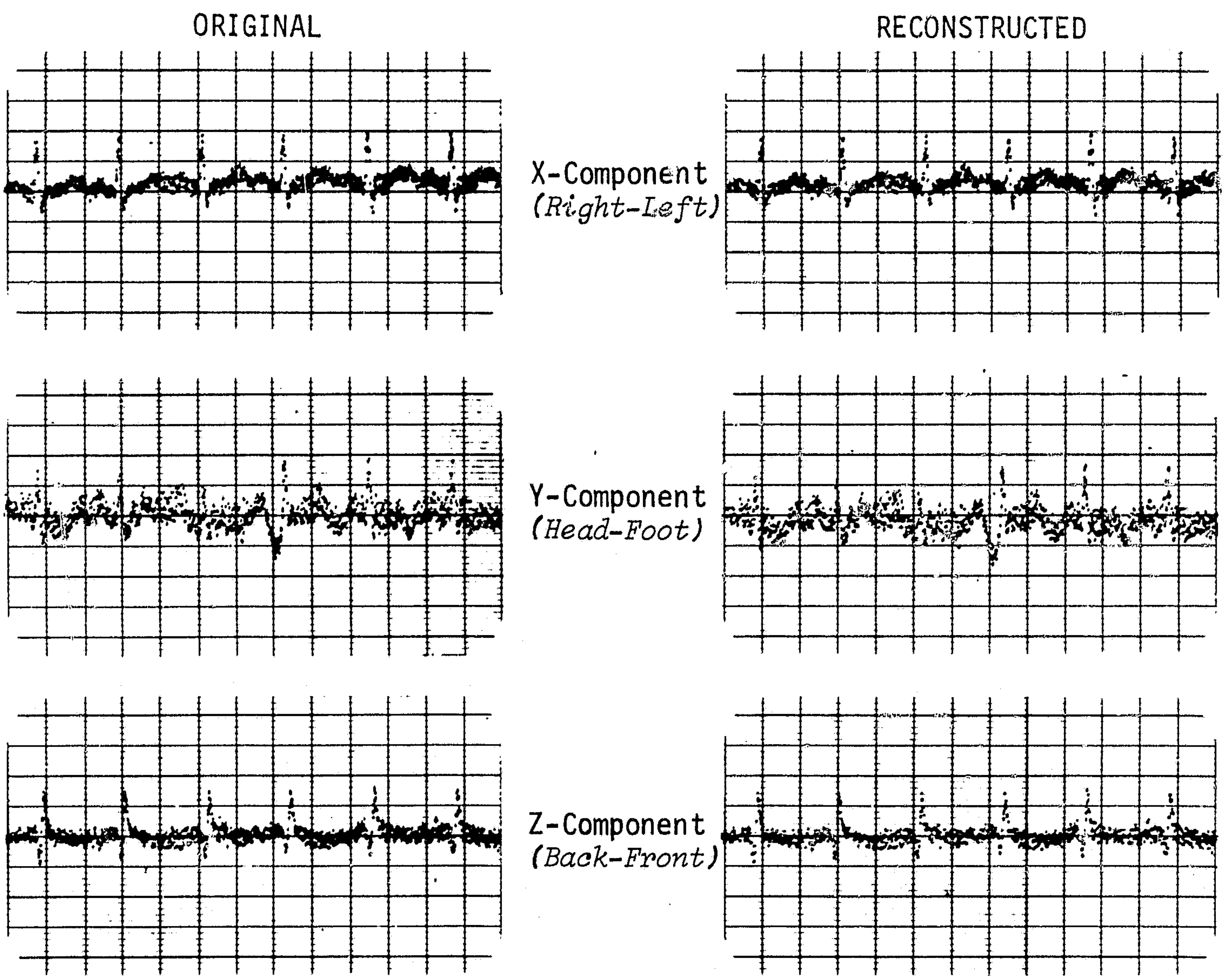

STUDY INPUT DATA DESCRIPTION

ACTIVITY GROUP:

I ☐ *II* ☐ *III* ☐ *IV* ■

SUBJECT IDENTIFICATION: Nu

SUBJECT TEST CONDITION:

0-g ☐ *Orbit* ☐ *Control/Recovery* ☐

1-g ■ *Ergometer* ■ *LBNP @ -40 mmHg* ☐

CARDIOGRAM CHARACTERISTICS:

VCG ■ *ECG* ☐ *Heart Rate* 136

QRS Amplitude (mv p-p): *Upper* 1.04 *Middle* 1.30 *Lower* 0.99

DATA COMPRESSION/RECONSTRUCTION RESULTS
(VCG Component Mean)

ALGORITHM:

Fast-Fourier ☐ *Cycle-to-Cycle* ☐

Fast-Hadamard ☐ *FFC2C* ☐

PAC *Z1/F1 Apertures* ■

COMPRESSION RATIOS:

Data (DCR) 1.3

Bandwidth (BCR) 0.5

DISTORTION (mv):

Maximum 0.01 *Average* 0.0 σ 0.0033

ERROR (%):

Maximum 0.91 *rms* 0.30

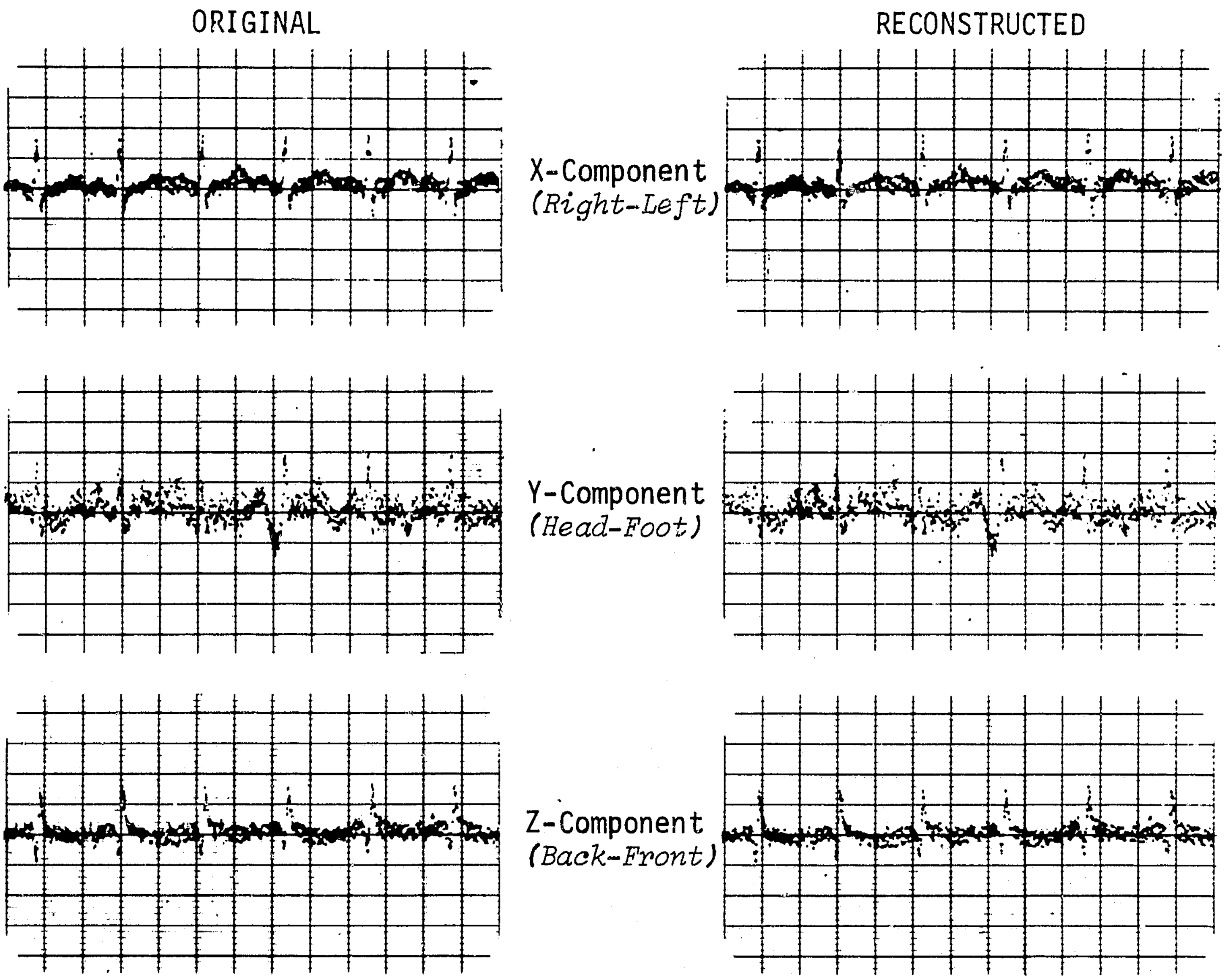

STUDY INPUT DATA DESCRIPTION

ACTIVITY GROUP:

I □ *II* □ *III* □ *IV* ■

SUBJECT IDENTIFICATION: Nu

SUBJECT TEST CONDITION:

0-g □ *Orbit* □ *Control/Recovery* □

1-g ■ *Ergometer* ■ *LBNP @ -40 mmHg* □

CARDIOGRAM CHARACTERISTICS:

VCG ■ *ECG* □ *Heart Rate* 136

QRS Amplitude (mv p-p): *Upper* 1.04 *Middle* 1.30 *Lower* 0.99

DATA COMPRESSION/RECONSTRUCTION RESULTS
(VCG Component Mean)

ALGORITHM:

Fast-Fourier □ *Cycle-to-Cycle* □

Fast-Hadamard □ *FFC2C* □

PAC Z3/F3 Apertures ■

COMPRESSION RATIOS:

Data (DCR) 1.7

Bandwidth (BCR) 0.7

DISTORTION (mv):

Maximum 0.03 *Average* 0.0001 σ 0.0117

ERROR (%):

Maximum 2.74 *rms* 1.08

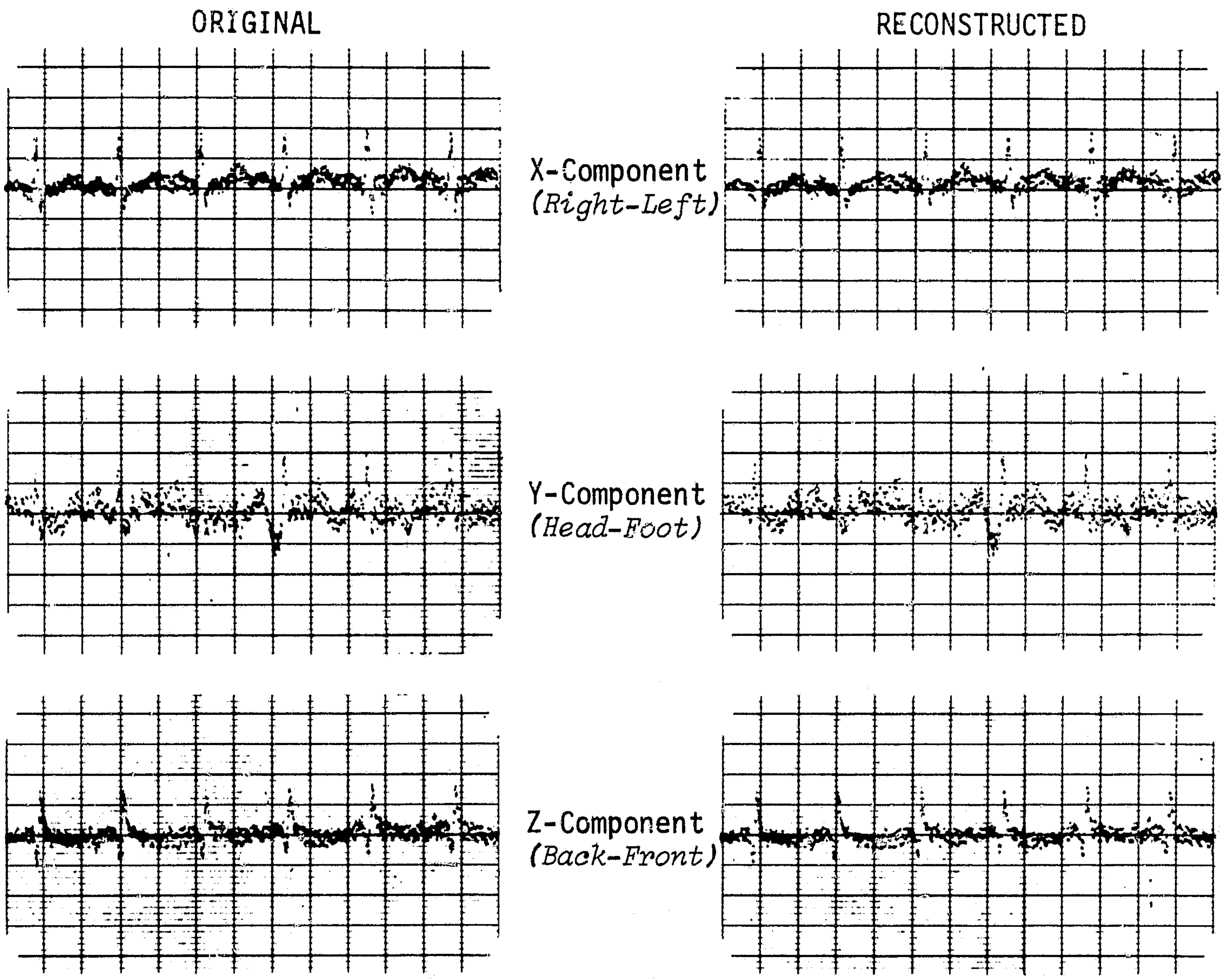

STUDY INPUT DATA DESCRIPTION

ACTIVITY GROUP:

I ☐ *II* ☐ *III* ☐ *IV* ■

SUBJECT IDENTIFICATION: Nu

SUBJECT TEST CONDITION:

0-g ☐ *Orbit* ☐ *Control/Recovery* ☐

1-g ■ *Ergometer* ■ *LBNP @ -40 mmHg* ☐

CARDIOGRAM CHARACTERISTICS:

VCG ■ *ECG* ☐ *Heart Rate* 136

QRS Amplitude (mv p-p): *Upper* 1.04 *Middle* 1.30 *Lower* 0.99

DATA COMPRESSION/RECONSTRUCTION RESULTS
(VCG Component Mean)

ALGORITHM:

Fast-Fourier ☐ *Cycle-to-Cycle* ☐

Fast-Hadamard ☐ *FFC2C* ☐

PAC Z5/F3 Apertures ■

COMPRESSION RATIOS:

Data (DCR) 1.9

Bandwidth (BCR) 0.8

DISTORTION (mv):

Maximum 0.05 *Average* 0.0007 σ 0.0159

ERROR (%):

Maximum 4.57 *rms* 1.71

2.4.3.2 Algorithm Speed

Evaluation of the PAC computation speed indicates that--congruent with its relative software simplicity--the algorithm can easily operate on real ECG/VCG data in real time. Further, as shown below, the PAC reconstruction algorithm is extremely fast performing in only one-fifth the compression time.

Subalgorithm Apertures	Percent of Real Time Required	
	Compression	Reconstruction
Z1-F1	72	14
Z3-F3	63	12
Z5-F3	45	9

2.4.4 Cycle-to-Cycle (C2C) Algorithm Test Results

A mathematical description of the C2C algorithm has been included in Appendix B.

2.4.4.1 Analysis

Probably the most impressive data compression ratios have been produced by the C2C algorithm. Test results for the C2C are presented in Table 2-4. Because of the algorithm software complexity and computation time requirements, only the VCG X-component was tested. The capability of this algorithm to process all three VCG components simultaneously in real time must remain a subject for future study. However, the C2C algorithm has proven excellent for ECG signals.

Two tolerances are required for the C2C algorithm as explained in Appendix B. Each tolerance is tested with each data point. Tolerances of 25 percent of the QRS p-p voltage, or 2.5 percent of the actual data sample value were selected to obtain the results shown in Table 2-4. Each test case was standardized at 20 complete cardiac complexes. The first eight beats stabilized the digital filter and the remaining 12 were compressed, reconstructed and analyzed to produce the Table 2-4 tabulations. An average test case contained 16 seconds of ECG/VCG data.

The C2C has a very attractive attribute in that with extremely large DCR = 1406, the reconstruction process does not suffer large increases in maximum or rms errors.

Four C2C algorithm plots are shown on pages 46 through 49. These particular subject plots were chosen to exemplify the extremes of DCR and rms error from Table 2-4. However, because the parallel digital filter used in the C2C algorithm provides substantial resistance to cardiac wave amplitude and duration changes (see Appendix B), eight complete cardiac changes must occur before a long duration change is fully observable. In the same manner, short duration changes (< eight beats) are either attenuated or not seen at all. The degree of acceptability to this algorithm characteristic is left to the cardiologist.

2.4.4.2 Algorithm Speed

The C2C algorithm has shown that when operating on a single ECG signal real time processing is easily accomplished.

Algorithm	Percent of Real Time Required: Compression	Reconstruction
C2C	58	34

The above figures, unfortunately, do not have the same meaning as for the FHT, FFT and PAC algorithms previously analyzed. Because of the C2C program size, the compressed and reconstructed data samples had to be intermediately written on tape rather than stored in core memory. Therefore, the above speed figures include tape writing time also. An engineering estimate has placed the probable actual compression and reconstruction times at approximately 35 and 10 percent respectively. It can be tentatively concluded from these computations that there is a strong probability the C2C algorithm can be made to work in real time on all three VCG components provided that computer memory size requirements are met.

Table 2-4. Test Results for the C2C Algorithm Using a 25/2.5 Percent Tolerance Set*

Activity Group	Subject	Test Condition	Compression Ratios		Distortion (mv)		Error (%)	
			Data	Bandwidth	RMS	Maximum	RMS	Maximum
I	ALPHA	Orbit	264.4	132.2	0.0087	0.040	0.79	3.64
(ECG)	BETA	Orbit	34.9	16.4	0.0120	0.050	1.38	5.75
	EPSILON	Orbit	41.5	18.2	0.0058	0.040	0.92	6.35
	Group I	Means	113.6	55.6	0.0088	0.043	1.03	5.25
II	ZETA	Recovery (LBNP)	49.1	20.2	0.0043	0.040	0.76	7.02
(VCG-X)	ETA	Control	**	**	**	**	**	**
	IOTA	Control	305.6	125.8	0.0050	0.040	0.67	5.41
	IOTA	Recovery (Ergometer)	68.1	29.8	0.0080	0.050	0.90	5.62
	KAPPA	Recovery (LBNP)	50.5	22.4	0.0146	0.070	1.18	5.65
	MU	Control	31.0	15.5	0.0124	0.150	0.64	7.73
	NU	Control	811.9	360.8	0.0077	0.050	0.83	5.43
	Group II	Means	219.3	95.8	0.0087	0.067	0.83	6.14
III	ZETA	LBNP @-40 mmHg	1406.3	579.0	0.0055	0.040	0.89	6.45
(VCG-X)	ETA	↓	**	**	**	**	**	**
	IOTA	↓	214.7	93.9	0.0085	0.040	1.12	5.26
	KAPPA	↓	1127.5	530.6	0.0041	0.040	0.38	3.77
	MU	↓	85.5	42.7	0.0222	0.210	1.38	13.04
	NU	↓	39.7	17.4	0.0088	0.060	1.19	8.11
	Group III	Means	574.7	252.7	0.0098	0.078	0.99	7.33
IV	IOTA	Ergometer (Erect)	64.6	30.2	0.0126	0.060	1.47	6.98
(VCG-X)	IOTA	Ergometer (Supine)	19.6	9.1	0.0101	0.060	1.44	8.57
	KAPPA	Ergometer (Supine)	40.6	20.3	0.0151	0.090	1.72	10.23
	NU	Ergometer (Erect)	21.8	10.2	0.0141	0.100	1.61	11.36
	Group IV	Means	36.7	17.5	0.0130	0.078	1.56	9.29

* VCG X-Component only.
** Signal amplitude insufficient for analysis.

FILTERED
X-Component
(Right-Left)

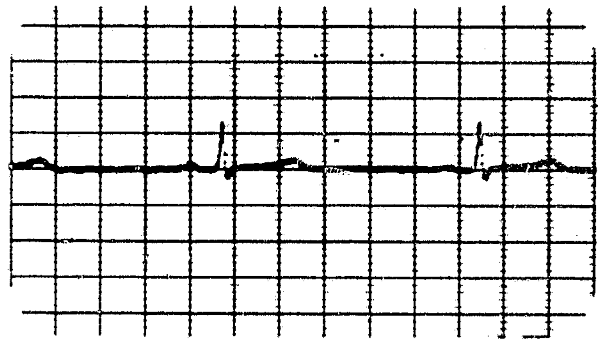

RECONSTRUCTED

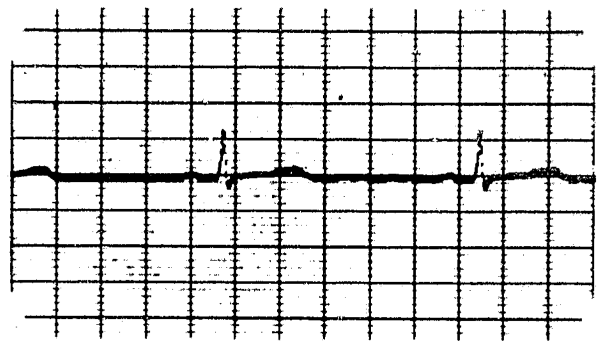

STUDY INPUT DATA DESCRIPTION

ACTIVITY GROUP:

I ☐ *II* ☐ *III* ■ *IV* ☐

SUBJECT IDENTIFICATION:	SUBJECT TEST CONDITION:		
Zeta	*0-g* ☐	*Orbit* ☐	*Control/Recovery* ☐
	1-g ■	*Ergometer* ☐	*LBNP @ -40 mmHg* ■

CARDIOGRAM CHARACTERISTICS:

VCG ■ *ECG* ☐ *Heart Rate* 54 — *QRS Amplitude (mv p-p)*: *Upper* 0.62 *Middle* --- *Lower* 0.6

DATA COMPRESSION/RECONSTRUCTION RESULTS

ALGORITHM:		COMPRESSION RATIOS:	
Fast-Fourier ☐	*Cycle-to-Cycle* ■	*Data (DCR)*	1406.3
Fast-Hadamard ☐	*FFC2C* ☐	*Bandwidth (BCR)*	579.0
PAC ☐			

DISTORTION (mv): *Maximum* 0.04 *Average* -0.0014 σ 0.0053

ERROR (%): *Maximum* 6.45 *rms* 0.89

FILTERED
X-Component
(Right-Left)

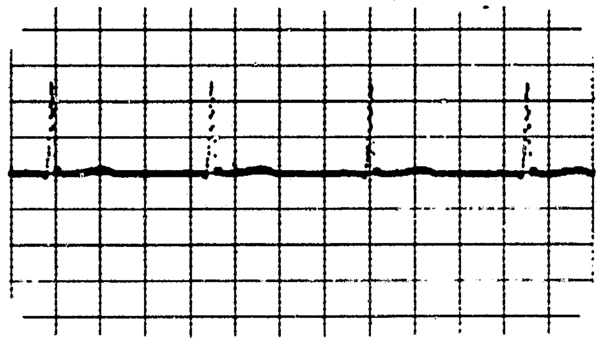

RECONSTRUCTED

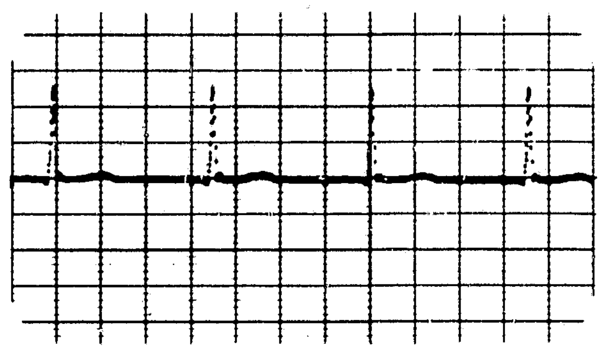

STUDY INPUT DATA DESCRIPTION			
ACTIVITY GROUP:			
I ☐	*II* ☐	*III* ■	*IV* ☐
SUBJECT IDENTIFICATION: Kappa	SUBJECT TEST CONDITION: *0-g* ☐ *1-g* ■	*Orbit* ☐ *Ergometer* ☐	*Control/Recovery* ☐ *LBNP @ -40 mmHg* ■
CARDIOGRAM CHARACTERISTICS: *VCG* ■ *ECG* ☐	*Heart Rate* 80	*QRS Amplitude (mv p-p)* *Upper* 1.06 *Middle* ---	*Lower* 1.1

DATA COMPRESSION/RECONSTRUCTION RESULTS

ALGORITHM:		COMPRESSION RATIOS:	
Fast-Fourier ☐	*Cycle-to-Cycle* ■	*Data (DCR)*	1127.5
Fast-Hadamard ☐	*FFC2C* ☐	*Bandwidth (BCR)*	530.6
PAC ☐			

DISTORTION (mv):			ERROR (%):	
Maximum 0.04	*Average* 0.0003	σ 0.0040	*Maximum* 3.77	*rms* 0.38

FILTERED
X-Component
(Right-Left)

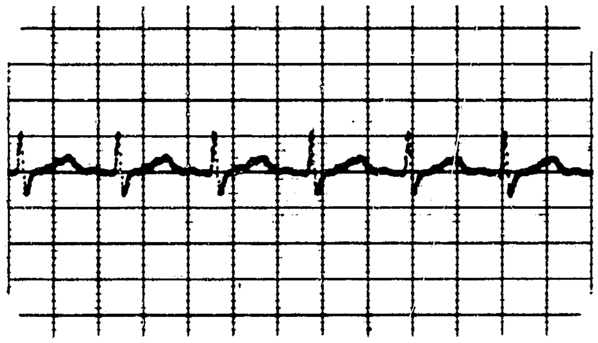

RECONSTRUCTED

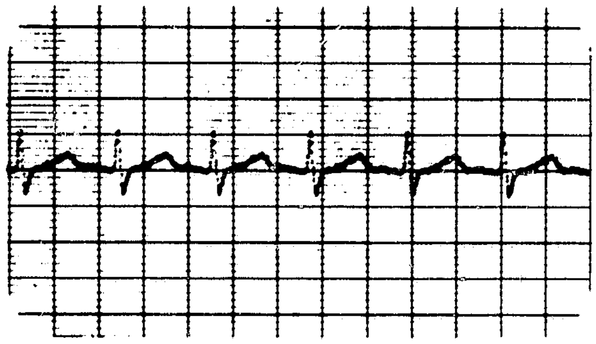

STUDY INPUT DATA DESCRIPTION

ACTIVITY GROUP:

I ☐ *II* ☐ *III* ☐ *IV* ■

SUBJECT IDENTIFICATION:	SUBJECT TEST CONDITION:					
Iota	*0-g*	☐	*Orbit*	☐	*Control/Recovery*	☐
	1-g	■	*Ergometer*	■	*LBNP @ -40 mmHg*	☐

CARDIOGRAM CHARACTERISTICS:

VCG ■ *ECG* ☐ *Heart Rate* 135 — *QRS Amplitude (mv p-p)*: *Upper* 0.70 *Middle* --- *Lower* 0.7

DATA COMPRESSION/RECONSTRUCTION RESULTS

ALGORITHM:

Fast-Fourier ☐ *Cycle-to-Cycle* ■
Fast-Hadamard ☐ *FFC2C* ☐
PAC ☐

COMPRESSION RATIOS:

Data (DCR) 19.6
Bandwidth (BCR) 9.1

DISTORTION (mv):

Maximum 0.06 *Average* -0.0027 σ 0.0097

ERROR (%):

Maximum 8.57 *rms* 1.44

FILTERED
X-Component
(Right-Left)

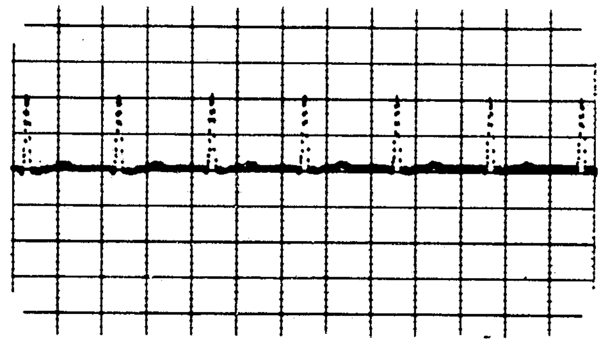

RECONSTRUCTED

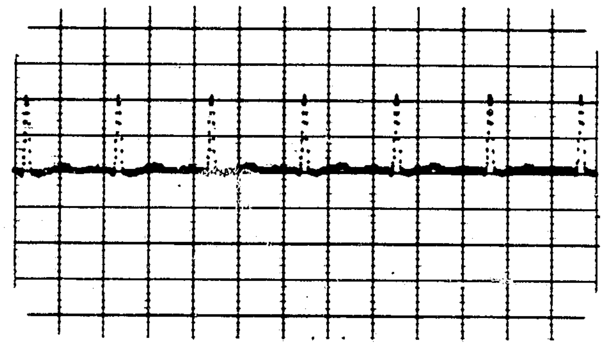

STUDY INPUT DATA DESCRIPTION

ACTIVITY GROUP:

I □ *II* □ *III* □ *IV* ■

SUBJECT IDENTIFICATION: Kappa

SUBJECT TEST CONDITION:

0-g □ *Orbit* □ *Control/Recovery* □
1-g ■ *Ergometer* ■ *LBNP @ -40 mmHg* □

CARDIOGRAM CHARACTERISTICS:

VCG ■ *ECG* □ *Heart Rate* 148

QRS Amplitude (mv p-p): *Upper* 0.88 *Middle* --- *Lower* 0.9

DATA COMPRESSION/RECONSTRUCTION RESULTS

ALGORITHM:

Fast-Fourier □ *Cycle-to-Cycle* ■
Fast-Hadamard □ *FFC2C* □
PAC □

COMPRESSION RATIOS:

Data (DCR) 40.6
Bandwidth (BCR) 20.3

DISTORTION (mv):

Maximum 0.09 *Average* -0.0045 σ 0.0144

ERROR (%):

Maximum 10.2 *rms* 1.72

2.4.5 Fast Fourier Cycle-to-Cycle (FFC2C) Algorithm Test Results

A description of the TRW FFC2C algorithm is included in Appendix B.

2.4.5.1 Analysis

This TRW innovation was tested using five selected subjects. The C2C algorithm results were reviewed (Table 2-4) and subjects Beta, II Mu, III Nu and IV Iota were chosen as those producing the smallest DCR/BCR in each activity group. Subject III Zeta was the outstanding best producer of all subjects. The FFC2C algorithm test results for the five subjects are presented in Table 2-5 below.

A tolerance of 40 (in the Fourier transform domain) was utilized, which represented a worst case percentage tolerance on the order of two percent. Accordingly, even with this relatively narrow tolerance, the FFC2C out-performed the C2C in three out of the five cases. Table 2-5 further shows the FFC2C to produce superior rms and maximum error magnitudes over those of the C2C algorithm.

Table 2-5. Test Results from Selected Subjects for the FFC2C Algorithm Using a Transform Domain Tolerance of 40*

Activity Group	Subject	Test Condition	Compression Ratios		Distortion (mv)		Error (%)	
			Data	Bandwidth	RMS	Maximum	RMS	Maximum
I	BETA	Orbit	26	19	0.00362	0.0154	0.48	2.05
II	MU	Control	57	41	0.00523	0.0516	0.25	2.51
III	ZETA	LBNP @-40 mmHg	14	10	0.00762	0.1370	0.47	8.38
III	NU	LBNP @-40 mmHg	298	217	0.00419	0.0359	0.53	4.56
IV	IOTA	Ergometer (Supine)	31	23	0.00484	0.0216	0.63	2.83

* VCG X-Component only.

Four FFC2C algorithm plots are presented on pages 52 through 55. For subject Beta on page 52, a noticable difference in QRS amplitude can be seen between the original and filtered (parallel digital filter) waveforms. This phenomena is accountable to the filter's resistance to change previously mentioned regarding the C2C algorithm above. A similar occurrence can be seen for subject II Mu (page 54) in that the second original R-peak is measurably lower than the adjacent peaks whereas the filtered and reconstructed R-peaks are not changed.

2.4.5.2 Algorithm Speed

Because of the extra resampling operation required to satisfy the FFT subalgorithm input requirement (see Appendix B) the FFC2C takes approximately five percent longer than the C2C algorithm. The corresponding FFC2C compression and reconstruction times are approximately 40 and 15 percent respectively.

ORIGINAL

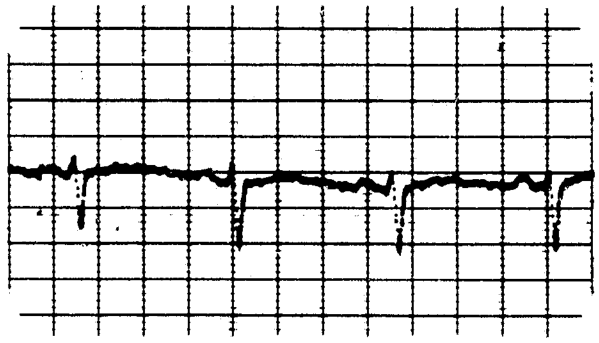

FILTERED

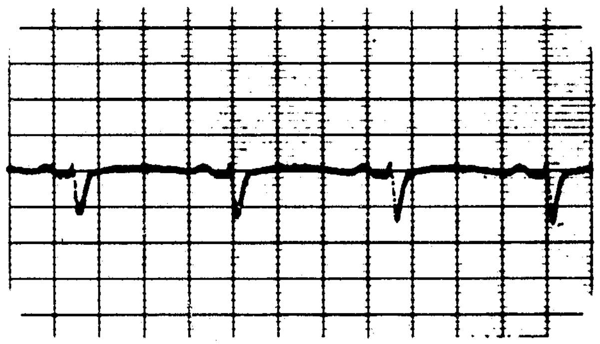

RECONSTRUCTED

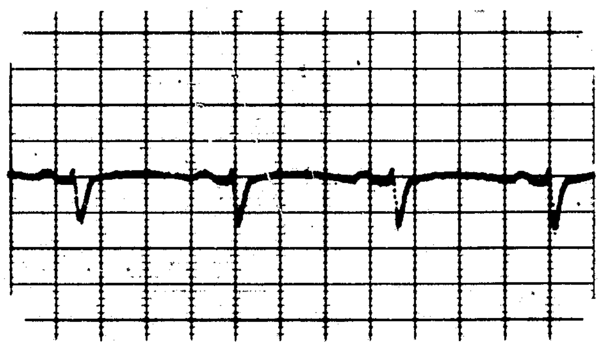

STUDY INPUT DATA DESCRIPTION

ACTIVITY GROUP:

I ■ *II* □ *III* □ *IV* □

SUBJECT IDENTIFICATION:	SUBJECT TEST CONDITION:		
Beta	*0-g* ■	*Orbit* ■	*Control/Recovery* □
	1-g □	*Ergometer* □	*LBNP @ -40 mmHg* □

CARDIOGRAM CHARACTERISTICS:

VCG □ *ECG* ■ *Heart Rate* 85

QRS Amplitude (mv p-p): *Upper* 0.87 *Middle* 0.7 *Lower* 0.7

DATA COMPRESSION/RECONSTRUCTION RESULTS

ALGORITHM:		COMPRESSION RATIOS:
Fast-Fourier □	*Cycle-to-Cycle* □	*Data (DCR)* 26
Fast-Hadamard □	*FFC2C* ■	*Bandwidth (BCR)* 19
PAC □		

DISTORTION (mv):			ERROR (%):	
Maximum 0.0154	*Average* 0.0	σ 0.0036	*Maximum* 2.05	*rms* 0.48

ORIGINAL
X-Component
(Right-Left)

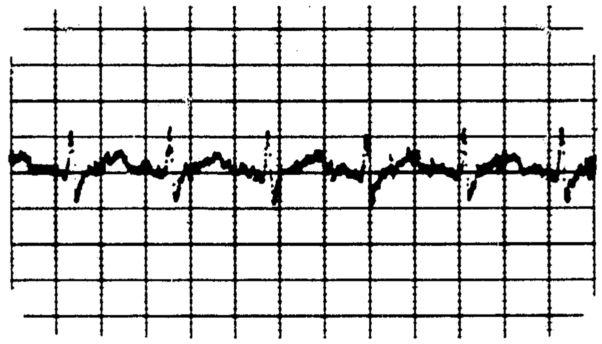

FILTERED

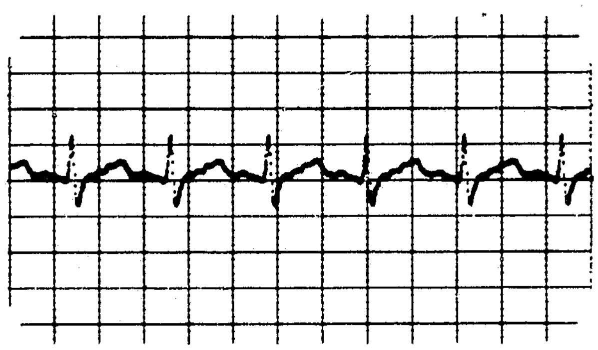

RECONSTRUCTED

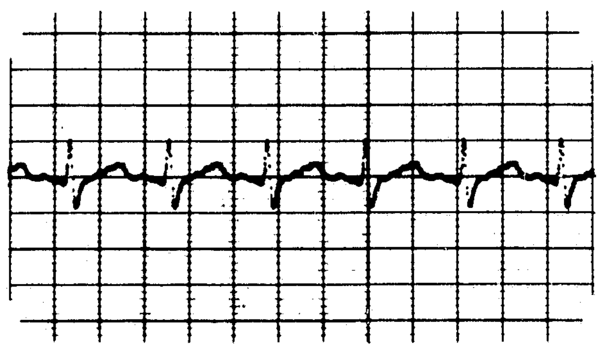

STUDY INPUT DATA DESCRIPTION

ACTIVITY GROUP:

I ☐ *II* ☐ *III* ☐ *IV* ■

SUBJECT IDENTIFICATION: Iota

SUBJECT TEST CONDITION:

0-g ☐ *Orbit* ☐ *Control/Recovery* ☐
1-g ■ *Ergometer* ■ *LBNP @ -40 mmHg* ☐

CARDIOGRAM CHARACTERISTICS:

VCG ■ *ECG* ☐ *Heart Rate* 135

QRS Amplitude (mv p-p): *Upper* 0.70 *Middle* 0.7 *Lower* 0.7

DATA COMPRESSION/RECONSTRUCTION RESULTS

ALGORITHM:

Fast-Fourier ☐ *Cycle-to-Cycle* ☐
Fast-Hadamard ☐ *FFC2C* ■
PAC ☐

COMPRESSION RATIOS:

Data (DCR) 31
Bandwidth (BCR) 23

DISTORTION (mv):

Maximum 0.0216 *Average* 0.0001 σ 0.0048

ERROR (%):

Maximum 2.83 *rms* 0.63

ORIGINAL
X-Component
(Right-Left)

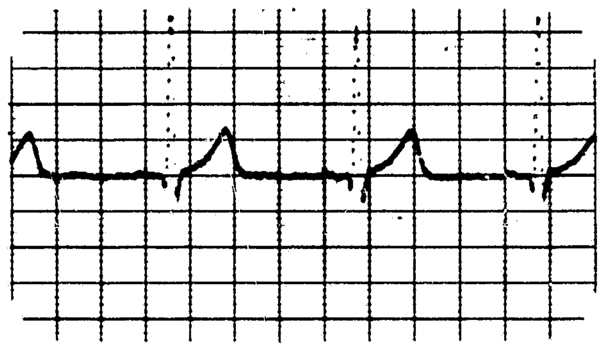

FILTERED

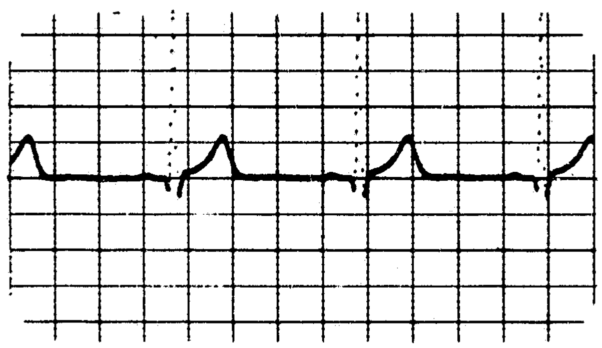

RECONSTRUCTED

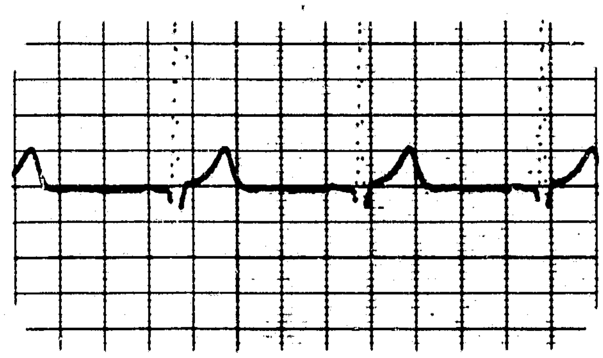

STUDY INPUT DATA DESCRIPTION

ACTIVITY GROUP:

I ☐ *II* ■ *III* ☐ *IV* ☐

SUBJECT IDENTIFICATION:	SUBJECT TEST CONDITION:		
Mu	*0-g* ☐	*Orbit* ☐	*Control/Recovery* ■
	1-g ■	*Ergometer* ☐	*LBNP @ -40 mmHg* ☐

CARDIOGRAM CHARACTERISTICS:

VCG ■ *ECG* ☐ *Heart Rate* 73

QRS Amplitude (mv p-p): *Upper* 1.94 *Middle* 2.0 *Lower* 2.0

DATA COMPRESSION/RECONSTRUCTION RESULTS

ALGORITHM:		COMPRESSION RATIOS:	
Fast-Fourier ☐	*Cycle-to-Cycle* ☐	*Data (DCR)*	57
Fast-Hadamard ☐	*FFC2C* ■	*Bandwidth (BCR)*	41
PAC ☐			

DISTORTION (mv):			ERROR (%):	
Maximum 0.0516	*Average* 0.0	σ 0.0052	*Maximum* 2.51	*rms* 0.25

ORIGINAL
X-Component
(Right-Left)

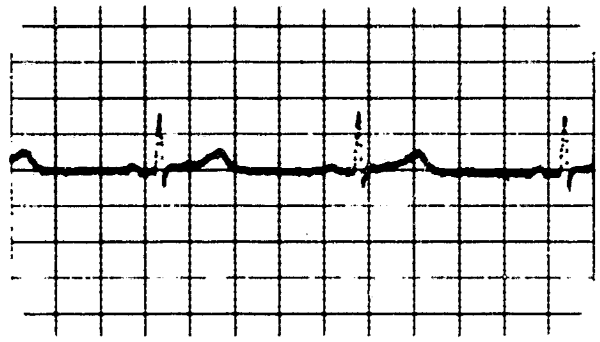

FILTERED

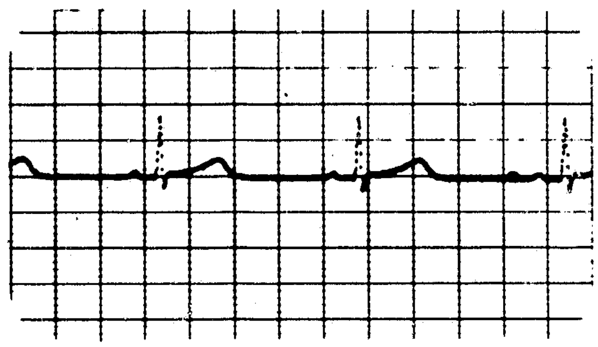

RECONSTRUCTED

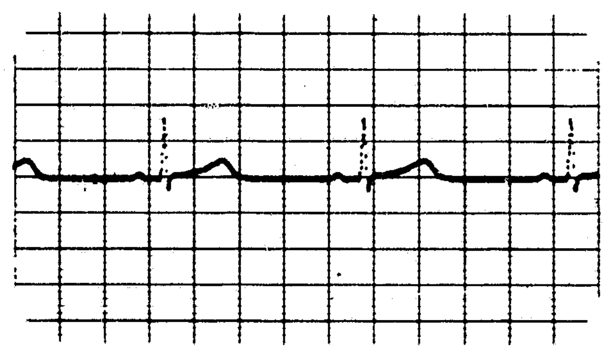

STUDY INPUT DATA DESCRIPTION

ACTIVITY GROUP:

I ☐ *II* ☐ *III* ■ *IV* ☐

SUBJECT IDENTIFICATION: Nu

SUBJECT TEST CONDITION:

0-g ☐	*Orbit* ☐	*Control/Recovery* ☐
1-g ■	*Ergometer* ☐	*LBNP @ -40 mmHg* ■

CARDIOGRAM CHARACTERISTICS:

VCG ■ *ECG* ☐ *Heart Rate* 67

QRS Amplitude (mv p-p): *Upper* 0.74 *Middle* 0.8 *Lower* 0.8

DATA COMPRESSION/RECONSTRUCTION RESULTS

ALGORITHM:

Fast-Fourier	☐	*Cycle-to-Cycle*	☐
Fast-Hadamard	☐	*FFC2C*	■
PAC	☐		

COMPRESSION RATIOS:

Data (DCR) 298

Bandwidth (BCR) 217

DISTORTION (mv):

Maximum 0.0359 *Average* -0.001 σ 0.0042

ERROR (%):

Maximum 4.56 *rms* 0.53

2.5 TESTING AND ANALYSES SUMMARY

Presented below in Table 2-6 is a summary of algorithm test results. These figures have been condensed from Figure 2-7 and Tables 2-3 through 2-5 as well as various listings within Section 2.

The intent of Table 2-6 is to present better visibility into algorithm comparisons from testing and analyses that were conducted on each of the six algorithms (the filter algorithm was incorporated in the C2C and FFC2C). Detailed conclusions cannot and should not be drawn from the Table 2-6. The reader is referred to the test results sections for detailed statistics.

Table 2-6. Summary of Algorithm Test Results

Algorithm	Aperture/ Tolerance	Algorithm Speed (% of Real Time)		Software Size	Performance Means by Activity Groups							
					I		II		III		IV	
		COMP	RECON		BCR	RMS Error (%)	BCR	RMS Error (%)	BCR	RMS Error (%)	BCR	RMS Error (%)
FHT	--	53	53	Large	2.2	2.3	2.3	3.2	2.3	2.7	2.5	4.0
FFT	--	55	55	Large	4.3	0.8	4.6	2.0	4.5	1.5	5.8	2.8
					17.0	5.2	17.6	5.4	18.0	6.0	19.4	7.6
PAC	Z1-F1	72	14	Small	1.8	0.68	1.8	0.85	1.8	1.71	0.8	0.49
	Z3-F3	63	12	Small	4.6	1.72	4.2	1.60	3.9	1.58	1.7	1.43
	Z5-F3	45	9	Small	7.6	2.63	7.4	2.28	6.8	2.40	2.5	2.16
C2C	25/2.5	35	10	Large	55.6	1.03	95.8	0.83	252.7	0.99	17.5	1.56
FFC2C	40	40	15	Large	19	0.48	41	0.25	114	0.50	23	0.63

PRECEDING PAGE BLANK NOT FILMED

3. CONCLUSIONS

3.1 BEST OVERALL ALGORITHM PERFORMANCE

TRW has concluded that while utilizing a variety of real ECG/VCG test data the parallel adaptive composite (PAC) redundancy reduction algorithm has produced the best overall performance. This conlusion was based on the factors outlined below for the PAC algorithm with both the ZOP-FA and FOI-Fan subalgorithm apertures equal to three millivolts.

a) A moderate range of DCR/BCR = 1.7/0.7 to 19.1/8.0.

b) Very good rms error figures ranging only from 1.08 to 2.24 percent.

c) Simple and fast software program requiring relative small core memory.

d) Excellent reconstructed waveform fidelity of original ECG/VCG waveforms.

With a small modification in the BCR computation philosophy the PAC algorithm BCR results can be increased by approximately 25 percent.

3.2 ANCILLARY CONCLUSIONS

3.2.1. Test Group ECG/VCG Data

Although using a group of real ECG/VCG signals with widely varying amplitudes might in one respect make a more realistic test signal population (as was the case in this study), it does add--or maintain--an uncontrolled dimension to the testing and analyses of data compression/reconstruction algorithms.

Better algorithm performance comparisons could be obtained if special standardized-amplitude test recordings (perhaps one millivolt p-p) were made for the algorithm testing; or the digitizing process could adjust each ECG/VCG analog signal so that all digitized data equalled a certain defined level.

3.2.2 Other Algorithms

The fast Fourier transform (FFT) algorithm was concluded to be superior in performance to the fast Hadamard transform (FHT) algorithm and only slightly slower in operation. In addition the FFT produces a smoothing effect to the ECG/VCG noise which may be of benefit to the cardiologist.

The cycle-to-cycle (C2C) and TRW fast Fourier cycle-to-cycle (FFC2C) redundancy reduction algorithms can produce fantastically large DCR>1400 with small corresponding error magnitudes. However their computer core requirements are large and their abilities to process three VCG components in real time requires further study. In addition, the time lag realized before significant changes to ECG wave amplitudes and durations are seen (because of the digital filter characteristics) in the algorithm output is a matter of evaluation for the cardiologist.

4. RECOMMENDATIONS

During the performance of this study TRW has become aware of several aspects of the data compression problem that should be investigated more extensively. In the following four points TRW will recommend investigations and the path these investigations should follow.

4.1 EFFECTS OF PRE-COMPRESSION FILTERING ON RECONSTRUCTED ECG

Some of the algorithms investigated during this study have used pre-compression filtering of the ECG data to improve the data compression performance. In particular the C2C and FFC2C techniques employ a digital filter whose output is heavily weighted in favor of periodic components in the raw ECG data. The excellent rms error performance of these two algorithms is, to some degree, the result of the pre-compression filtering. No detailed examination of the effects of such filtering on the reconstructed ECG waveform has been possible. A thorough examination of filter effects is needed to insure that the distortion of ECG signals caused by filtering does not significantly impair the usefulness of the reconstructed ECG waveforms. Therefore an investigation of pre-compression filtering should:

a) Perform a high resolution spectral analysis of raw (original) ECG data to determine the true degree of periodicity of the data.

b) Verify the results above by determining the time averaged autocorrelation function over multiple cycles of the ECG data.

c) Develop filters for the raw ECG data which are matched to the spectrum of the raw data so as to minimize the rms error introduced by the filter.

d) Reproduce filtered ECG data in a form suitable for evaluation of the subjective effects of filtering by cardiologists.

e) Obtain an evaluation of these filtered ECG data by cardiologists.

4.2 SUBJECTIVE EVALUATION CRITERIA

In evaluating the distortion of ECG data produced by the various data compression algorithms the rms error between the original and reconstructed ECG data has been used as an error criterion. A cardiologist's evaluation of these same reconstructed ECG waveforms would be based on subjective criteria related to his training and experience. It is not clear that a one-to-one relationship exists between the rms error and the cardiologist's subjective evaluation criteria. An orderly test program is needed encompassing a variety of types of ECG data distortion to determine the degree with which these two criteria are correlated. This test program would require:

a) The establishment of a list of compression algorithms whose distortion of ECG data is typical of that produced by most data compression algorithms.

b) The reproduction of a variety of compressed ECG data taken from a range of representative raw ECG data. These compressed data would possess controlled degrees of rms distortion.

c) The evaluation of these representative compressed data by cardiologists.

4.3 APPLICATION OF DATA COMPRESSION TECHNIQUES TO VECTORCARDIOGRAMS

This study has been primarily concerned with compressing and accurately reconstructing the time-amplitude relationship of scalar electrocardiograms. However the accurate production of a vectorcardiogram requires the simultaneous use of two scalar ECG derived from two orthogonal axes. The resulting shape of the Lissajous display depends not only on the relative amplitudes of the two orthogonal ECG signals but also on their relative phase angles. Since the application of many data compression/reconstruction algorithms to a scalar ECG involves inherent filtering and time scaling of the original data a careful study should be made to determine the detailed nature of these phase shifts and to evaluate their effects on the vectorcardiogram display. Specifically the investigation should:

a) Analyze representative data compression algorithms to determine the phase shifts associated with each algorithm. This analysis would determine the time delay of each algorithm as well as any time delay dispersion caused by filtering of the ECG data.

b) Compute the differential phase shift produced by the application of each algorithm to each channel of actual VCG data.

c) Determine the effects of these differential phase shifts on the shape of the vectorcardiogram display.

d) Develop techniques for equalizing the differential phase shifts produced by the data compression/reconstruction algorithms.

4.4 OPERATIONAL IMPLEMENTATION OF SELECTED ALGORITHMS

The computer program implementations of the algorithms developed during the course of this study have included many features which are not required in the operational use of these algorithms. For example the TBED program saves the original ECG data for computing many statistical parameters between the original and reconstructed ECG waveforms. The algorithms selected as most promising in this study should be examined to determine the most efficient means of operational implementation. This examination should:

a) Determine the basic program requirements for each candidate algorithm for operational implementation.

b) Examine alternate means of meeting the above requirements.

c) Perform trade-off studies of these alternatives using core storage, computation time, and simplicity requirements as trade-off criteria to select the most practical operational implementations of the data compression/reconstruction algorithms.

REFERENCES

1. D. R. Weber, "A Synopsis on Data Compression," *IEEE National Telemetering Conference Proc.,* 1965.

2. M. Schwartz, W. R. Bennett and S. Stein, *Communications Systems and Techniques,* New York: McGraw-Hill, 1966.

3. E. K. Franke, J. F. Braunstein and D. C. Zillner, "Study of High Frequency Components in Electrocardiogram by Power Spectrum Analysis," *Circulation Research,* 10:8701, 1962.

4. P. H. Langner, Jr., D. V. Geselowitz and F. T. Mansure, "High Frequency Components in the Electrocardiograms of Normal Subjects and of Patients with Coronary Heart Disease," *American Heart Journal,* 62:746, 1961.

5. Ellersick, "Data Compactors for Space Vehicles," *IEEE National Telemetering Conference Proc.,* 1961.

6. G. D. Bergland, "A Guided Tour of the Fast Fourier Transform," IEEE *Spectrum,* July 1969.

7. H. F. Harmuth, *Transmission of Information by Orthogonal Functions,* New York: Springer-Verlag New York, Inc., 1969.

8. D. F. Specht and P. E. Drapkin, "Biomedical Data Compression," *IEEE National Telemetering Conference Proc.,* 1965.

9. P. H. Fuijkschot, "A Simple First Order Digital Filter," *IEEE National Telemetering Conference Proc.,* 1967.

10. C. A. Steinberg, S. Abraham and C. A. Caceres, "Pattern Recognition in the Clinical Electrocardiogram," *IRE Transactions on Bio-Medical Electronics,* 1962.

11. R. Van Blerkom, G. R. Schwarz, and R. J. Ward, "An Adaptive Composite Data Compression Algorithm with Reduced Computation Requirements," *IEEE National Telemetering Conference Proc.,* 1968.

12. Ernest Frank, "An Accurate, Clincally Practical System for Spatial Vectorcardiography," *Circulation,* Volume XIII, May 1966.

13. C. E. Kossman, "Recommendations for Standardization of Leads and of Specification for Instruments in Electrocardiography and Vectorcardiography," *Circulation,* 35:596, 1967.

14. Hubert V. Pipberger, et al., "Digital Computer Analysis of the Normal and Abnormal Electrocardiogram," *Progress in Cardiovascular Diseases,* Volume 5, No. 4, January 1963.

PRECEDING PAGE BLANK NOT FILMED

BIBLIOGRAPHY

Andrews, C. A. and Schwarz, G. R. "Analysis and Simulation Compression Techniques," *IEEE National Telemetering Conference Proc.*, 1967.

Bechtold, W. R., Medlin, J. E. and Weber, D. R. *PCM Telemetry Data Compression Study, Phase I*, Final Report M-62-65-2, Contract NAS 5-9729, Lockheed Missiles and Space Company, Sunnyvale, California, October 1965.

Blackman, R. B. and Tukey, J. W. *The Measurement of Power Spectra*, New York: Dover Publications, Inc., 1958.

Blasbalg, H. and Van Blerkom, R. "Message Compression," *IRE Transactions on Space Electronics and Telemetry*, vol. SET-8, pp. 228-238, September 1962.

Breaux, J. N. "A Maximum RMS Error Comparison of Several Redundancy Reduction Techniques," The Boeing Company, New Orleans, Louisiana.

Burch, G. E. and Winsor, T. *A Primer of Electrocardiography*, Philadelphia: Lea & Febiger, Fourth Edition 1960.

Carlton, A. G., et al., "A Real-Time Data Compression for Apollo PCM Telemetry," Johns Hopkins University, Applied Physics Lab, TG 1093, December 1969.

Corday, E. and Irving, D. W. *Disturbances of Heart Rate, Rhythm and Conduction*, Philadelphia: W. B. Saunders Company, 1961.

Daley, F. D., Jr. "Some General Considerations of the Role of the Computer in Airborne and Spaceborn Data Handling Systems," *IEEE National Telemetering Conference Proc.*, 1967.

Dorland's Illustrated Medical Dictionary, Philadelphia: W. B. Saunders Company, 24th Edition, 1965.

Drapkin, P. E. and Pentz, R. M. "An Associative Data Compressor," *IEEE International Convention Proc.*, March 1965.

Dotson, W. P., Jr. "Dynamic Reconstruction Errors in Digital-to-Analog Systems with Biomedical Applications," NASA/MSC.

Frost, W. "A Telemetry Technique for Wideband Data," *PGSET Transactions*, December 1962.

Furstenau, B. W. "PCM Telemetry and Data Compression Applied to Real-Time Flight Evaluation," *AIAA/AFLC/ASD Support for Manned Flight Conference*, Dayton, Ohio, April 1965.

Gardenhire, L. W. "Data Redundancy Reduction for Biomedical Telemetry," *Biomedical Telemetry*, New York: Academic Press, 1965.

Gardenhire, L. W. "Redundancy Reduction-The Key to Adaptive Telemetry," *IEEE National Telemetering Conference Proc.*, 1964.

Gardenhire, L. W. "Data Compaction of Rocket Booster PCM Telemetry Data," *Second Space Congress*, Cocoa Beach, Florida, 1965.

Gentleman, W. M. and Sande, G. "Fast-Fourier Transforms-For Fun and Profit," *Fall Joint Computer Conference Pro.*, 1966.

Germond, H. H. "Compression of Bioastronautical Data," *IEEE National Telemetering Conference Proc.*, 1965.

Grant, R. P. and Estes, E. H., Jr. *Spatial Vector Electrocardiography*, New York: The Blakiston Company, 1952.

Hulme, J. R. and Schomberg, R. A. "A Data Bandwidth Compressor for Space Vehicle Telemetry," *IEEE National Telemetering Conference Proc.*, May 1962.

Hurst, J. W. and Logue, R. B. *The Heart*, New York: The Blakiston Division of McGraw-Hill Book Company, 1966.

Klotz, L. A. B. and Duffin, P. M. "Remote-Site Data Compression," *IEEE National Telemetering Conference Proc.*, 1968.

Kurtenbach, A. J. and Wintz, P. A. "Data Compression for Second Order Processes," *IEEE National Telemetering Conference Proc.*, 1968.

Lamb, L. E. "Aerospace Cardiology," *The Heart and Circulation*, vol. I/ Research, Second National Conference on Cardiovascular Diseases, Washington, D.C., 1964.

Ledley, R. S. "Practical Problems in the Use of Computers in Medical Diagnosis," *IEEE Proc.*, vol. 57, November 1969.

Massey, H. N. "An Experimental Telemetry Data Compressor," *IEEE National Telemetering Conference Proc.*, 1965.

Medlin, J. E. "Sampled-Data Prediction for Telemetry Bandwidth Compression," *IEEE, Transactions on Space Electronics and Telemetry*, March 1965.

Medlin, J. "The Comparative Effectiveness of General Telemetry Data Compression Techniques," *IEEE International Telemetering Conference*, September 1963.

Pratt, W. K., Kane, J., and Andrews, H. C. "Hadamard Transform Image Coding," *IEEE Proc.*, vol. 57, no. 1, January 1969.

Schaefer, D. H. "Logarithmic Compression of Binary Numbers," *IRE Proc.*, p. 1219, 1961.

Schomburg, R. A. "Computer Simulation of a Data Compressor for Aerospace Telemetry Systems," *IRE National Symposium on Space Electronics and Telemetry*, October 1962.

Schwartz, M. *Information Transmission, Modulation, and Noise*, New York: McGraw-Hill Book Company, Inc., 1959.

Shannon, C. E. and Weaver, W. *The Mathematical Theory of Communication*, Urbana: The University of Illinois Press, 1963.

Sheldahl, S. A. "Comparison of Hardware Requirements for Polynomial Data Compressors," *IEEE National Telemetering Conference Proc.*, 1968.

Simpson, R. S., et al., "A Study of Redundancy Removal for Saturn Telemetry Data," *University of Alabama*, November 1964.

Stiltz, H. L. *Aerospace Telemetry*, Englewood Cliffs, N. J.: Prentice-Hall, 1961.

Stumpe, J. W. "Redundancy Reduction Techniques and Applications," *IEEE National Telemetering Conference Proc.*, 1967.

Tzannes, N. S. and Sarantakis, A. J. "Entropy and Data Compression," *IEEE Transactions on Information Theory*, vol. IT-16, no. 1, January 1970.

Wait, J. V. "Sampled Data Reconstruction Errors," *Instruments and Control Systems*, June 1970.

Weber, D. R. "Some Economic Factors in the Application of Data Compression," *IEEE National Telemetering Conference Proc.*, 1967.

Weber, D. R. and Wynhoff, J. "The Concept of Self-Adaptive Bandwidth Compression," *PGSET Record*, October 1962.

APPENDIX A

ALGORITHM SYNOPSES

1. TRANSFORMS

This algorithm family operates on data samples via mathematical transformation whereby all the original data samples are irretrievably lost.

1.1 Fast Fourier Transform

The "fast" term is used to denote a much different computer program which can generate the required output in a fraction of the time required by the usual Fourier program. An operator (the Fourier integral) is used to transform the input data samples from a time base to the frequency base yielding the amplitudes as a function of frequency. The transformed data (or same portion thereof) may be transmitted and the data reconstructed by performing the inverse operation on the ground. Noise immunity is gained through the averaging of channel errors in the reconstruction process; and data compression is derived from the exploitation of redundancy in the frequency base (high frequency components may have very small amplitudes and need not be transmitted).

1.2 Fast Hadamard Transform

This method uses a linear operator to transform the data samples from a time base to a sequency base, the transform having similar advantages described immediately above in addition to being much simpler to implement. This algorithm is even faster than the Fourier in that no multiplication or division operations are performed.

1.3 Spectrum Analysis

Usually performed during post flight, the activity examines particular frequency energy aspects of the signal time history. The original data samples cannot be reconstructed from the analysis output which would preclude use with ECG.

1.4 Thresholding

Limits can be defined (such as amplitude, slope, frequency parameters) whereby data is transmitted only during the time the limit is exceeded.

Bandwidth is thereby reduced; however, the entire original data cannot be reproduced since an *a priori* judgment was made that eliminated transmission of some data bandwidth.

1.5 Frequency Discrimination

If a signal has a reference frequency, then instead of transmitting the actual signal a discriminated output that represents the change from the reference frequency can be derived and transmitted. Since the deviation from the reference is usually orders of magnitude less than the reference frequency, a bandwidth conservation can be made.

1.6 Hotelling's Method

This is a very complex scheme requiring mathematical operations similar to those used in the Fourier transform technique, but with the additonal burden of an algorithm to diagonalize matrices (Eigenvalue, Eigenvector problem).

1.7 Filtering

Any transform scheme can be described as a filter. Preprocessing filters (with amplitude or slope thresholds) may be utilized to smooth out undesirable noise prior to the initiation of a specific data compression technique. This process usually limits the higher frequencies thus permitting lower data sampling rates and/or narrower bandwidths.

2. ADAPTIVE SAMPLING

These methods advocate real-time adjusting of the data sampling rate to correspond to its information rate. In this manner, the total sample rate of all sensors is adjusted to conform with the channel capacity and, if necessary, *a priori* data priorities are implemented so as not to exceed the channel capacity.

2.1 Associative

This is essentially a threshold-controlled-multiplex algorithm for reducing the total number of bits transmitted from a set of data sample sources. Each channel in the set is tested periodically to see if data above the threshold level is available. Those sources with available data are then sequentially scanned.

2.2 Command-Adaptive

Also a multiplexer scheme, the algorithm must be triggered by a command from where automated decisions are made regarding which data are significant at any point in time.

2.3 Self-Adaptive

In this method, each sensor has an analyzer for channel-sampling-frequency regulation.

2.4 Transient Event

Sensor analyzers detect amplitude changes (or rates of change) to trigger transmission of bursts of sequential data samples.

3. REDUNDANCY REDUCTION

Redundancy reduction techniques are successful because sampling rates are fixed and generally greater than the usual data information rates. These algorithms eliminate data samples that can be implied by examination of preceding or succeeding samples; or by comparison with arbitrary reference patterns.

3.1 Predictors

3.1.1 Zero-Order Polynomial (ZOP)

The algorithm predicts that the next data sample will be within the programed, fixed aperture (± tolerance) around the present data sample. If it is, the next data sample is not transmitted; if the next sample is outside the aperture limits, it is transmitted and the process is repeated.

3.1.2 Zero-Order Polynomial, Floating Aperture (ZOP-FA)

Same as above, except the aperture is repositioned symmetrically about each successive transmitted data sample.

3.1.3 Zero-Order Polynomial, Offset (ZOP-O)

A modification of ZOP-FA above. The predicted value is offset (by a fixed, predetermined amount) from the last transmitted value. The direction of the offset is determined by noting the most recent out-of-tolerance deviation of the data samples.

3.1.4 Exponential

Rather than using straight lines for predictions, this algorithm can handle data that exhibits exponential curves by utilizing exponential functions to predict the next data sample.

3.1.5 Cyclic Patterns

As repetitive cycles are measured, each is compared to a stored pattern determined *a priori*, and information indicating which pattern matches the closest is transmitted.

3.1.6 Cycle-to-Cycle Comparison (C2C)

Each data sample of a cyclic pattern (such as a cardiac complex) is compared to each corresponding sample of the reference cycle. Appropriate stored, amplitude limits are used as comparison criteria on each data sample. If the present cycle falls within the tolerances about the reference cycle, a message is transmitted instructing the ground to utilize the reference cycle. This process is similar to the ZOP-floating aperture. The process repeats until a new out-of-limits data sample is detected. The new data sample is transmitted and also displaces its predecessor in the reference cycle.

3.2 Interpolators

3.2.1 Zero-Order Polynomial (ZOI)

Similar to ZOP, except that the reference sample for the interpolator is determined at the end of a redundant set as contrasted with the first sample in the case of the predictors.

3.2.2 First-Order Polynomial, Two Degrees of Freedom (FOI-2DF)

This scheme calculates a straight line between the present sample (time) and the last transmitted sample so that all intermediate points are within a tolerance of the interpolated value on the straight line.

3.2.3 First-Order Polynomial, Two Degrees of Freedom, Fan Implementation (FOI-Fan)

This is a modification of FOI-2DF above. In order to avoid storing all the data between the last non-redundant sample and the point being considered, two line shapes are calculated for each new sample. The upper slope passes through the original sample and a point some specified tolerance above the next sample, and the lower slope goes similarly below this next sample. If the third sample falls between the elements of this fan shape, an interpolation line can be drawn between points one and three such that any point on this line is within this desired tolerance.

3.2.4 First-Order Polynomial, Modified (FOIM)

This scheme is twice as fast as the FOI-Fan above and takes advantage of the fact that computer division or multiplication operations with binary numbers can be performed by a simple shift operation.

3.2.5 FOI3DF and FOI4DF

These differ from the FOI-2DF in that computed values are transmitted for the beginning and ending points of the interpolation lines as opposed to sample points. The next line is started from the next sample value after the last transmitted point.

3.2.6 Sync Function

This is an approximation to the ideal low pass filter, (sin x)/x. The operation remains "in sync" with the sampled data which is by definition over-sampled, thus generating redundant data samples. The filter function thus deletes the excessive data points and allows only those to pass that are sufficient to describe the frequency content.

3.2.7 Fourier

The same mathematical techniques are required as for the Fourier transform. The inverse transform is evaluated in the middle interval of the data points to obtain interpolated values.

3.2.8 Least Squares Polynomials

The object here is to find a general polynomial which fits the data points as well as possible so that the sum of the squares of the differences between the original data points and the polynomial are minimized via the least-squares method. The polynomial coefficients are found by solving a set of (n+1) simultaneous equations which yields a polynomial of order (n). A perfectly general, least-square, curve-fitting computer program is a fairly complex and computer-time-consuming tool.

3.2.9 Lagrange Polynomials

The object is to replace the original signal with a Lagrange polynomial derived from the sample points. Presumably some data compression will result from transmitting only the coefficients of the polynomial instead of all the sample points. Lagrange polynomials result when it is required that the signal and the polynomial are equal at every sample data point. In general, it cannot be determined what order polynomial will give the best results for a set of data points. So, while Lagrange's formulation is a valuable theoretical tool in numerical analysis, it has little virtue in practical computation.

3.2.10 Difference Methods

Basically, all differencing methods are initiated by constructing and storing a difference table of all data points. The process is best applied to data tables whose characteristics are well known, and even in this restricted case several different methods may have to be used in different portions of the same table. Difference schemes are very sensitive to round-off and truncation errors and therefore detract from accurate data compression.

3.2.11 Fourier Coefficients

If a signal may be considered to be pseudo-periodic, piecewise continuous in an interval, and to possess derivatives throughout the interval, then the signal may be represented by a Fourier series which is convergent. The Fourier series coefficients may be transmitted rather than the actual data points.

3.3 Composite

3.3.1 Parallel Adaptive Composite (PAC)

Two methods already described, the ZOP-FA and the FOIM, are used simultaneously on each data sample. A decision is made (when each of the algorithms reaches a non-redundant sample) as to which has produced the longest run of redundant samples. An algorithm identification tag must accompany each transmitted data sample so that reconstruction may be done using the appropriate method.

4. ENCODING

4.1 Non-Adaptive

4.1.1 Delta Modulation

This model integrates combinations of positive and negative pulses in time so that the value of the integral closely approximates the magnitude of the original signal. Transmittal data consists of a stream of zeros and ones which can be used to synthesize the original signal. Since sampling frequency determines the transmission bit rate (a one or a zero must be transmitted for each sample), a low upper bound is placed on the compression ratio.

4.1.2 Difference Modulation

The technique utilizes the high probability that the difference between two adjacent data samples is small compared to full scale and therefore shorter binary words can be used to transmit their differences. This method is very sensitive to channel (bit) errors and results in only small compression ratios.

4.1.3 Probabilistic

The amplitude probability density function of the signal must be known *a priori* (and all data words must have different probabilities of occurrence). This scheme codes the data such that short words are assigned to values which frequently occur and long words are available to values which rarely occur. Variable word length gives serious problems in synchronizing words and equally serious problems in queuing buffer control.

4.2 Adaptive

4.2.1 Probabilistic

This is basically the same as the non-adaptive probabilistic, with the addition of an algorithm to compute new distribution functions so that code word assignments can be made to non-stationary data. The method is also subject to the same problems as the non-adaptive scheme.

4.2.2 Bit Plane

This is a complex scheme requiring very large data storage and long time delays between signal initiation and transmission. Data samples from many samples are compared on a bit-by-bit basis and the "bit planes" are recoded into variable length words for transmission, causing again the above mentioned problems.

APPENDIX B

ALGORITHM MATHEMATICAL DESCRIPTIONS

1. FAST FOURIER TRANSFORMATION

The fast Fourier transformation (FFT) algorithm can perform data compression by transforming the time domain sampled waveform to the frequency domain representation and then transmitting the lower positive frequency components. A reconstructed version of the original waveform is computed at the receiver by performing the inverse fast Fourier transformation.

1.1 General

The Fourier transform and inverse transform pair for continuous signals are defined:

$$X(f) = \int_{-\infty}^{\infty} x(t)e^{-i2\pi ft}dt \qquad \text{(B-1a)}$$

$$x(t) = \int_{-\infty}^{\infty} X(f)e^{i2\pi ft}df \qquad \text{(B-1b)}$$

where the uppercase X(f) denotes the frequency domain function and the lowercase x(t) denotes the time domain waveform; also, $i = \sqrt{-1}$. Since the original signal is a sampled (rather than continuous) waveform, the analogous discrete Fourier transforms of (B-1) are used. If the continuous waveform is sampled every Δt seconds for a time period T seconds long, N discrete samples are obtained. The following relations for time t, frequency f, and fundamental frequency f_o may be then defined:

$$T = N\Delta t$$
$$t = K\Delta t$$
$$f_o = 1/T$$
$$f = jf_o = j/N\Delta t$$
$$\text{and } ft = jK/N$$

where j, K are integers. Thus, the discrete Fourier transform pair is:

$$X(j) = \frac{1}{N}\sum_{K=0}^{N-1} x(K)e^{-i2\pi jK/N} \qquad \text{(B-2a)}$$

$$x(K) = \sum_{j=0}^{N-1} X(j) e^{i2\pi jK/N} \qquad \text{(B-2b)}$$

for j,K = 0, 1, 2, ..., N-1.

In general, (B-2a) and (B-2b) are applicable to both real and complex x(K). For either case, however, X(j) is complex. When x(K) is real, as in the present case of interest, the real part of X(j) is symmetric about the folding frequency f_f and the imaginary part is anti-symmetric. The folding frequency f_f is defined:

$$f_f = f_s/2$$

where f_s is the rate at which the continuous signal is sampled. Thus, the real part of X(j) is an even function and the imaginary part is an odd function. Consequently, components between 1 and N/2 may be interpreted as positive frequency harmonics of f_o; components between N/2 and N-1 may be interpreted as negative frequency harmonics between -N/2 and -1. The zeroth component is the direct current (DC), i.e., zero frequency, component. The N/2 component corresponds to the folding frequency.

The fast Fourier transform is simply an efficient (computationally fast) implementation which eliminates the numerous redundant operations inherent in the direct application of (B-2). This efficiency exists only when the number of samples to be transformed is restricted to a power of two; i.e., $N = 2^n$, where n is a positive integer. Elimination of the redundant operations is possible because the transform may be computed by a recursive procedure which defines a larger Fourier transform in terms of smaller transforms. A detailed mathematical development of the formulation is presented in Reference 6.

1.2 Filter

Data compression is achieved by performing a filtering operation on the transform components. The filtering operation may be conveniently described using the equivalent matrix form of (B-2). Thus,

$$\overline{X} = \frac{1}{N} \overline{F}\, \overline{x} \quad \text{and} \quad \overline{x} = \overline{F}\, \overline{X}$$

where $\overline{x}$ is a column matrix containing N real (or complex) samples of the signal waveform; $\overline{X}$ is a column matrix containing N complex transform components; and $\overline{F}$ is an NXN Fourier transformation matrix. In component form:

$$
\begin{bmatrix} X_0 \\ X_1 \\ X_2 \\ \cdot \\ \cdot \\ \cdot \\ \cdot \\ X_{N-1} \end{bmatrix} = \frac{1}{N} \begin{bmatrix} 1 & 1 & 1 & \cdots & 1 \\ 1 & a & a^2 & \cdots & a^{N-1} \\ 1 & a^2 & a^4 & \cdots & a^{2(N-1)} \\ \cdot & \cdot & \cdot & & \cdot \\ \cdot & \cdot & \cdot & & \cdot \\ \cdot & \cdot & \cdot & & \cdot \\ \cdot & \cdot & \cdot & & \cdot \\ 1 & a^{N-1} & a^{2(N-1)} & \cdots & a^{(N-1)(N-1)} \end{bmatrix} \begin{bmatrix} x_0 \\ x_1 \\ x_2 \\ \cdot \\ \cdot \\ \cdot \\ \cdot \\ x_{N-1} \end{bmatrix}
$$

where $a^{jK} = e^{-i2\pi jK/N}$.

The data compression/reconstruction scheme is based on the technique of zonal sampling and uses the symmetry properties mentioned previously. In zonal sampling, only positive frequency components below a specified cutoff frequency f_c are transmitted. Thus, compression is achieved by computing N complex transform domain components and removing (filtering) positive frequency components greater than f_c and all negative frequency components from the transmitted components.

Reconstruction is performed using the inverse procedure. The received components are loaded into locations $j = 0$ to $j = f_c/f_o$ of an input array. Then, negative frequency components, the absolute value of which are less than f_c, are computed using the symmetry properties and loaded into locations $j = N-1$ to $N-f_c/f_o$. The remaining locations are filled with zeros. Finally, the reconstructed time signal is obtained by performing the inverse FFT.

The above description may be illustrated by the highly artificial case $N = 2^3 = 8$ and $f_c = f_o$. Thus, only the DC and fundamental components are transmitted.

$$
\begin{bmatrix} X_0 \\ X_1 \\ X_2 \\ X_3 \\ X_4 \\ X_5 \\ X_6 \\ X_7 \end{bmatrix} = \begin{bmatrix} R_0 + iIm_0 \\ R_1 + iIm_1 \\ R_2 + iIm_2 \\ R_3 + iIm_3 \\ R_4 + iIm_4 \\ R_3 - iIm_3 \\ R_2 - iIm_2 \\ R_1 - iIm_1 \end{bmatrix}
\begin{matrix} \left.\begin{matrix} \\ \\ \end{matrix}\right\} \bullet \text{ Transmitted} \\ \left.\begin{matrix} \\ \\ \\ \\ \\ \end{matrix}\right\} \bullet \text{ Not transmitted, zero magnitude assumed at receiver} \\ \left.\begin{matrix} \\ \end{matrix}\right\} \bullet \text{ Not transmitted, reconstructed using symmetry} \end{matrix}
$$

R and Im denote the real and imaginary parts of X.

1.3 Simultaneous Transformations

The compression ratio may be increased by a factor of two without any increase in rms error by utilizing the FFT capability for transforming complex time signals. In a straight-forward application of (B-3), the imaginary part of the N samples $x_0, x_1, x_2, \ldots x_{N-1}$ would be set equal to zero, since the original signal is real. A more efficient procedure is to locate the first N samples in the real part of $x_0, x_1, \ldots x_{N-1}$ and the next N samples in the corresponding imaginary part. Twice as many samples may be transformed without any increase in the number of computations.

The N complex transmitted components X, however, now represent both sets of N samples. Thus, a procedure for separating X into the two individual transform sets is required. Let the first and second sets of real time samples be denoted by a and b, respectively. Then, substituting a into the real part of x, and b into the imaginary part,

$$x = a + ib$$

with Fourier transform

$$\mathcal{F}\{x\} = \mathcal{F}\{a + ib\} = \mathcal{F}\{a\} + i\mathcal{F}\{b\}$$

or $$X = A + iB. \qquad \text{(B-4a)}$$

The complex conjugate X^* is

$$X^* = A - iB. \qquad \text{(B-4b)}$$

Solving (B-4) for the individual transform sets A and B yields:

$$A = \frac{1}{2}(X + X^*)$$

and $$B = \frac{1}{2}(X - X^*).$$

Both A and B possess the symmetry properties.

An interesting result of the above is that a compression ratio of two may always be achieved without any rms error. An FFT functional flow diagram is presented in Figure B-1.

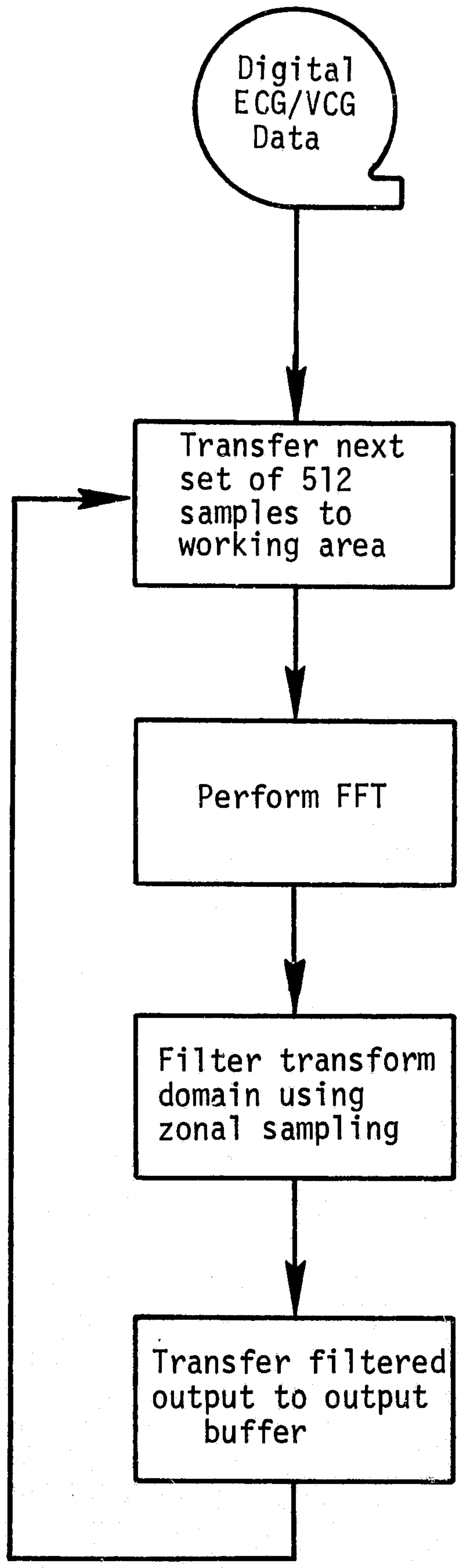

Figure B-1. FFT Data Compression Algorithm Functional Flow Diagram

1.4 Selection of N

The value $N = 2^9 = 512$ was selected for the present study. This value was obtained based on an examination of the rms error between the original and reconstructed signals as a function of N for several test subjects. The rms error was constant for $N = 2^{10}$, 2^9, 2^8, and 2^7 and increased significantly as N was decreased further.

2. PARALLEL ADAPTIVE COMPOSITE

2.1 General

The parallel adaptive composite (PAC) compression/reconstruction algorithm combines the advantages of the zero-order predictor with floating aperture algorithm (ZOP-FA) and the first-order interpolator with two degrees of freedom and fan implementation (FOI-Fan) algorithm. The ZOP-FA has the advantage of implementation simplicity and is efficient for compressing step-like signals; i.e., signals which contain time intervals during which the signal magnitude remains relatively constant. The FOI-Fan has been found to be efficient for general types of original waveforms, but requires considerably more implementation complexity than the ZOP-FA. Figure B-2 presents a PAC algorithm functional flow diagram.

A detailed description of the PAC and the compression performance when applied to several signal types, including electrocardiograms, is presented in Reference 11.

2.2 Zero-Order Predictor - Floating Aperture

In prediction methods, the compressor forms an estimate $\hat{s}_n$ of the next sample value based on past sample values (as interpreted by the receiver) y_{n-1}, y_{n-2}, y_{n-3}, ... y_{n-j}. Then, the prediction error magnitude $|\hat{s} - s_n|$ (where s_n is the present sample value) is computed. If the prediction error is within a specified aperture ($\pm K$) about $\hat{s}_n$, s_n is not transmitted, but is replaced at the receiver by its predicted value $\hat{s}_n$. If the prediction error magnitude is greater than $|K|$, the present value s_n and a time/position identifier are transmitted and the aperture is repositioned about the present value s_n which then becomes the estimated $\hat{s}_n$ value for the next prediction. Thus, the aperture essentially "floats" with non-redundant (transmitted) samples.

2.3 First-Order Interpolator, Two Degrees of Freedom, Fan Implementation

In interpolation methods, the estimates $\hat{s}_{n+1}$, $\hat{s}_{n+2}$, ..., $\hat{s}_{n+j-1}$ are computed for all sample values between the last transmitted sample s_n and a later sample s_{n+j}. If s_{n+j} is the most distant later sample value such that the maximum interpolation error is less than the specified tolerance K ; i.e.,

$$\max_{1 \leq i \leq j-1} \left| \hat{s}_{n+i} - s_{n+i} \right| \leq K \qquad \text{(B-5)}$$

then s_{n+j} is transmitted.

The FOI-Fan corresponds to the special case in which the estimates $\hat{s}_{n+1}$, $\hat{s}_{n+2}$, ..., $\hat{s}_{n+j-1}$ are intermediate values along a straight line connecting the last transmitted sample s_n and s_{n+j}. The slope M of this line is:

$$M = \frac{s_{n+j} - s_n}{j} .$$

Thus, the estimates $\hat{s}_{n+i} = s_n + Mi$.

First-order interpolators may be implemented with two, three, or four degrees of freedom depending upon whether both ends, one end, or neither end of the line of interpolation is confined to a sample. In the present two-degrees-of-freedom case, the end points are constrained to terminate on s_n and s_{n+j}.

The procedure for implementing the FOI-Fan is detailed below. First, however, the initial value for the upper bound U and lower bound L, corresponding to the first estimate $\hat{s}_{n+1}$, are computed:

$$U_1 = s_n + K \text{ and } L_1 = s_n - K.$$

Then, the following procedure is repeated as many times as required.

Step 1. Compute U and L for the ith estimate $\hat{s}_{n+i}$.

$$U_i = \frac{U_{i-1} - s_n}{i-1} + U_{i-1}$$

$$L_i = \frac{L_{i-1} - s_n}{i-1} + L_i - 1.$$

Step 2. Compute

$$U_i^* = s_{n+i}+K$$

$$L_i^* = s_{n+i}-K$$

for later use.

Step 3. Compute

$$\Delta_i^1 = U_i - s_{n+i}$$

$$\Delta_i^2 = L_i - s_{n+i}$$

If either Δ_i^1 is negative or Δ_i^2 is positive, then (B-5) has been violated. The previous sample s_{n+i-1} is transmitted along with the position (or run length) identifier i-1.

Step 4. If Δ_i^1 is positive or Δ_i^2 is negative, proceed by comparing U and L with U* and L*, respectively.

$$\Delta_i^3 = U_i - U_i^*$$

$$\Delta_i^4 = L_i - L_i^*$$

Step 5. Determine if U* or L* should be used in place of U_{i-1} and L_{i-1}, respectively, in the recursive formula of Step 1 when the entire procedure is repeated. If $\Delta_i^3 > 0$, use U*; otherwise use U. If $\Delta_i^4 < 0$, use L*; otherwise use L.

Step 6. Repeat starting at Step 1.

2.4 Parallel Adaptive Composite

Both algorithms (ZOP-FA and FOI-Fan) become a subalgorithm of the composite algorithm and operate in parallel on the same data samples. Each subalgorithm operates on the samples until each finds a non-redundant sample. The subalgorithms may have the same, or differing, tolerances ($\pm K$). The subalgorithm which provides the longest run of consecutive redundant samples is identified as compressing that particular "run" and the procedure is repeated on subsequent data. The transmitted information consists of the non-redundant data sample and a subalgorithm identifier. The identifier is a positive or negative quantity if the compressing subalgorithm was the ZOP-FA or FOI-Fan, respectively. The subalgorithm identifier is used to accomplish reconstruction using the proper algorithm.

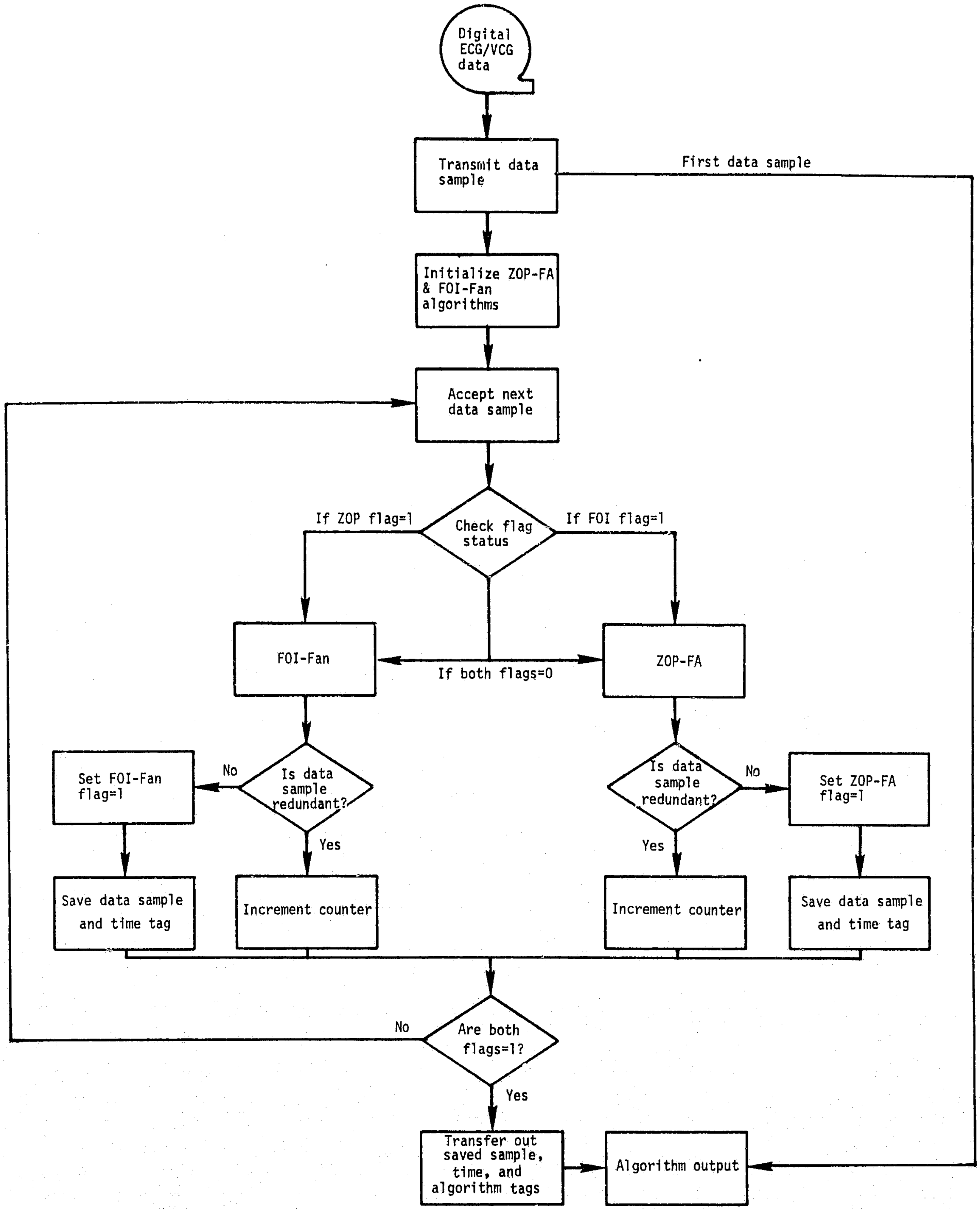

Figure B-2. PAC Data Compression Algorithm Functional Flow Diagram

3. FAST HADAMARD TRANSFORMATION

The fast Hadamard transformation (FHT) algorithm performs data compression by transforming the time domain sampled waveform to the sequency domain representation and transmitting the lower sequency components. A reconstructed version of the original waveform is computed at the receiver by performing the inverse fast Hadamard transformation.

Use of the FHT is motivated by the fact that the transform computation requires only additions and subtractions (no multiplications or divisions). Thus, the FHT is significantly faster than the fast Fourier transform.

3.1 General

The FHT is similar to the fast Fourier transformation (FFT), described above, except that a rectangular instead of sinusoidal orthogonal basis is used for representing the waveform. When using a sinusoidal basis, the sampled waveform, x(t), is represented as a weighted sum of harmonically related sine and cosine components. In the rectangular basis, x(t) is represented as a weighted sum of related rectangular components. Several sinusoidal and rectangular components W(s) are compared in the sketch below:

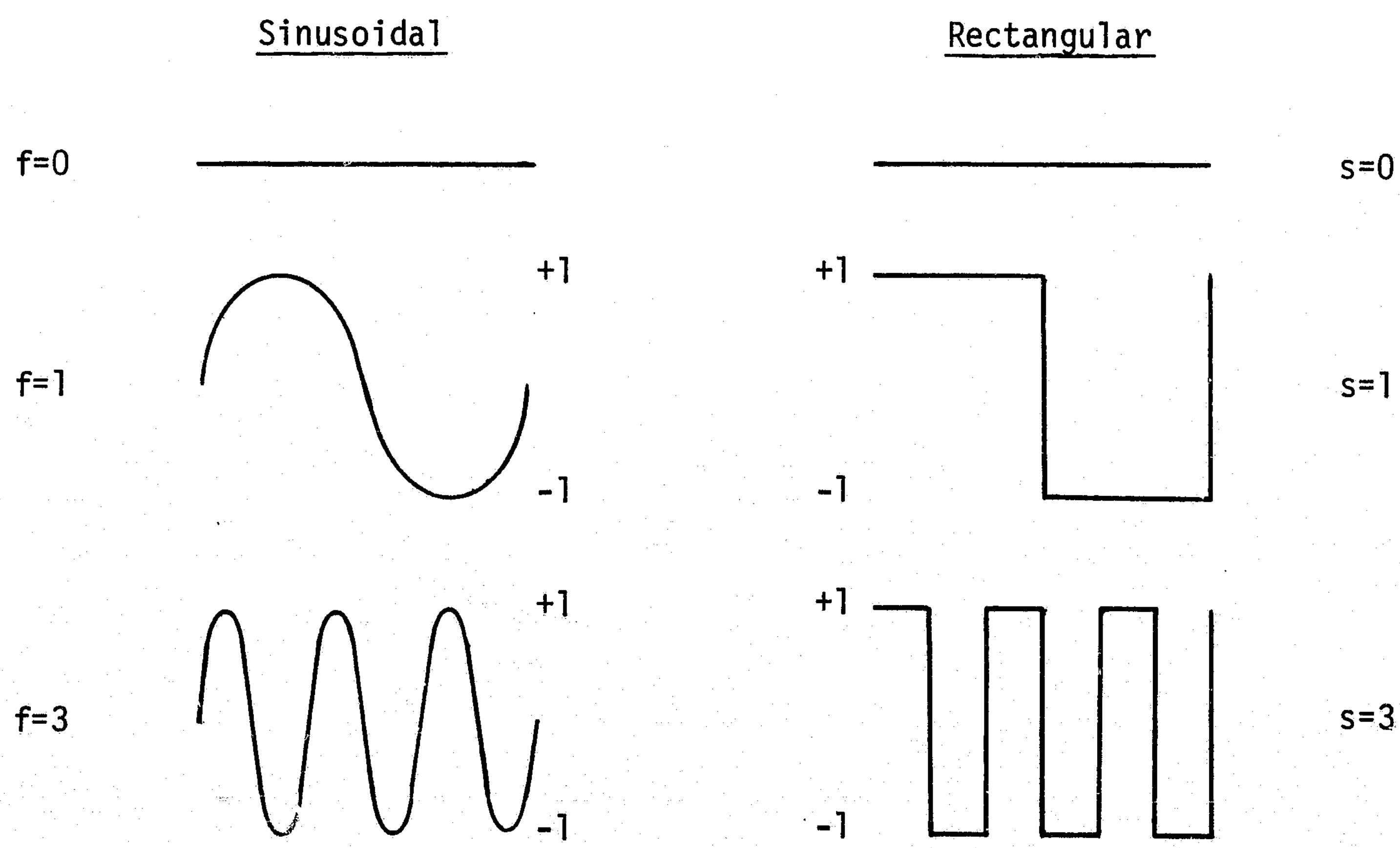

f and s denote frequency and sequency, respectively, and hence, the similarity between the concept of frequency and sequency.

The Hadamard transform X(j) of N samples of the signal x(K) is defined:

$$X(j) = \frac{1}{N}\sum_{K=0}^{N-1} x(K)W(j,K) \qquad \text{(B-6a)}$$

for j,K = 0, 1, 2, ..., N-1 and where W(j,K) represents the rectangular orthogonal basis. Similarly, the inverse Hadamard transform is:

$$x(K) = \sum_{j=0}^{N-1} X(j)W(K,j). \qquad \text{(B-6b)}$$

The form of W(j,K) may be clarified by using the equivalent matrix form of (B-6). Thus,

$$\overline{X} = \frac{1}{N}\overline{H}\,\overline{x} \quad \text{and} \quad \overline{x} = \overline{H}\,\overline{X}$$

where $\overline{x}$ is a column matrix containing N samples of the original signal, $\overline{X}$ is a column matrix containing N transform domain components, and $\overline{H}$ is an NXN Hadamard transformation matrix. In component form,

$$\begin{bmatrix} X_0 \\ X_1 \\ X_2 \\ \cdot \\ \cdot \\ \cdot \\ \cdot \\ X_{N-1} \end{bmatrix} = \frac{1}{N}\begin{bmatrix} H \end{bmatrix}\begin{bmatrix} x_0 \\ x_1 \\ x_2 \\ \cdot \\ \cdot \\ \cdot \\ \cdot \\ x_{N-1} \end{bmatrix}$$

The form of $\overline{H}$ depends on N and is given below for several N. The symbols (+) and (-) denote (+1) and (-1), respectively.

N	Matrix	Sequency
2	$\begin{bmatrix} + & + \\ + & - \end{bmatrix}$	0 1
4	$\begin{bmatrix} + & + & + & + \\ + & - & + & - \\ + & + & - & - \\ + & - & - & + \end{bmatrix}$	0 3 1 2

N	Matrix								Sequency
8	+	+	+	+	+	+	+	+	0
	+	-	+	-	+	-	+	-	7
	+	+	-	-	+	+	-	-	3
	+	-	-	+	+	-	-	+	4
	+	+	+	+	-	-	-	-	1
	+	-	+	-	-	+	-	+	6
	+	+	-	-	-	-	+	+	2
	+	-	-	+	-	+	+	-	5

The fast Hadamard transform is simply an efficient (computationally fast) implementation which eliminates the numerous redundant operations inherent in the direct application of (B-6). This efficiency exists only when the number of samples to be transformed is restricted to a power of two; i.e., $N = 2^n$, where n is a positive integer. Elimination of the redundant operations is possible because the transform may be computed by a recursive procedure which defines a larger Hadamard transform in terms of smaller transforms. A detailed mathematical development of the formulation is presented in Reference 7.

3.2 Filter

Data compression is achieved by performing a filtering operation on the transform components. In the particular filtering technique used (termed zonal sampling), only sequency components below a specified cutoff sequency s_c are transmitted. For example, in the artificial case where $N = 2^3 = 8$ and $s_c = 1$, only the DC and first sequency component are transmitted, as shown below:

$$\begin{bmatrix} X_0 \\ X_1 \end{bmatrix} \quad \bullet \text{ Transmitted}$$

$$\begin{bmatrix} X_2 \\ X_3 \\ X_4 \\ X_5 \\ X_6 \\ X_7 \end{bmatrix} \quad \bullet \text{ Not transmitted, zero magnitude assumed at receiver}$$

Figure B-3 presents an FHT functional flow diagram.

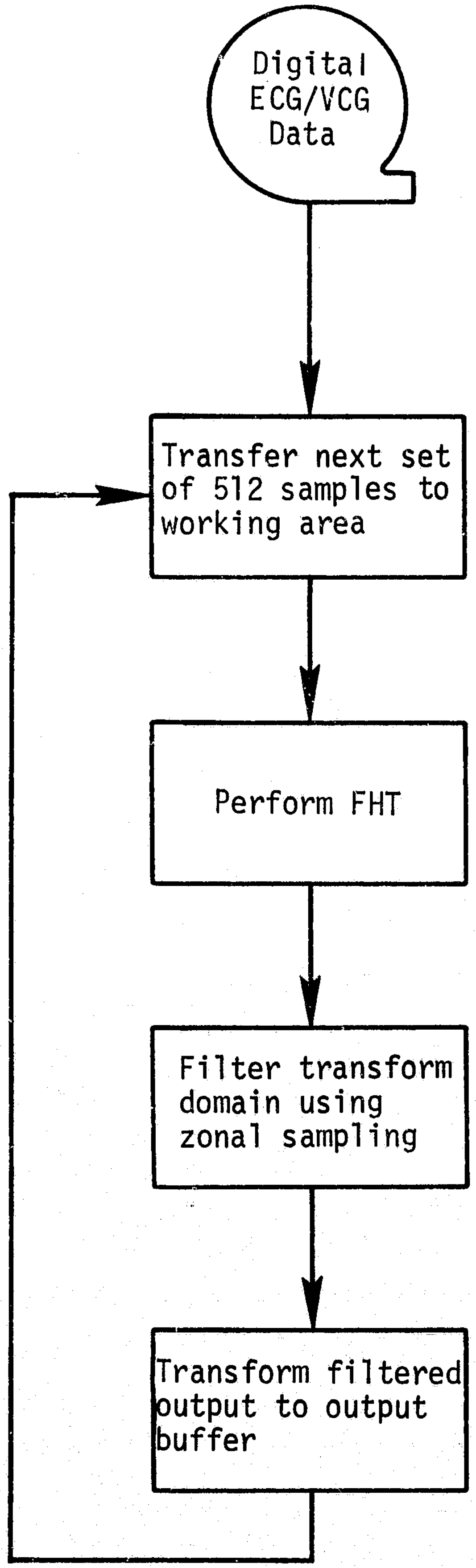

Figure B-3. FHT Data Compression Algorithm Functional Flow Diagram

3.3 Selection of N

The value $N = 2^9 = 512$ was selected for the present study. An examination of the rms error between the original and reconstructed signals for $N = 2^{10}, 2^9, \ldots, 2^2$ for several test subjects revealed that the rms error was constant. N = 512 was chosen to facilitate comparison of the FHT algorithm with the fast Fourier transform algorithm (which also used N = 512).

4. CYCLE-TO-CYCLE

4.1 General

The cycle-to-cycle redundancy reduction algorithm is based on the assumption that the ECG waveform is cyclic and hence repeats itself in an almost periodic fashion. If this is the case, any two consecutive cycles are almost identical in information content. The basic idea of the cycle-to-cycle redundancy reduction algorithm is to compare each cycle of ECG data with a base reference cycle on a sample by sample basis. If the comparison is outside of a required tolerance, the sample is transmitted and also replaces the old value in the base reference cycle. If the comparison is within the required tolerance, the sample is ignored. The comparison is carried out cycle after cycle with the appropriate updates being made to the base reference cycle. In this manner, only extreme variations to the current base reference cycle need be transmitted in order to reconstruct the data to within a required tolerance. A functional flow diagram is presented in Figure B-4. Reference 8 presents additional data.

4.2 Cardiac Cycle Identification

The first step in the algorithm is to locate a complete cardiac cycle (P, Q, R, S, T waves). This is done by stepping through the raw data while computing slopes since the R-wave contains the most drastic change in slope from a positive to a negative direction. A kurtosis (peakedness) parameter is computed which registers slope changes in the negative direction. When the peakedness parameter registers a negative slope change, it is tested against an input threshold.

The peakedness parameter (DEL) is defined using differences between points spaced 8 time samples apart. The differences are spaced 8 samples apart to minimize the effect of random static within the data. Differences along the R-wave show a sequence of positive differences (δ_j^+) followed by a sequence of negative differences (δ_i^-). The peakedness parameter (DEL) is defined as follows:

$$\text{DEL} = \text{Minimum}\ (\delta_i^-) - \text{Maximum}\ (\delta_j^+) \qquad \text{(B-7)}$$

For a given subject under a given condition, the most negative values of DEL consistently fall on the R-wave. Values of (B-7) for all other upward pointing waves are far less negative. A threshold value (AMPTØL) is set as a trigger against which each value of (B-7) is compared. If AMPTØL is set to a large negative value, only values of (B-7) on the R-wave will be triggered by the comparison, thus consistently detecting only the R-wave.

The extreme value of the peakedness parameter will trigger the process of finding the R-peak on the ECG waveform. The R-peak is found by searching the ECG data points for a maximum (δ_j^+) value. The points will be found to be monotonically increasing up to the R-peak. When a new value is smaller than the preceding value, the R-peak is the preceding value. Each cycle is aligned with other cycles using its R-peak as a reference. As R-peaks are found, complete data cycles are located and aligned.

4.3 Parallel Digital Filter

The next step of the process is to compute filtered data using the parallel digital filters. Each data sample of the cycle is input to a parallel filter along with the previous output of the parallel filter. The equation for the parallel filter is:

$$X_n = \frac{(\tau-1)\ X_{n-1} + D_n}{\tau}$$

where

X_n = filtered sample for cycle n

X_{n-1} = filtered sample for cycle n-1

D_n = unfiltered sample for cycle n

τ = time constant in number of cardiac cycles

The purpose of the parallel digital filters is to eliminate random noise in the samples of a cycle prior to compression. The equation defines a filter which is exponential in the digital domain and has the same frequency rejection characteristics as a simple resistance-capacitance low-pass filter which is exponential in the analog domain. For these studies, $\tau = 8$ was used which means that an initial filter stabilization period of eight cardiac cycles was required. In addition, one can see that the parallel digital filter is resistant to change; or, it can be stated that the filter somewhat amplifies ECG periodic characteristics while attenuating short-term perturbations. Thus it is more than a digital version of a low-pass filter.

4.4 Isoelectric Adjuster

At the output end of the parallel filter, a section of the ECG isoelectric region is used to compute a zero amplitude reference value. The zero amplitude reference value is a simple average of filtered data from a portion of the ECG isoelectric region between the T- and P-waves. The zero-amplitude reference is subtracted from each filtered value of the cycle in order to position each cycle about the zero-millivolt point and thus eliminate any biasing artifacts.

Finally, the cycle is compared with the base reference cycle on a sample by sample basis in order to determine whether or not to transmit the sample. Only samples which fall outside of a required tolerance are transmitted, as well as being used to update the base reference cycle.

4.5 Tolerances

The tolerance used for each sample is the larger of two values as follows:

$$T\emptyset LA = MAX\ (.1*T\emptyset LPC*T\emptyset L,\ T\emptyset LPC*|B|)$$

where:

TØLA = tolerance for a given data sample in millivolts
TØLPC = a percent value of tolerance which is input
TØL = peak-to-peak excursion of the base reference QRS complex
B = base reference cycle value for the given data sample in millivolts

For these studies, TØLPC = 25 was used.

The absolute value of the difference between each sample and its corresponding value in the base reference cycle is computed and tested against .01*TØLA. If the absolute value is greater than or equal to .01*TØLA, the sample is transmitted and also used to update that position within the base reference cycle. Otherwise, the next sample is examined.

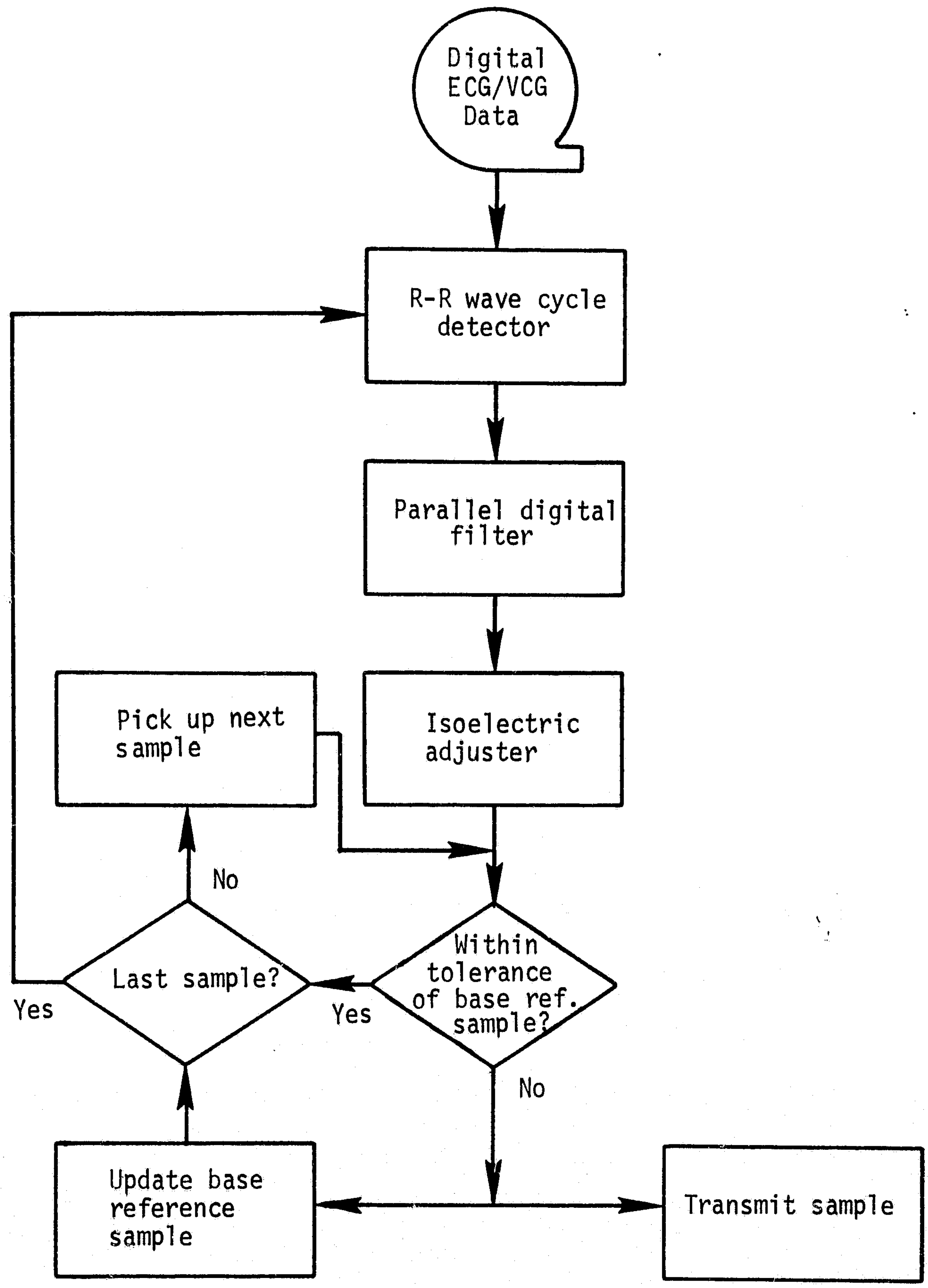

Figure B-4. C2C Data Compression Algorithm Functional Flow Diagram

5. FAST FOURIER CYCLE-TO-CYCLE

5.1 General

The FFC2C algorithm is an innovation of TRW and is a composite of the C2C and the FFT previously decribed. An FFC2C functional flow diagram is shown in Figure B-5.

The basic premise of this algorithm holds that more redundancy exists in the Fourier transform frequency domain for an ECG than exists in the usual input time domain. When the substantial periodicity of the cardiac complex is reviewed one can observe that for a given physiological condition the ECG is relatively unchanging except for rhythm, instrumentation noise, and various artifacts.

5.2 Interpolator

As previously explained in the FFT algorithm and shown in Figure B-5, the FFT will process only 2^n numbers of input data samples at a time. Since all the study ECG/VCG data are digitized at 500 sps, little probability exists that even a single cardiac complex will contain exactly $2^8 = 512$ data samples (512 was chosen as an optimum FFT input figure) because of the wide ranges of subject heart rates and rhythms. Actually, a cardiac complex in this study will contain from 200 (heart rate = 150) samples to 580 (R = 52) data samples.

An interpolator subprogram is incorporated to satisfy the FFT input requirement of 512 samples (Figure B-5). After a complete R-R cycle is identified a straight-line (first-order polynomial) interpolator connects each data sample value using

$$y = m\Delta t + b$$

where y is the next original data sample, m is the slope between the present and next sample, Δt is the original sampling interval (1/500 = 2 ms), and b is the y value for $\Delta t = 0$. Resampling is accomplished by then digitizing the ECG amplitude level at the new sampling interval which is 1/512th of the R-R interval. Accordingly the next cardiac complex will in all probability be a different length which merely modifies the sampling interval to produce exactely 512 samples for the new R-R interval.

5.3 Cycle-to-Cycle Transformation Filtering

After transformation and truncation--via zonal filtering--an initial transform domain set of Fourier coefficients are stored for use as a reference cycle. Subsequent cardiac complexes are each transformed and in turn arrive for comparison with the reference transform coefficients. Each new coefficient is compared to its corresponding reference position and if the difference magnitude is $<40_{10}$, the new coefficient is determined to be redundant and is discarded.

However if a new Fourier coefficient is compared and the difference magnitude is $\geq 40_{10}$, then it is considered to be non-redundant and is transmitted as an algorithm output while simultaneously replacing its corresponding reference coefficient; thus, it becomes the new reference coefficient.

The value for the transform domain tolerance is an input variable. The value of 40 used for this study represented about two percent of the smallest Fourier coefficient's magnitude.

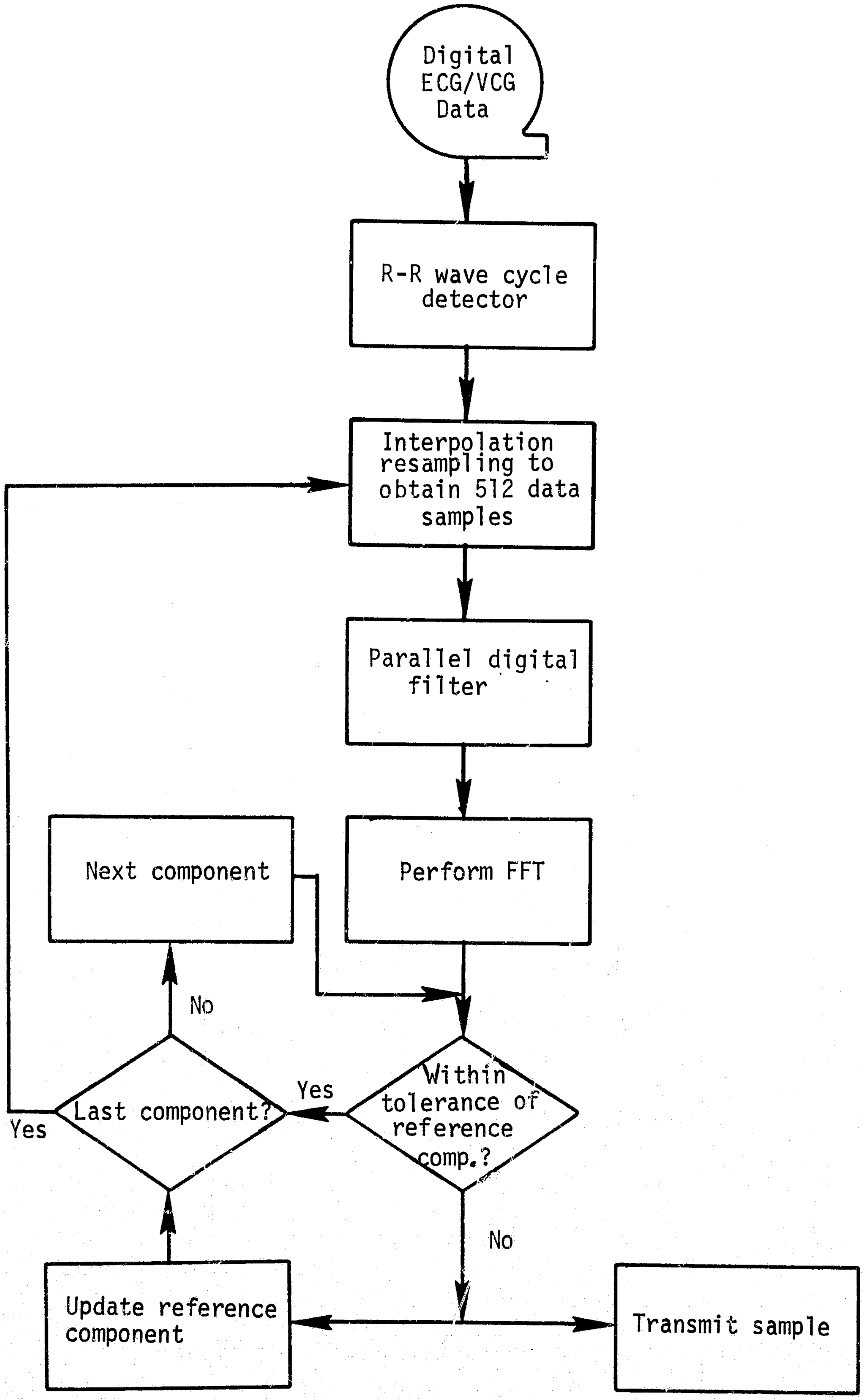

Figure B-5. FFC2C Data Compression Algorithm Functional Flow Diagram